

Open access  
**virtual testing protocols**  
for enhanced  
**road user safety**

# **Results of Application of Integrated Virtual Test Chain for VRUs**

## **WP Number: 4**


WP Title: Vulnerable Road User Protection

Deliverable D4.2

**Please Refer to this Report as Follows:**

Leo, Christoph; Klug, Corina; Schachner, Martin; Kocic, Veljka; Lackner, Christian; Heinzl, Philipp; Tidborg, Fredrik; Fredriksson, Anders; Kranjec, Matej (2022). Results of Application of Integrated Virtual Test Chain for VRUs, Deliverable 4.2. of the H2020 VIRTUAL project.

**Project details:**

Project start date:	01/06/2018
Duration:	54 months
Project name:	Open access virtual testing protocols for enhanced road user safety – VIRTUAL
Coordinator:	Astrid Linder, Prof Traffic Safety Swedish National Road and Transport Research Institute (VTI) Regnbågsgatan 1, 417 55 Gothenburg, Sweden
	This project has received funding from the European Union Horizon 2020 Research and Innovation Programme under Grant Agreement No. 768960.

**Deliverable details:**

Version:	Final (D4.2)
Dissemination level:	PU (Public)
Due date:	31/10/2022
Submission date:	28/10/2022
Online location:	<a href="https://secure.webforum.com/atvirtual/doc/?dfRefID=31603696">https://secure.webforum.com/atvirtual/doc/?dfRefID=31603696</a>

**Lead Contractor for this Deliverable:**

Corina Klug, TU Graz

<b>Report Author(s):</b>	Christoph Leo, Corina Klug, Martin Schachner, Veljka Kocic (TU Graz) Christian Lackner, Philipp Heinzl (Siemens) Fredrik Tidborg, Anders Fredriksson (Volvo Car Corporation) Matej Kranjec (UL)
<b>Reviewer:</b>	Luis Martinez (UPM), Ingrid Skogsmo (VTI)

**Legal Disclaimer**

All information in this document is provided "as is" and no guarantee or warranty is given that the information is fit for any particular purpose. The user, therefore, uses the information at its sole risk and liability. For the avoidance of all doubts, the European Commission and INEA has no liability in respect of this document, which is merely representing the authors' view.

© 2022 by VIRTUAL Consortium.

## Revision History

Date	Version	Reviewer	Description
30.09.2022	Draft 1.0. (M4.6.)	Luis Martinez	Draft shared with the reviewers and all WP4 partners for internal review
12.10.2022	Draft 2.0.	Elisabet Agar	Draft for language review
18.10.2022	Draft 3.0.	Ingrid Skogsmo	Draft for quality review
26.10.2022	Draft 4.0.	Elisabet Agar	Draft for second language review
27.10.2022	Draft 5.0.	Astrid Linder	Draft for review of the coordinator
28.10.2022	Final version	Astrid Linder	Submitted to portal



# Table of Contents

<b>1</b>	<b>Introduction.....</b>	<b>12</b>
1.1	Terminology.....	12
1.2	Background.....	12
1.3	Objectives.....	13
<b>2</b>	<b>Parts of the Assessment Framework.....</b>	<b>15</b>
2.1	VIRTUAL Testing Scenarios.....	15
2.2	Pre-Crash Simulation.....	16
2.2.1	Virtual Testing Catalogue for cars.....	18
2.2.2	Virtual testing catalogue for trams.....	19
2.3	Probability of Collision Scenarios.....	20
2.3.1	In-crash Simulation Matrix.....	21
2.4	In-crash simulations.....	22
2.5	Injury Prediction.....	22
2.5.1	Meta-Modelling.....	24
2.5.2	Overall Injury Probability.....	25
2.5.3	Transfer to the Cost Benefit Analysis tool.....	25
2.6	Cost Benefit Analysis Tool.....	25
2.7	User Interface.....	26
<b>3</b>	<b>Holistic Assessment for Car-Pedestrian cases.....</b>	<b>27</b>
3.1	Method.....	27
3.1.1	Generic AEB.....	27
3.1.2	In-Crash Simulations.....	27
3.2	Results.....	30
3.2.1	Generic AEB simulations.....	30
3.2.2	Generic Sedan in-crash simulations.....	31
3.2.3	State of the Art SUV Model.....	35
3.3	Discussion.....	37
3.3.1	Robustness of In-Crash Simulation Results.....	38
<b>4</b>	<b>Holistic Assessment of Car-Cyclist cases.....</b>	<b>45</b>
4.1	Method.....	45
4.1.1	Generic AEB.....	45
4.1.2	In-Crash Simulations:.....	45
4.1.3	Car Models.....	45
4.1.4	Cyclist Model.....	45
4.1.5	FE Bicycle Model for in-crash simulations.....	47
4.2	Results.....	48
4.2.1	Generic AEB simulations.....	48
4.2.2	Generic Sedan In-crash Simulations.....	49
4.2.3	State of the Art SUV in-crash simulations.....	53
4.3	Discussion.....	55
<b>5</b>	<b>Holistic Assessment for tram-pedestrian cases.....</b>	<b>57</b>
5.1	Method.....	57

5.1.1	Generic AEB for trams .....	57
5.1.2	Generic tram models .....	57
5.1.3	Pedestrian Model.....	59
<b>5.2</b>	<b>Results .....</b>	<b>59</b>
5.2.1	Generic AEB for trams .....	59
5.2.2	Generic tram models .....	59
<b>5.3</b>	<b>Discussion.....</b>	<b>64</b>
<b>6</b>	<b>Dissemination .....</b>	<b>65</b>
<b>6.1</b>	<b>OpenVT .....</b>	<b>65</b>
<b>6.2</b>	<b>Publications .....</b>	<b>65</b>
<b>7</b>	<b>Discussion and Outlook .....</b>	<b>67</b>
<b>8</b>	<b>Conclusions.....</b>	<b>68</b>
<b>9</b>	<b>References .....</b>	<b>69</b>
<b>10</b>	<b>Appendix A: Pedestrian Simulations Matrix .....</b>	<b>74</b>
<b>11</b>	<b>Appendix B: Cyclist Simulations Matrix.....</b>	<b>78</b>
<b>12</b>	<b>Appendix C: Tram Simulations Matrix .....</b>	<b>82</b>
<b>13</b>	<b>Appendix D: GV and Windscreen Validation.....</b>	<b>84</b>
<b>13.1</b>	<b>GVE Validation .....</b>	<b>84</b>
<b>13.2</b>	<b>Windscreen Validation .....</b>	<b>84</b>
<b>14</b>	<b>Appendix E: Results of the meta-model for pedestrian-car cases .....</b>	<b>86</b>
<b>15</b>	<b>Appendix F: Results of the meta-model for cyclist-car cases .....</b>	<b>95</b>
<b>16</b>	<b>Appendix G: Results of Tram in-crash simulations.....</b>	<b>104</b>

# Abbreviations

Abbreviation	Description
AEB	Autonomous Emergency Braking
AIS	Abbreviated Injury Scale
CARE	Community Database of Accidents on the Roads in Europe
CBA	Cost Benefit Analysis
CDF	Cumulative Distribution Function
CoG	Centre of Gravity
CPU	Central Processing Unit
CS	Conflict Situation
DoE	Design of Experiments
DYNASAUR	Dynamic Simulation Analysis of Numerical Results
Euro NCAP	European New Car Assessment Programme
GV	Generic Vehicle
HBM	Human Body Model
ID	Identifier
IS	Injury Severity
MPS	Maximum Principal Strain
OEM	Original Equipment Manufacturer
PEARS	Prospective Effectiveness Assessment for Road Safety
PDF	Probability Density Functions
PVB	Polyvinyl butyral
SotA	State of the Art
TTC	Time to Collision
VISAFE-VRU	VIRTUAL integrated assessment framework for Vulnerable Road Users
VRU	Vulnerable Road User
VT	Virtual Testing

# List of Tables

Table 2-1: Clustered quantities describing the collision scenario. ....	20
Table 2-2: Injury Prediction for different types of injuries. ....	23
Table 2-3: Parameters of the GaussianProcessRegressor for the meta-model created with Scikit-learn (Pedregosa et al., 2011). ....	25
Table 3-1: Parameters of the conceptual AEB System. ....	27
Table 3-2: Specification of VIVA+ shoes example shown for LS-Dyna. ....	30
Table 3-3: Results of the overall injury assessment for pedestrian to generic Sedan scenarios based on the predicted injuries by the meta-model and the occurrence probability. ....	32
Table 3-4: Results of the overall injury assessment for AEB pedestrian generic Sedan and SotA SUV scenarios based on the predicted injuries by the meta-model and the occurrence probability. ....	35
Table 3-5: Simulation Matrix for Round-robin Simulations. ....	39
Table 3-6: System properties used in the simulations performed by the different partners. ....	39
Table 3-7: Results of the round-robin simulations of Load Case 1 with the VIVA+ 50F pedestrian and the generic Sedan (struck side in bold). ....	40
Table 3-8: Results of the round-robin simulations of Load Case 2 with the VIVA+ 50M pedestrian and the generic Sedan (struck side in bold). ....	41
Table 3-9: Variation in maximum principal strains of the single ribs for 50M and 50F simulations performed on the four different systems. ....	42
Table 3-10 Kinematics of the VIVA+ 50F model in the generic Sedan crash until head impact. ....	43
Table 3-11: Kinematics of the VIVA+ 50M model in the generic Sedan crash until head impact. ....	44
Table 4-1: Reference Postures of 50F and 50M cyclists. ....	46
Table 4-2: Target geometry for trapeze frame VIVA+ 50F. ....	48
Table 4-3: Target geometry for diamond frame VIVA+ 50M. ....	48
Table 4-4: Results of the overall injury assessment for cyclist-generic Sedan cases based on the predicted injuries by the meta-model and the occurrence probability. ....	50
Table 4-5: Results of the overall injury assessment for AEB cyclist generic Sedan and SotA SUV scenarios based on the predicted injuries by the meta-model and the occurrence probability. ....	53
Table 5-1: Parameters of the conceptual Tram AEB System. ....	57
Table 5-2: Results of the overall injury assessment for pedestrian to tram scenarios based on the predicted injuries and the occurrence probability. ....	60
Table 10-1: In-Crash Simulation Matrix for Pedestrian baseline simulations. ....	74
Table 10-2: In-Crash Simulation Matrix for Pedestrian AEB simulations. ....	75
Table 11-1: In-crash Simulation Matrix for Cyclist baseline simulations. ....	78
Table 11-2: In-crash Simulation Matrix for Cyclist AEB simulations. ....	80
Table 12-1: Probabilities for tram collision speeds. ....	82
Table 12-2: Probabilities for pedestrian collision speeds. ....	82
Table 12-3: Probability for tram conflict situations. ....	82
Table 12-4: In-crash Simulation Matrix for Tram simulations. ....	83
Table 13-1: Response of the impactor test (black) compared to the results reported in Feist et al. (2019). ....	84
Table 13-2: Results reported by Alvarez and Kleiven (2016) (left), Impactor results with CFC180 filtered impactor acceleration (middle) and location of the head impactor impact on the windscreen (right). ....	85
Table 14-1: Results of the meta-model for generic Sedan pedestrian Baseline in-crash cases. ....	86
Table 14-2: Results of the meta-model for generic Sedan pedestrian in-crash AEB cases. ....	88
Table 14-3: Results of the meta-model for the SotA SUV pedestrian in-crash AEB scenarios. ....	91
Table 15-1: Results of the meta-model for generic Sedan cyclist in-crash baseline scenarios. ....	95

Table 15-2: Results of the meta-model for the generic Sedan cyclist in-crash AEB scenarios. .... 97  
Table 15-3: Results of the meta-model for SotA SUV cyclist in-crash AEB scenarios. ....100



# List of Figures

Figure 2-1: VIRTUAL assessment framework for VRU protection.....	15
Figure 2-2: Approach to calculate the occurrence probability of a specific VT scenario. ....	16
Figure 2-3: VIRTUAL pre-crash tool. ....	17
Figure 2-4: Identifier for VIRTUAL VRU testing scenarios. ....	17
Figure 2-5: Definition of collision point relative to vehicle front.....	18
Figure 2-6: SCPPR Scenarios implanted in the pre-crash tool to investigate the VIRTUAL pedestrian to tram testing scenarios. ....	19
Figure 2-7: Distribution of collision speeds as proposed in (Lackner et al., 2022).....	19
Figure 2-8: 3D scatter plots for 270 [°] and 90 [°] collision angle.....	21
Figure 2-9: Workflow of the in-crash simulations within VIRTUAL. ....	22
Figure 2-10: Injury Risk curve for proximal femur fractures (Schubert et al., 2021). ....	24
Figure 2-11: Injury Risk curve for femur shaft fractures (Schubert et al., 2021). ....	24
Figure 2-12: Injury Risk curve for tibia shaft fractures. ....	24
Figure 2-13: Scripts and files prepared as part of the VISAFE-VRU workflow. ....	26
Figure 3-1: Generic Sedan front model enhanced within WP4. ....	28
Figure 3-2: Positioned VIVA+ 50F model in accordance with the Euro NCAP Technical Bulletin TB024 (Euro NCAP, 2019). ....	29
Figure 3-3: Positioned VIVA+ 50M model in accordance with the Euro NCAP Technical Bulletin TB024 (Euro NCAP, 2019). ....	29
Figure 3-4: Structure of the VIVA+ shoe model.....	30
Figure 3-5: VIVA+ shoe model. ....	30
Figure 3-6: Results of the pre-crash simulations for car-pedestrian cases.....	31
Figure 3-7: Cost-Benefit Analysis for pedestrian to generic Sedan cases. ....	34
Figure 3-8: Relative mean error for all pedestrian load cases (relative to the max values over all four use cases) comparing 50F, 50M and both vehicle models.....	38
Figure 4-1: Reference Posture of 50F and 50M cyclists with left foot down.....	46
Figure 4-2: Positioned 50F cyclist model in front of GV Sedan Model. ....	47
Figure 4-3: Positioned 50M cyclist model in front of GV Sedan Model.....	47
Figure 4-4: Trapeze Frame Bicycle for VIVA+ 50F simulations. ....	48
Figure 4-5: Diamond Frame Bicycle for VIVA+ 50M simulations.....	48
Figure 4-6: Results of the pre-crash simulations for car-cyclist cases. ....	49
Figure 4-7: CBA for cyclist-generic Sedan cases.....	52
Figure 4-8: Relative mean error for all cyclist load cases (relative to the max values over all four use cases) comparing 50F, 50M and both vehicle models.....	56
Figure 5-1: Generic tram front model developed within WP4. ....	58
Figure 5-2: Beams (red) at the back of the Tram front to adjust the stiffness and achieve an improved generic tram. ....	58
Figure 5-3: Characteristics of the beams fixing the panels to the tram body. The baseline variant is shown red and the "Improved" version in green.....	58
Figure 5-4: Results of the pre-crash simulations for tram-pedestrian cases. ....	59
Figure 5-5: CBA for pedestrian to generic tram cases. ....	63
Figure 14-1: Results of the overall injury assessment for pedestrian to generic Sedan scenarios based on the predicted injuries by the meta-model and the occurrence probability. ....	90
Figure 14-2: Results of the overall injury assessment for the AEB pedestrian generic Sedan and SotA SUV scenarios based on the predicted injuries by the meta-model and the occurrence probability....	93
Figure 14-3: CBA analysis of generic Sedan baseline simulations compared with SotA SUV AEB simulations for pedestrians. ....	94

Figure 15-1: Results of the overall injury assessment for cyclist-GV scenarios based on the predicted injuries by the meta-model and the occurrence probability..... 99

Figure 15-2: Results of the overall injury assessment for AEB cyclist generic Sedan and SotA SUV scenarios based on the predicted injuries by the meta-model and the occurrence probability. ....102

Figure 15-3: CBA analysis of generic Sedan baseline simulations compared with SotA SUV AEB simulations for cyclists. ....103

Figure 16-1: Results of the overall injury assessment for pedestrian-tram scenarios based on the predicted injuries and the occurrence probability.....104

# Executive Summary

---

Within this report, the VIRTUAL Integrated Assessment Framework for Vulnerable Road User (VISAFE-VRU) protection is presented together with five different application examples.

By means of the integrated assessment framework, a holistic safety evaluation considering both active and passive safety measures for a population of accidents is considered. The likelihood of a specific virtual testing (VT) scenario occurring in real life has been derived from accident databases. Based on pre-crash simulations it has been determined how likely it is that VT scenarios could be avoided by a specific Autonomous Emergency Braking (AEB) system. For the unavoidable cases, probabilities for specific crash scenarios have been determined and finally from in-crash simulations with the VIVA+ Human Body Models the injury risk for these crash scenarios can be determined. The whole workflow is implemented and available as VISAFE-VRU notebooks and scripts on the OpenVT<sup>1</sup> platform.

The VISAFE-VRU was applied for the holistic assessment of car-related pedestrian and cyclist protection using a generic and a State of the Art (SotA) car model to assess the safety benefits of a generic AEB system combined with current passive safety structures. The fifth use case involved the assessment of an optimised tram front for pedestrian protection. Cost-Benefit Analysis (CBA) was applied for all use cases in which the generic safety system had been implemented, indicating when break-even had been achieved.

---

<sup>1</sup> <https://openvt.eu>

# 1 Introduction

## 1.1 Terminology

For consistency in terms of terminology, the consortium has agreed on common definitions that are used throughout the report:

- **Vulnerable Road Users (VRUs):** Defined as unprotected road users, who have to rely heavily on partner-protection of the vehicles in case of a collision (Wegman et al., 2008). The only VRUs considered within the Work Package (WP) 4 of the VIRTUAL project are pedestrians and cyclists, although motorcyclists and wheelchair users are often also associated with this group.
- **Conflict Situations:** Rough description of the participants' intention, (e.g., pedestrian crossing from the right and vehicle driving straight).
- **Accident Parameters:** Parameters necessary for describing the boundary conditions of an accident, (e.g., initial velocities, road conditions, weather conditions, collision velocities, etc.).
- **Accident Scenario:** Specification of a conflict situation and all accident parameters. It therefore includes a detailed description of the environment, (e.g., street width, lightning conditions, weather conditions, visual obstructions), as well as the velocity profile and trajectory of road users. The term is used for actual (and not potential) accidents, (i.e., collisions between vehicle and VRU).
- **Virtual Testing Scenario:** Detailed virtual description of the environment, (e.g., street width, lightning conditions, weather conditions, visual obstructions), as well as the velocity profile and trajectory of road users. Together with the motion profile and the environmental parameters, a single conflict situation can lead to a variety of possible VT scenarios. The term is used for scenarios that represent the Baseline for the assessment. Hence not all VT scenarios will lead to accidents and impact scenarios in the treatment simulations.
- **Baseline:** Baseline simulations are based on the original VT scenarios. Active safety systems have not been considered (w/o AEB).
- **Treatment:** Treatment is applied based on the Baseline. AEB systems have been considered (with AEB). In treatment simulations described in this report, vehicle models are equipped with generic virtual AEB systems.
- **Impact Scenario:** Describes the boundary conditions of the VRU impact, (i.e., collision), relative to the vehicle.

## 1.2 Background

In the year 2019, 48% of all road fatalities in Europe affecting the lives of VRUs amounted to 10,895 fatalities (European Commission, 2021). Besides other strategies, car manufactures and governments are expecting that the introduction and market penetration of new active safety systems, such as AEB and emergency evasion, respectively, will significantly change the overall number of pedestrian accidents (Chen et al., 2015; Detwiller & Gabler, 2017; Hummel et al., 2011; Isaksson-Hellman &

Lindman, 2019; Lindman et al., 2010; Luttenberger et al., 2014; Strandroth et al., 2016; Vertal & Steffan, 2016). However, the studies also conclude that it will not be possible to avoid all VRU accidents.

Pedestrian AEB Systems are already being assessed in current European New Car Assessment Programme (Euro NCAP) assessments and have, therefore, gained increasing importance in the last few years. From 2024 onwards they will become mandatory. Hence, the distribution of crash configurations of VRU accidents is predicted to change in the near future. Consequently, new priorities of crash configurations will have to be considered in-crash performance testing since simply analysing contemporary accidents will not suffice. Hence, it is also necessary to predict how the priorities will change due to the continued implementation of crash avoiding safety systems, such as different versions of AEB.

In case of unavoidable accidents, the impact configuration will be significantly affected, due to active safety systems influencing the relative velocity between VRUs and vehicles (Gruber et al., 2019). Therefore, developing an integrated assessment procedure, considering the ratio of avoided cases as well as the effect on unavoidable cases, is anticipated within VIRTUAL.

A common approach to determine testing scenarios involves using reconstructed real-world accidents. Each conflict scenario is represented in a detailed, explicit way, comprising trajectories of all accident participants based on evidence collected in case records. The use of reconstructed accident scenarios is a fundamental method for the evaluation of safety systems. However, they also represent the extremes of possible scenarios, which are determined and influenced by many different parameters that may not be present in a sampled accident. An attempt to tackle this issue is applying the stochastic determination of conflict situations. Such an approach attempts to determine potential conflict scenarios by objectively analysing the variation of "possible" influencing factors.

By means of virtual pre-crash simulation, the effectiveness of active safety systems (such as AEB) can be assessed on a variety of generic or real-world conflict scenarios (Barrow et al., 2018; Jeppsson et al., 2018; Lindman et al., 2010; Page et al., 2015; Rosen et al., 2010; Roth et al., 2018; TRL et al., 2018).

Within cities, the importance of public transport is increasing in order to make cities more sustainable, and a "renaissance" of trams has been observed within the last few years. Currently, trams run in 204 cities in Europe, with the tram network continuously increasing in length (UIC: International union of Railways, 2009). Hence, the consequence of an increased number of trams in the cities is that the interaction between trams and other road users is more prominent and consequently potential crashes more likely. Ensuring safety and mitigating tram related accidents is a major concern in the design, operation and development of tram systems (Naznin et al., 2016). Current knowledge is almost entirely based on analyses of reported accident data (Naznin et al., 2017), related to several shortcomings, such as underreporting, especially for less severe accidents (Budzynski et al., 2019). For the assessment of passive safety of tram fronts, a recently published Technical Recommendation 17420 (Technical Committee CEN/TC, 2019) defines pedestrian tram front design safety requirements for the first time, mainly based on geometrical guidelines.

### 1.3 Objectives

The aim of WP4 is to bridge the gap between active and passive safety assessments. In our approach we aim to take current real-world crash data into consideration for defining VT scenarios, without limiting our assessments to specific real-world crashes available in the databases, investigating a wider variation of scenarios instead to studying the potential relevance of scenarios after implementing active safety systems. For cases which are not avoided by the active safety systems, our aim has been to

perform a detailed injury assessment which can be used as input for a CBA. This means that the risk for specific injuries and severities has to be predicted for both females and males. The assessment of these injury risks has to be feasible with conventional simulation resources, while still providing a sufficient level of accuracy.

In Task 4.1 the relevance of different conflict situations as well as the relevance of different parameters (for specific conflict situations) for car-pedestrian, car-cyclists and tram-pedestrian crashes, has been identified. This information has then been considered to define VT scenarios, in which the integrated safety systems addressing VRUs can be assessed. Our ambition, therefore, was to use real life crash data from different databases to weigh VT scenarios, suitable for weighing each VT scenario according to its relevance. By using this approach, the potential of an integrated safety system can be derived and used to estimate how the relevance of different conflict situations and scenarios change due to a higher market penetration of enhanced safety systems. A hybrid approach is applied to determine a catalogue of potential conflict scenarios for a particular virtual pre-crash simulation and to derive future impact scenarios, (i.e., impact locations and relative velocities among accident participants). Potential factors that influence scenarios have been retrieved from accidents records and combined with possible conflict scenarios (based on motion patterns) to derive future accident and impact scenarios.

In Task 4.2 these future impact scenarios have been investigated in more detail. VT scenarios not avoided by the generic AEB system, were taken into account for the in-crash simulation. The Design of Experiments (DoE) method was applied to select a reasonable number of VT scenarios for the in-crash simulations. A trade-off between occurrence probability of the scenarios and good coverage (space filling) of the study area was achieved through the DoE. The in-crash simulations were performed to predict the injury probability for specific body regions using the VIVA+ Human Body Models (HBMs). As only a small number of collision scenarios can be considered in the in-crash simulations (due to high computational effort) a meta-model was used to predict the injury probability of the collision scenarios not considered. The injury prediction for each collision scenario together with the occurrence probability of each scenario were used to establish the overall injury risk. The total benefit of introducing an active safety system was calculated through CBA.

In Task 4.3., the developed framework was demonstrated in five different use cases as proof of concept and guideline for future application. The following use cases are included in this report:

1. Generic Sedan front in pedestrian crashes with and without generic AEB.
2. SotA SUV model in pedestrian crashes with generic AEB.
3. Generic Sedan front in bicycle crashes with and without generic AEB.
4. SotA SUV model in bicycle crashes with generic AEB.
5. Generic tram front in pedestrian crashes with conventional and optimised front structure.

The scope of this deliverable is to demonstrate the whole VIRTUAL Integrated Safety Assessment Framework (VISAFE-VRU) for the above mentioned different VRUs and collision partners.

## 2 Parts of the Assessment Framework

The workflow of the VIRTUAL assessment framework for VRU protection is shown in Figure 2-1. The data flow and transformation for the individual steps is done with Jupyter Notebooks. These interactive notebooks are a combination of documentation in markdown language with code blocks, (i.e., a combination of clear documentation of the performed steps as well as easy user interaction is achieved). The virtual testing protocol, which should be applied by future users who aim to apply the framework, is described in Deliverable 1.2 (Klug et al., 2020). The current deliverable summarises the methodological background instead.

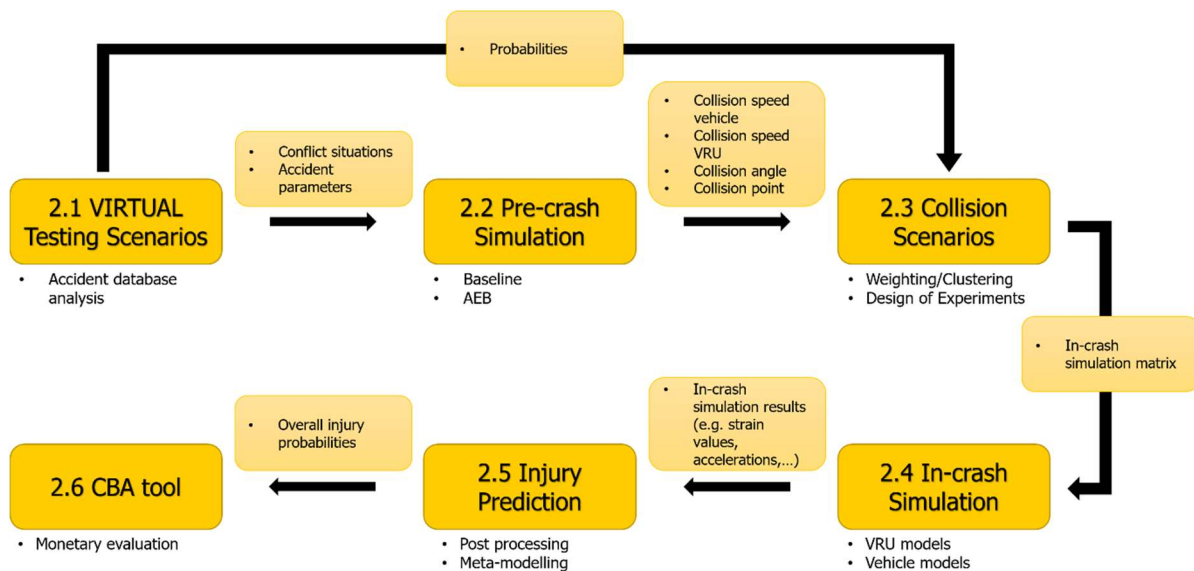


Figure 2-1: VIRTUAL assessment framework for VRU protection.

### 2.1 VIRTUAL Testing Scenarios

Based on the conducted analysis of accident statistics in D4.1, occurrence probabilities of major influencing factors on the accident scenario have been evaluated as shown in Figure 2-2.

In D4.1, data has been split into three different injury severity (IS) categories: *minor*, *severe* and *fatal*; each having a certain occurrence probability  $P(IS)$ . Further, occurrence probabilities for each conflict situation (CS)  $P(CS | IS)$  have been determined with respect to the injury severities.

Besides the conflict situation, which defines the pathways of the accident participants, initial speeds and road conditions represent major boundary conditions of an accident scenario. Probability Density Functions (PDF) for vehicle and VRU speeds  $f_{v_e}$ ,  $f_{v_{VRU}}$  have been determined from the accident statistics for each IS and CS. PDFs allow sampling, equally distributed speed percentile values, which are then used to initialise the scenario. Thus, the occurrence probabilities of individual speeds  $P(v_{veh} | IS, CS)$  and  $P(v_{VRU} | IS, CS)$  cover certain ranges of their distribution. Road conditions can either be *dry* or *non-dry*, the occurrence probability  $P(RC | IS, CS)$  has also been determined with respect to IS and CS. Road conditions and initial speeds are assumed to be conditional independent. The occurrence probability of

an individual scenario  $P(\textit{Scenario})$  can then be calculated as described in Equation 1 and Figure 2-2. These occurrence probabilities are based on current accidents, where active safety systems, such as AEB play a negligible role. These cases are used as baseline and the change due to an AEB system can be evaluated by means of the pre-crash simulations in the next step.

Equation 1:

$$P(\textit{Scenario}) = P(IS) \cdot P(CS | IS) \cdot P(v_{veh} | IS, CS) \cdot P(v_{VRU} | IS, CS) \cdot P(RC | IS, CS)$$

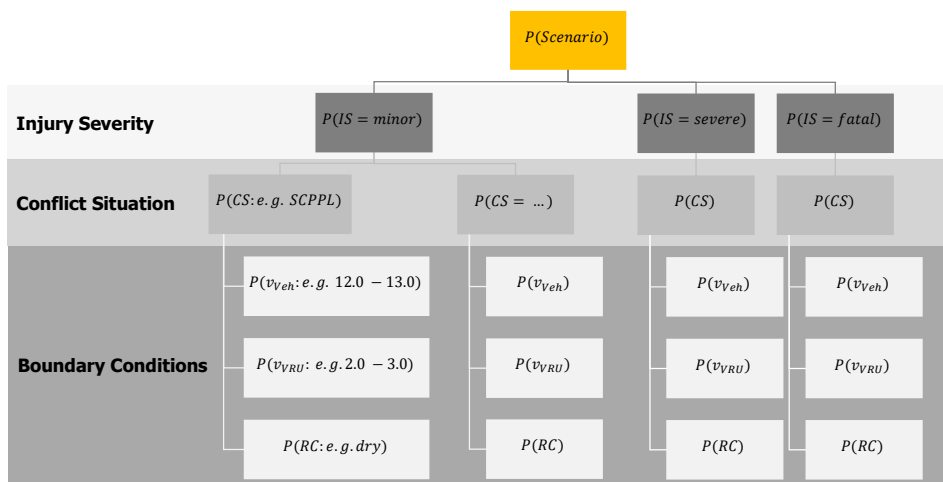


Figure 2-2: Approach to calculate the occurrence probability of a specific VT scenario.

## 2.2 Pre-Crash Simulation

Pre-crash simulations are performed with the VIRTUAL VRU-pre-crash-tool, which has been introduced in previous reports and also published (Schachner, Schneider et al., 2020). An overview on the method is shown in Figure 2-3. The entire source code is publicly available on <https://OpenVT.eu>, together with instructions of how to set up the tool and how to generate and simulate a scenario catalogue.



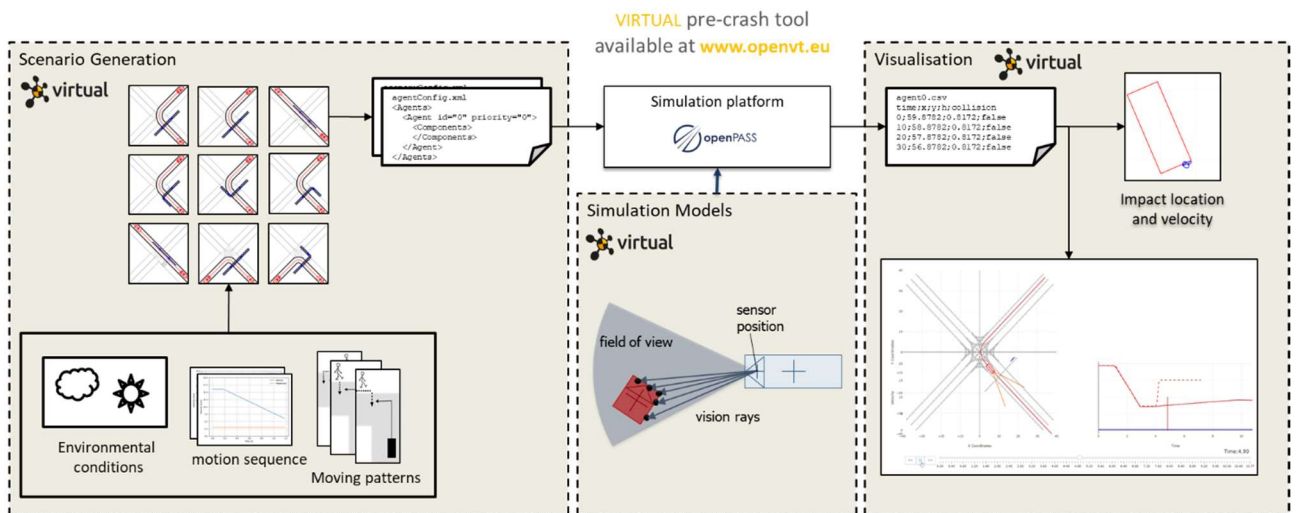


Figure 2-3: VIRTUAL pre-crash tool.

With the described approach in (Schachner, Schneider et al., 2020) and D 4.1, an individual VT scenario can be built by providing the following scenario parameters:

- Conflict situation
- Initial speed of the vehicle  $v_{Ve}$
- Initial speed of the VRU  $v_{VRU}$
- Road condition (dry/non-dry)
- Collision point (point where vehicle and VRU trajectory cross each other)

For each VT scenario of the catalogue, a unique Identifier (ID) is created by combining all scenario parameters. An example ID is shown in Figure 2-4. The ID represents the scenario at 50<sup>th</sup> percentile initial speed for both vehicle and VRU, a collision point of 0% and dry road conditions.

Overall, the two derived catalogues consist of more than 90.000 baseline scenarios for the pedestrian and more than 120.000 scenarios for the cyclist.

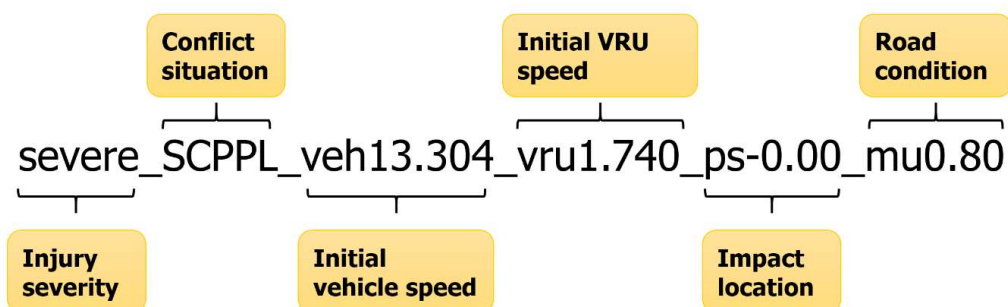


Figure 2-4: Identifier for VIRTUAL VRU testing scenarios.

For each VT scenario, a baseline simulation (no driver reaction or AEB system intervention) is performed as well as a simulation with a virtual AEB system, described in (Schachner, Schneider et al., 2020). The AEB can be calibrated to an individual system by the following system parameters, which are in line

with the suggestions of the Prospective Effectiveness Assessment for Road Safety (PEARS) consortium (Wimmer et al., 2019):

- Maximum sensor range in [m]
- Azimuth sensor opening angle [°]
- Azimuth sensor resolution [°]
- Trigger at which braking is induced – implemented based on Time to Collision (TTC) [s]
- Brake Delay [s]
- Braking Gradient [m/s<sup>3</sup>]

The parameters of the virtual AEB system, were selected as described in (Schachner, Schneider et al., 2020) and should be further validated by means of physical testing in the Euro NCAP scenario.

For each scenario, the following obtained quantities are stored in a CSV file:

- IDs
- Collision speed baseline
- Collision point baseline
- Collision angle baseline
- Collision speed VRU
- Collision speed AEB
- Collision point AEB
- Collision angle AEB

### 2.2.1 Virtual Testing Catalogue for cars

The entire catalogue of VT scenarios for the car - pedestrian and car - cyclist use cases is derived by varying the scenario-parameters described above. For each type of conflict situation, the initial speeds are varied based on the derived PDFs representative of *minor*, *severe* and *fatal* accidents. The speeds are selected based on the derived percentiles for the three different accident severities (5 percentile increments for  $v_{veh}$ , 10 percentile increments for  $v_{VRU}$ ).

The effects of dry or non-dry road conditions are taken into account by road friction values. For dry road conditions  $\mu$  is set to 0.8 and for non-dry conditions to 0.5.

Five different collision points (Figure 2-5) were selected (-40%, -20%, 0%, 20%, 40%) except for the cluster "Car and pedestrian/cyclist in longitudinal traffic", where the collision point was set to 0%. This was done because of collision point determination based on road layouts as described in Schachner, Sinz et al. (2020).

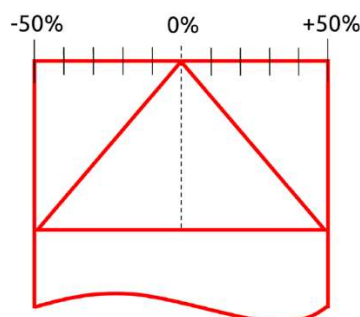


Figure 2-5: Definition of collision point relative to vehicle front.

## 2.2.2 Virtual testing catalogue for trams

The VT catalogue for the tram-pedestrian use case was created based on the analysis of real-world crashes performed in WP4 & WP6, published in Lackner et al. (2022). In comparison to the pre-crash matrix for pedestrian-car and car-cyclist scenarios, the distribution of impact speeds has not been further split into severity levels or conflict situations (Figure 2-7). Furthermore, the friction coefficient (0.8) was selected in accordance with the tram performance to reach a maximum deceleration of 3 m/s<sup>2</sup> as reported in Lindemann et al. (2021) and was not varied for the tram.

The conflict situations Left Turn, Pedestrian from Same Direction (LTSD), Right Turn, Pedestrian from Opposite Direction (RTOD), Right Turn, Pedestrian from Same Direction (RTSD), Straight Crossing Path, Pedestrian from Left (SCPPL), Straight Crossing Path, Pedestrian from Right (SCPPL), Straight, Pedestrian Same Direction (SD) have been considered based on the accident analysis. An example of the pre-crash simulation setup can be seen in Figure 2-6 where the SCPPL Scenario is displayed and used to investigate the VIRTUAL pedestrian-tram testing scenarios. In order to define meaningful trajectories, the initial velocity of the VRU and the vehicle have been considered together with each defined type of conflict situation and varying baseline collision points as described in Section 2.2.

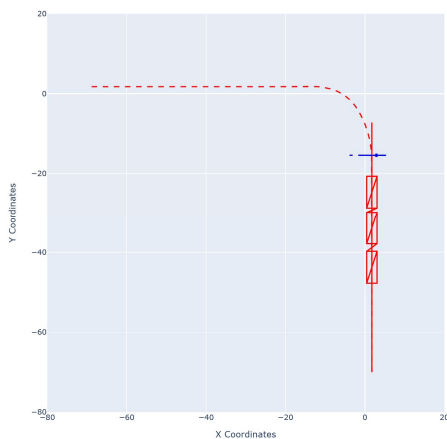


Figure 2-6: SCPPR Scenarios implanted in the pre-crash tool to investigate the VIRTUAL pedestrian to tram testing scenarios.

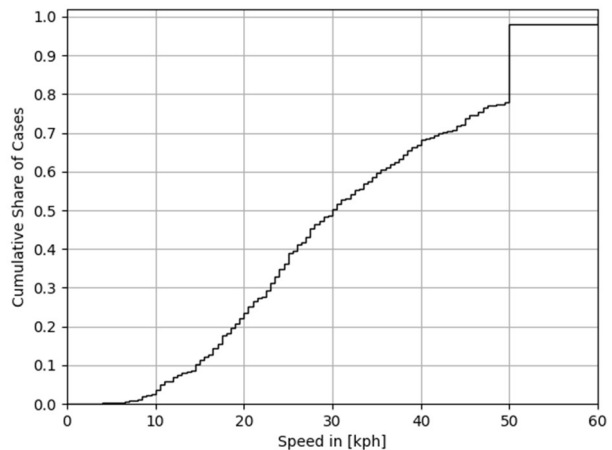


Figure 2-7: Distribution of collision speeds as proposed in (Lackner et al., 2022).

The probability of a scenario  $P(\text{Scenario})$  is the result of the probability of occurrence of the Conflict Situation (CS), (i.e., the probability of the tram and the pedestrian speed). In contrast to the pedestrian/bicycle scenarios, the probability of the tram speeds were directly sampled from the cumulative distribution function (CDF), which were taken from the real-world crash scenarios (Lackner et al., 2022). As tram-specific data was unavailable for pedestrian speeds, the overall distribution for vehicle-pedestrian scenarios has been used, which was reported in Deliverable 4.1. The used values can be found in Appendix C, Table 12-1 and Table 12-2. Therefore, the proposed probability calculation in Equation 1 has been modified in this use case to Equation 2 for the tram assessment.

Equation 2:

$$P(\text{Scenario}) = P(\text{CS}) \cdot P(v_{\text{veh}}) \cdot P(v_{\text{VRU}})$$

The probability for different tram-pedestrian conflict situations have also been retrieved from the field data (Lackner et al., 2022) and can be found in Table 12-3 (Appendix C).

## 2.3 Probability of Collision Scenarios

The AEB system intervenes in many cases of an impending accident, which alters the collision scenario in comparison to the baseline. This section describes the calculation of new collision scenarios, which are determined by the following quantities:

- Collision angle  $A$
- Collision point  $CP$
- Vehicle collision speed  $\hat{v}_{veh}$
- VRU collision speed  $\hat{v}_{VRU}$

In order to calculate the probability of a certain collision scenario, the obtained quantities are clustered. Obtained collision angles are clustered in  $30^\circ$  steps. The collision speed of the pedestrian is clustered in 1 km/h steps to remain high resolution. Due to the extended range of occurring collision speeds, it was decided to cluster the collision speed of the cyclist in 5 km/h steps. The collision point relative to the vehicle front has been clustered in bins of 5%, starting at -50%. All parameters describing a collision scenario and related clusters are shown in Table 2-1.

Table 2-1: Clustered quantities describing the collision scenario.

	Pedestrian		Cyclist	
	Range	Cluster	Range	Cluster
Collision speed vehicle $\hat{v}_{veh}$	0 - 120 [km/h]	5 [km/h]	0-120 [km/h]	5 [km/h]
Collision speed VRU $\hat{v}_{VRU}$	0 - 20 [km/h]	1 [km/h]	0 - 50 [km/h]	5 [km/h]
Collision angle $A$	0 - 360 [°]	30 [°]	0 - 360 [°]	30 [°]
Collision point $CP$	-50 [%] - +50 [%]	5 [%]	-50 [%] - +50 [%]	5 [%]

Equation 3 is suitable for calculating the probability for a specific collision scenario  $P(A \cap CP \cap \hat{v}_{veh} \cap \hat{v}_{VRU})$ , using the probability of a certain VT scenario as described in Chapter 2.1.

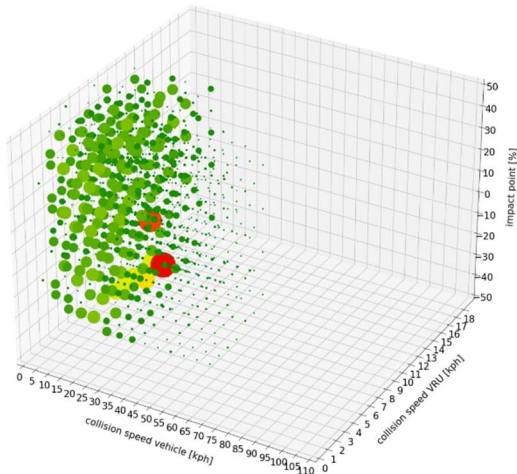
Equation 3:

$$P(A \cap CP \cap v_{veh} \cap v_{VRU}) = \sum_i P(A \cap CP \cap v_{veh} \cap v_{VRU} | Scenario_i) \cdot P(Scenario_i)$$

The huge amount of data requires sophisticated assessment scripts. Jupyter Notebook is a popular framework, which allows fast data processing and visualisation based on Python. The developed script (available on <https://OpenVT.eu/wp-4/VISAFE-VRU>) extracts the simulated results stored in the CSV files and clusters them. Afterwards the probability of each collision scenario is calculated.

The results are visualised in 3D scatter plots where the size of the dots indicates the occurrence probability of a specific collision scenario. Those with the highest probabilities are highlighted in red. An example for  $P(CP \cap v_{veh} \cap v_{VRU} | A = 270^\circ)$  and  $P(CP \cap v_{veh} \cap v_{VRU} | A = 90^\circ)$  is shown in Figure 2-8.

Occurrence probability for pedestrian conflict scenarios at 270 [°] collision angle



Occurrence probability for pedestrian conflict scenarios at 90 [°] collision angle

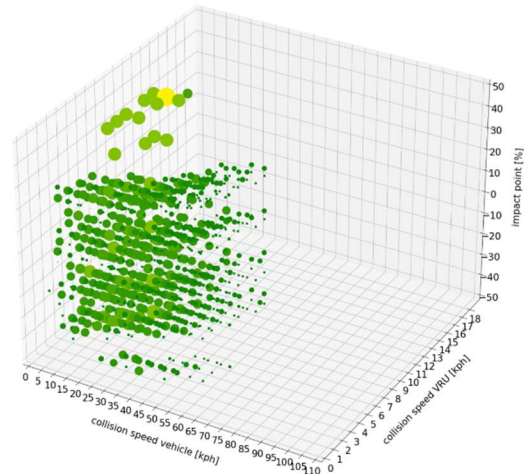


Figure 2-8: 3D scatter plots for 270 [°] and 90 [°] collision angle.

### 2.3.1 In-crash Simulation Matrix

The Design of Experiments (DoE) method is required to select a reasonable number of simulations suitable for the in-crash simulation. A trade-off has been found between the feasibility of running the simulations at the vehicle manufacturers and accuracy of the predicted injury risks for the whole range of scenarios. Based on the feedback of the industry partner, 50 cases were considered as appropriate number of simulations for load cases.

Through our simulation matrix design, we have aimed to address both occurrence probability of the scenarios and good space filling. If only high occurrence probability scenarios would have been selected, the study area would not have been covered sufficiently. Another requirement was that the DoE must be repeatable and reproducible (each user should achieve the same simulation matrix when applying the method). Furthermore, the used algorithms must be available open source as the integrated assessment framework, including the DoE, has to be openly available. Eventually, the DoE and the whole workflow should be easily managed without much effort by users.

With these restrictions in mind, we decided to try the so called MaxPro Criteria. For further information on the MaxPro Criteria see Joseph et al. (2015) and Joseph et al. (2020). This criterion is commonly used in deterministic computer experiments and is currently SotA. The MaxPro criterion should facilitate finding space-filling designs that ensure good projections to subspaces of the factors. One further advantage of the MaxPro criterion is that a certain number of scenarios can be selected by the occurrence probability, and consequently rendering the remaining scenarios - based on the first selection - selected to obtain good space filling.

As a starting point for the DoE, the scenarios which were not avoided by the generic AEB system were weighted according to their occurrence probability. This led to a distribution of collision parameters as shown exemplary in the 3D scatter plots in Figure 2-8.

The 50 simulation cases have been selected such that 60% of the cases (30 cases) are selected by MaxPro from the scenarios, representing the upper 50% quantile based on the occurrence probability of the clustered collision scenario. The other 40% were selected by MaxPro from all scenarios.

## 2.4 In-crash simulations

The in-crash simulations are performed to predict the injury probability for specific body regions, using the VIVA+ pedestrian HBM model (John et al., 2022) in different postures and anthropometries. The boundary conditions, (e.g., collisions speed, collision angle,...), are based on the in-crash simulation matrix described in Section 2.3.1. The results of the in-crash simulations are then processed with the help of the Open Source post-processing tool DYNASAUR and a Jupyter notebook to finally establish an injury probability for different body regions for each in-crash simulation. An overview of the workflow is shown in Figure 2-9. Subsequently, the derived injury probabilities can then be used as input for the CBA tool.

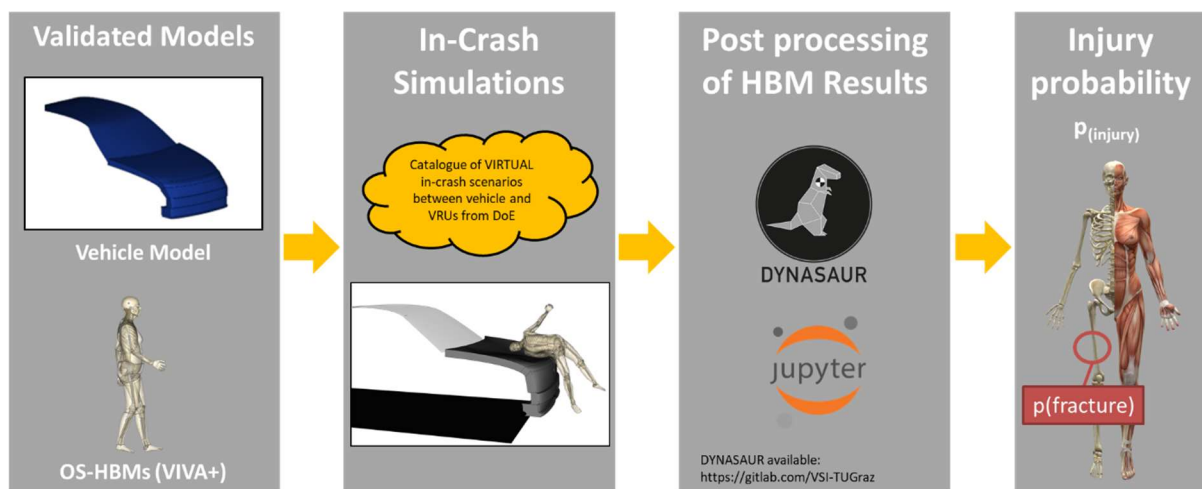


Figure 2-9: Workflow of the in-crash simulations within VIRTUAL.

## 2.5 Injury Prediction

A summary of the applied injury criteria is shown in Table 2-2. For some of the criteria, model-specific injury risk curves have already been developed. Definition files were developed for the post-processing tool DYNASAUR, which include all the listed injury criteria and can be used for the current version of the VIVA+ models. The specific type of injuries were determined from the analysis of real-world injuries (Leo et al., 2021; Leo, Klug, Ohlin, Bos et al., 2019; Leo, Klug, Ohlin, & Linder, 2019) and aligned with validation requirements of the VIVA+ VRU models.

Table 2-2: Injury Prediction for different types of injuries.

Criteria	CBA Tool Name	Based on	Sources
HIC	Other skull–brain injury	Resultant Head CoG accelerations filtered with CFC1000.	Schmitt et al., 2019
DAMAGE MPS	Concussion injuries	DAMAGE Implementation in Dynasaur using head rotation sensors implemented in VIVA+ definition files, filtered with CFC60.	Gabler et al., 2019 Wu et al., 2022 Euro NCAP, 2022
Risk of fractured ribs	Rib fractures	Risk per rib determined based on maximum strain per rib. Combined to overall risk of fractured ribs using probabilistic method.	Larsson et al., 2021 Forman et al., 2012
Proximal Femur Fracture Risk	Fracture of hip	Risk based on MPS99 using risk curves calibrated for VIVA+ model.	Schubert et al., 2021
Femur Shaft Fracture Risk	Fracture of femur shaft	Risk based on MPS99 using risk curves calibrated for VIVA+ model.	Schubert et al., 2021
Tibia Shaft Fracture Risk	Fracture of knee/lower leg	Risk based on MPS99 using risk curves calibrated for VIVA+ model.	Developed in WP2 of VIRTUAL (unpublished)
Knee Ligament Rupture Risk	Dislocation/sprain/strain of knee	Risk based on beam elongation/original length with corresponding risk curve from (Nusia et al., 2021).	Nusia et al., 2021

The injury risk curves for proximal Femur and Femur shaft fractures which was developed within VIRTUAL and published by Schubert et al. (2021) can be seen in Figure 2-10 and Figure 2-11. Furthermore, injury risk curves have been developed for the tibia shaft within VIRTUAL, (manuscript under preparation), which are shown in Figure 2-12.

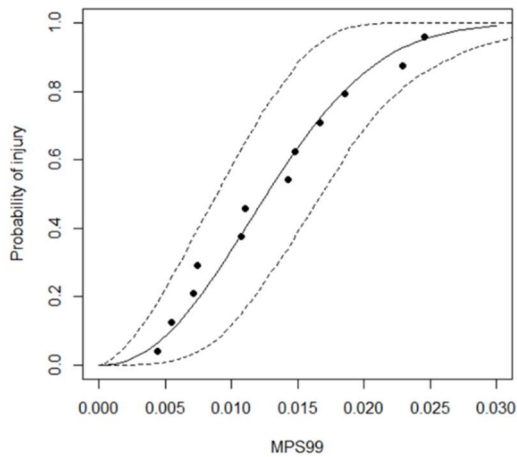


Figure 2-10: Injury Risk curve for proximal femur fractures (Schubert et al., 2021).

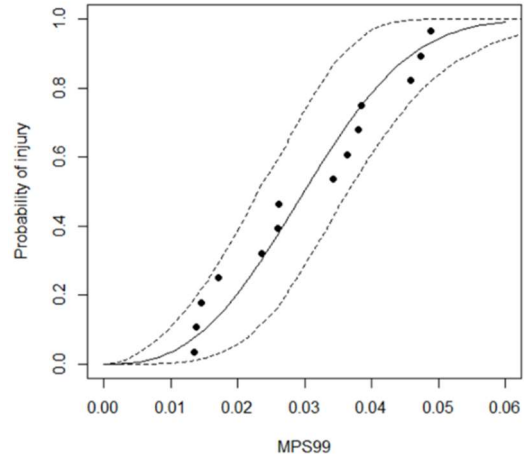


Figure 2-11: Injury Risk curve for femur shaft fractures (Schubert et al., 2021).

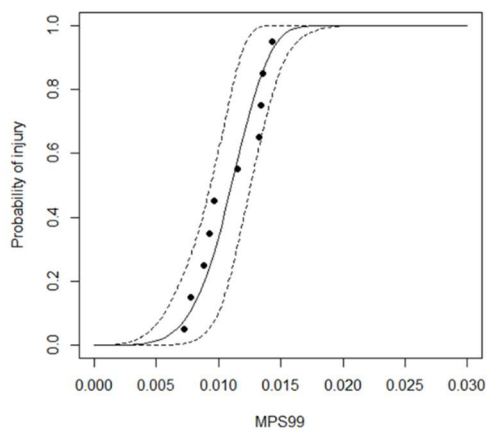


Figure 2-12: Injury Risk curve for tibia shaft fractures.

### 2.5.1 Meta-Modelling

A meta-model is used to also predict the injury probability of the unavoidable cases, which are not part of the in-crash simulation matrix. The development of the meta-model is done with the help of the openly available python library Scikit-learn (Pedregosa et al., 2011). With this library, it is possible to develop different meta-models based on a set of simulation results. The GaussianProcessRegressor (Duvenaud, 2014; K. I. Williams, 2006; Rasmussen, 2004) was used in these particular cases as it shows the best results, and the Matern kernel with its default values was also used. The other parameters of the GaussianProcessRegressor were determined with the help of the GridSearchCV algorithm of the Scikit-learn (Pedregosa et al., 2011) package. This algorithm can find the optimised parameters with the help of cross-validated grid-search over the parameter grid. A summary of the used values can be found in Table 2-3.



Table 2-3: Parameters of the GaussianProcessRegressor for the meta-model created with Scikit-learn (Pedregosa et al., 2011).

Name	Value
kernel	Matern
n_restarts_optimizer	1000
normalize_y	True
random_state	42

Based on the 50 simulations from the in-crash simulations matrix, the results were split into a training dataset (85% of data) and a test dataset (15% of data). Both datasets have been scaled using the StandardScaler provided in Scikit-learn (Pedregosa et al., 2011). Scaling the data is necessary as the provided data should be standard normally distributed, as the accuracy of the meta-model algorithm may otherwise be unsatisfactory. The training dataset was used to develop the meta-model and the test dataset was used to check how good the prediction of the meta-model works based on the training data. The developed meta-model was then applied to predict the injury risk for all non-avoidable collision scenarios resulting from the pre-crash simulations. The injuries which have been predicted can be seen in Table 2-2.

### 2.5.2 Overall Injury Probability

After predicting the injury probability for the individual collision scenarios, the overall injury probability for each injury criterion can be calculated. The overall injury probability is calculated by adding the injury probability of each collision scenario multiplied with its occurrence probability. This single value can then be used in the CBA tool.

### 2.5.3 Transfer to the Cost Benefit Analysis tool

The final output is prepared with a Jupyter notebook such that it can be directly included into the CBA tool (Bützer et al., 2022).

## 2.6 Cost Benefit Analysis Tool

For details of the CBA tool, readers are referred to Deliverable 6.1 of the VIRTUAL project (Bützer et al., 2022).

## 2.7 User Interface

The current user interface can be seen in Figure 2-13, below.

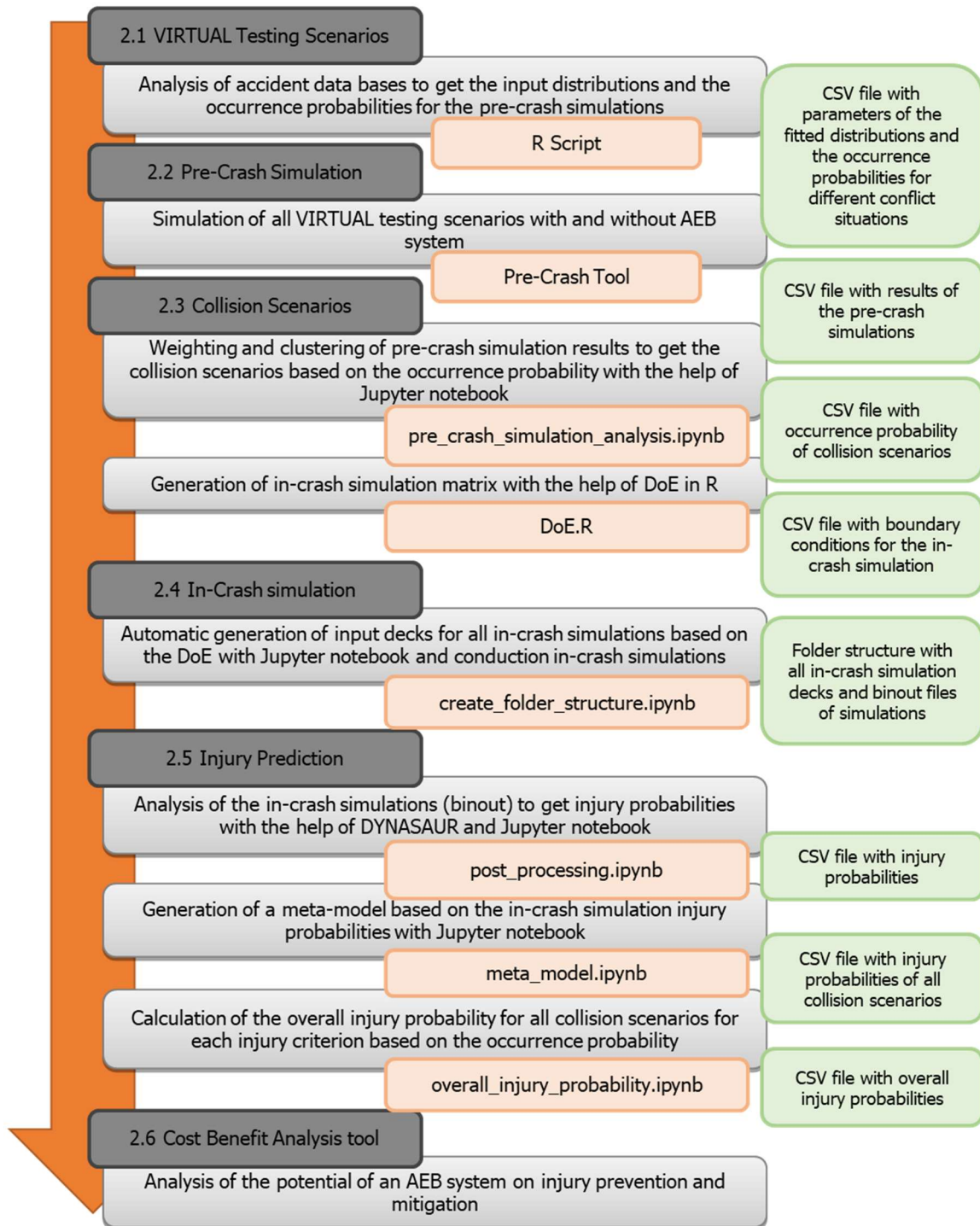


Figure 2-13: Scripts and files prepared as part of the VISAPE-VRU workflow.

# 3 Holistic Assessment for Car-Pedestrian cases

The aim of this use-case was to investigate the effect of a generic AEB system on the overall benefit for pedestrian protection considering a reduction of the crash risk and injury risk. For the in-crash, two different vehicle models were used – a generic Sedan and a SotA SUV model to investigate the vehicle-specific effect on the determined overall benefit.

## 3.1 Method

### 3.1.1 Generic AEB

A conceptual AEB system, modelled on previous studies (Barrow et al., 2018; Gruber et al., 2019; TRL et al., 2018), was applied. A geometric sensor with a range of 60 m and a field of view of 60° was positioned 0.25 m behind the most frontal point of the vehicle (2.2 m ahead of vehicle CoG). The VRU was detected when fully in view for 150 ms while braking was induced when the TTC was  $\leq 1$  s. The geometric sensor was modelled with an Azimuthal resolution of 0.5° and a time resolution of 10 ms. Following the brake delay, the deceleration was increased in line with the braking gradient until the maximum acceleration (depending on road friction) was reached. The Parameter of the AEB system is summarised in Table 3-1.

Table 3-1: Parameters of the conceptual AEB System.

Sensor range [m]	Field of view (sensor angle) [°]	Acquisition time [s]	TTC threshold [s]	Azimuthal resolution [°]	Brake delay [s]	Braking gradient [m/s <sup>2</sup> ]
60	60	0.15	1.0	0.5	0.2	36.0

### 3.1.2 In-Crash Simulations

The Simulation Matrix for the in-crash pedestrian simulations can be found in Appendix A for the pedestrian Baseline and AEB simulations.

#### 3.1.2.1 Generic Sedan Model

The generic Sedan front model has been based on the generic vehicle models which were developed for the Euro NCAP certification of pedestrian models (Klug et al., 2017; Klug et al., 2019). These car models were originally developed for kinematic evaluations, focusing on the time and location of the head impact of pedestrian models.

The generic vehicle (GV) model has been updated in order to improve the interaction between the HBM and the car front, and to make it more realistic for injury assessments. The generic Sedan front model is shown in Figure 3-1. The interface layer between the bonnet leading edge and the bonnet was removed from the original model. The coincident nodes of the neighbouring parts were fused to connect them. The improvement of the impact response was analysed by comparing force-penetration curves gained from impactor simulations on the bonnet leading edge with data from the literature (Feist et al., 2019). Also, the stiffness of the other parts of the GV were re-evaluated, comparing them with data available from the literature regarding different stiffness levels of the current European fleet (Feist et al., 2019). The results of this re-evaluation can be found in Appendix D.

Further, the rigid windscreen was remodelled to represent a deformable glass-PVB composite. The modelling method was adopted from the tram model, modelling two glass layers with shell elements and a connecting PVB layer modelled by solid elements. The response of the new windscreen was analysed by impact simulations and compared to data from the literature (Alvarez & Kleiven, 2016). The results of the windscreen impactor tests can be found in Appendix D.

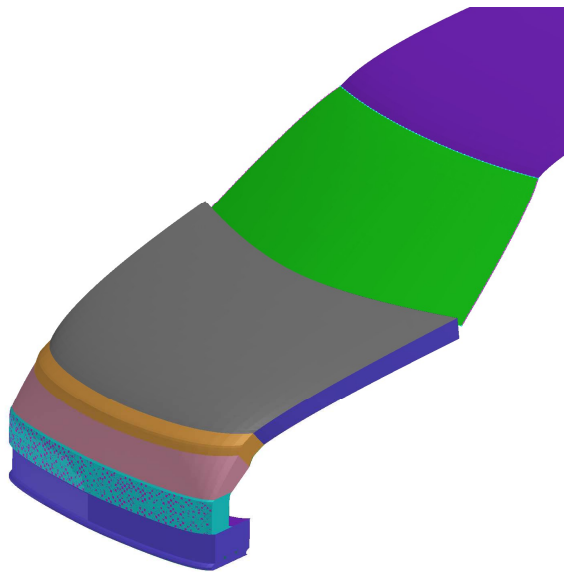


Figure 3-1: Generic Sedan front model enhanced within WP4.

### 3.1.2.2 State of the Art SUV Model

To compare the results of the generic Sedan model with a current serial car, simulations were performed with a complete vehicle model of a SUV currently in production. The base model is a SotA, complete vehicle model specifically used for low speed and pedestrian load cases (legal, rating and development simulations). Good correlation is achieved in the load cases it is primarily used for, pedestrian impactors (head and leg forms) and low speed barriers. The base model includes all internal and external components making up the vehicle. All components, and their supporting structures, which might come into contact with the HBM are modelled in detail with applicable material models. To reduce the required central processing unit (CPU) time for each simulation, the complete vehicle model was reduced to a half model where everything behind the B-pillars and the interior, out of reach for a VRU, was replaced by an equivalent lumped mass with corresponding inertia. Comparing reference runs with the complete vehicle model with the half model, shows no difference in HBM results between the simulations.

For the simulations with the SotA vehicle model, some additional definitions were required in contrast to the generic Sedan model. The collision position is defined as the position of the centre of the HBM, relative an effective vehicle width at first contact between the VRU and the vehicle. The effective vehicle width is defined as the total vehicle width at the front axle minus the hip width of the female HBM (380 mm). The HBM width is subtracted from the actual vehicle width to avoid defining scenarios with little (glancing off) or no HBM-vehicle contact. In this setup the initial vehicle-VRU contact is set to occur with  $VRU_x = 0$  and  $VRU_y$  in accordance with the scenario boundary conditions. The vehicle position  $veh\_X0$  is calculated to create minimal initial contact. The initial displacement parameters  $veh\_dX$ ,

$vru_{dX}$  and  $vru_{dY}$  are then calculated to ensure there are no initial penetrations at the start of the simulation.

### 3.1.2.3 Pedestrian Models

For the in-crash simulations, the VIVA+ 50F and 50M models (John et al., 2022) were positioned in accordance with the Euro NCAP Technical Bulletin TB024 (Euro NCAP, 2019). The positioned models can be seen in Figure 3-2 and Figure 3-3. Version 0.3.2<sup>2</sup> of the VIVA+ (John et al., 2022) models was used in the simulations. In some simulations with the generic Sedan model at high severities, instabilities were observed in the pelvic floor of the HBM, which have been fixed in revision 0.3.2.a<sup>3</sup> of the models and have been rerun with this particular model.

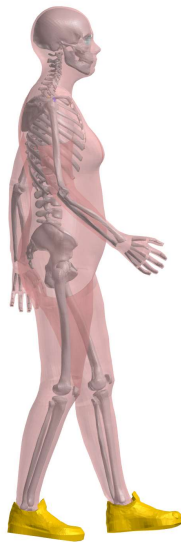


Figure 3-2: Positioned VIVA+ 50F model in accordance with the Euro NCAP Technical Bulletin TB024 (Euro NCAP, 2019).



Figure 3-3: Positioned VIVA+ 50M model in accordance with the Euro NCAP Technical Bulletin TB024 (Euro NCAP, 2019).

The pedestrian model was also fitted with a pair of shoes, in accordance with the Euro NCAP Technical Bulletin TB024 (Euro NCAP, 2019). The material properties of the VIVA+ shoes are based on Cho et al, 2009. The baseline shoe geometry is based on freely available geometry data<sup>4</sup>. Each shoe consists of the following parts: Fabric outer, Fabric inner, Sole inner, Sole mid and Sole outer. This can also be seen in Figure 3-4 and Figure 3-5.

To fit the shoe on the VIVA+ model, the geometry of the VIVA+ foot (50F and 50M) was used to generate the inner fabric. All other parts were then adjusted on this geometry. The specifications for the 50M and 50F shoes are given in Table 3-2.

<sup>2</sup> <https://openvt.eu/fem/viva/vivaplus/-/commit/ce7074e7094ff93f3c7af5bf26da78da76f0e7a0>

<sup>3</sup> <https://openvt.eu/fem/viva/vivaplus/-/commit/07cfc0cb1972689a2cd8590396ee55b5350ee4c4>

<sup>4</sup> <https://free3d.com>

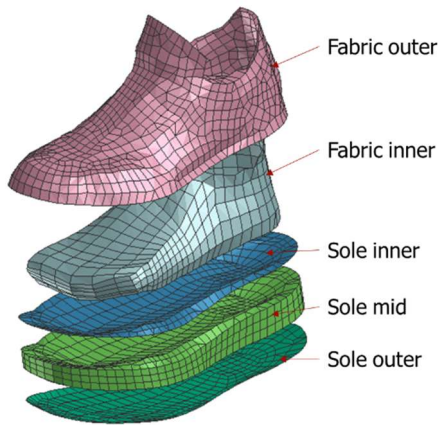


Figure 3-4: Structure of the VIVA+ shoe model.

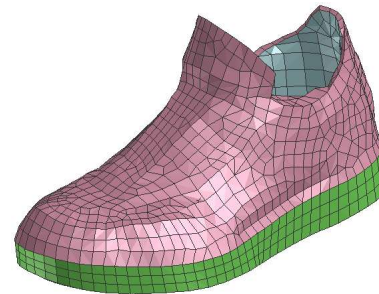


Figure 3-5: VIVA+ shoe model.

Table 3-2: Specification of VIVA+ shoes example shown for LS-Dyna.

	50M	50F
Sole thickness (at the heels)	26.5 mm	26.5 mm
Weight of one shoe	694 g	532 g
Fabric outer	Section: Shell 1mm; Material: *MAT_ELASTIC (LS-Dyna)	
Fabric inner	Section: Shell 1mm; Material: *MAT_ELASTIC (LS-Dyna)	
Sole inner	Section: Shell 1mm; Material: *MAT_ELASTIC (LS-Dyna)	
Sole mid	Section: Solid; Material: *MAT_ELASTIC (LS-Dyna)	
Sole outer	Section: Shell 1mm; Material: *MAT_ELASTIC (LS-Dyna)	
Contact Fabric outer to Fabric inner	*CONTACT_AUTOMATIC_SINGLE_SURFACE (LS-Dyna)	
Contact right shoe to left shoe	*CONTACT_AUTOMATIC_SINGLE_SURFACE (LS-Dyna)	
Contact Foot to Shoe	*CONTACT_AUTOMATIC_SURFACE_TO_SURFACE (LS-Dyna)	

## 3.2 Results

### 3.2.1 Generic AEB simulations

In total, 61,914 VT scenarios have been derived for car-pedestrian cases. With the help of the implemented AEB system, 24,081 of those cases can be avoided. Although 37,833 cases were unavoidable by the AEB system, considering the occurrence probability of the VT scenarios, a total crash risk reduction of 81.70% was achieved. The results of the pre-crash simulations can be seen in Figure 3-6 where the grey bars represent the baseline occurrence probabilities, and the yellow bars represent the probabilities based on the simulations with the AEB system. A clear trend towards lower collision speeds can be seen by implementing an AEB system.

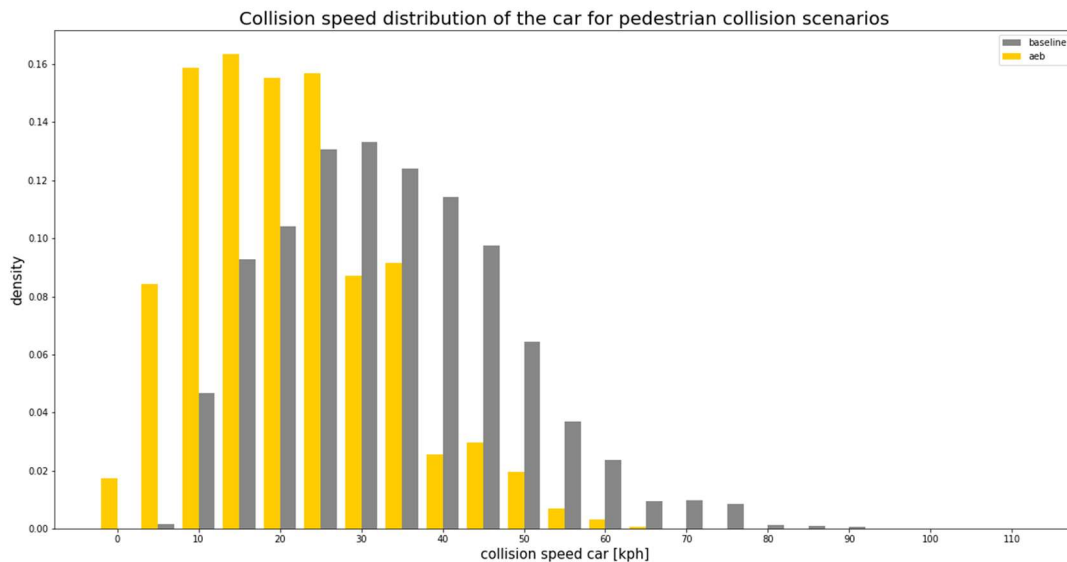


Figure 3-6: Results of the pre-crash simulations for car-pedestrian cases.

## 3.2.2 Generic Sedan in-crash simulations

### 3.2.2.1 Holistic Assessment Simulations

For GV in-crash simulations, baseline as well as AEB cases have been analysed. For both cases, 50 in-crash simulations have been conducted for males and females resulting in a total of 200 simulations. These simulations have then been used to train the meta-model which was used to predict the injuries of the excluded cases. The performance of the meta-model for the different injury criteria can be seen in Table 14-1 and Table 14-2 of Appendix E. It can also be seen that the prediction of the meta-model is performing better for some of the injury criteria than others. This is why the results should be discussed more in the terms of trends than in absolute injury values. In Figure 14-1 of the Appendix E, the results of the overall injury analysis can be seen, based on the injury prediction from the meta-model, combined with the occurrence probability of each collision scenario.

The values presented in Figure 14-1 are also presented graphically in Table 3-3. By having a look at the injury risk for Abbreviated Injury Scale (AIS)4+ concussion injuries it can be seen, that by implementing the generic AEB system, it was predicted that the injury risk would be reduced by approximately 20% for males as well as for females. Also, for the other concussion injury levels a reduction was observed. For skull injuries, a similar trend was observed, resulting in a lower injury risk due to the AEB system. For AIS3+Rib injuries (3+ Ribs broken) the injury risk was also reduced. It was observed that females showed a lower AIS3+ rib injury risk than males for the baseline as well as for the AEB simulations. In contrast, for the right hip injury risk, females showed a higher fracture risk than males. The risk was reduced by the AEB system for both genders. For femur shaft fractures, a comparable injury risk was observed for males and females, for baseline and AEB simulations. The injury risk was also lowered by the AEB system for this type of injury. Only a very low injury risk was observed for tibia shaft fractures in both sexes, which was reduced even further by the AEB System. The risk for ligament rupture is very high for the baseline as well as AEB simulations, although it was reduced by implementing this active safety system, which was observed for males as well as for females.

Table 3-3: Results of the overall injury assessment for pedestrian to generic Sedan scenarios based on the predicted injuries by the meta-model and the occurrence probability.







### 3.2.2.2 Cost Benefit Analysis

In Figure 3-7 the final results of the CBA for generic Sedan-pedestrian cases can be seen. Due to the lack of available data, the manufacturing costs have only been roughly estimated. The crash risk before intervention is based on data analyses which have been presented in Deliverable 6.1 of the VIRTUAL project (Bützer et al., 2022). Implementing the AEB system for pedestrians, achieved an avoidance rate of 81.70% (see Section 3.2.1). This avoidance rate is also affecting the crash risk resulting in a lower crash risk after intervention. The average age was set to 50 years for males and females, as this age was found to be the average in the CARE database (Klug et al., 2020; Linder et al., 2020). The proportion between males and females was also analysed based on the CARE database. With all this information and the injury risks calculated in Section 3.2.2.1, a total benefit of €1,549 to €2,436 can be achieved by implementing an AEB system, indicating that system costs in that range would lead to an overall positive Net present value. If costs for the AEB system between €2,000-€3,000 are assumed, this would only be true for the prediction of the "upper" benefits. However, one has to consider that one AEB system can avoid or mitigate several types of crashes and not only pedestrian crashes.


COST-BENEFIT TOOL FOR VEHICLE SAFETY						
						
<i>Measure: AEB pedestrians</i>						
Input				Results		
	<i>lower</i>	<i>best estimate</i>	<i>upper</i>	<i>lower</i>	<i>best estimate</i>	<i>upper</i>
<b>Costs per vehicle</b>						
- Development costs						
- Manufacturing costs	€ 2,000	€ 2,500	€ 3,000			
- Repair/replacement costs after a crash						
<b>Crash risk (number of target crashes per vehicle per year)</b>						
- before intervention	0.0003959	0.0003993	0.0004027			
- after intervention	0.0000740	0.0000747	0.0000753			
<b>Road user characteristics</b>						
- Number of target road users per vehicle		1				
- Average age casualties: - male		50				
- female		50				
- Life expectancy: - male		78				
- female		83				
- Proportion male target road user		52%				
<b>Vehicle life time (years)</b>		15				
<b>Discount rate</b>		3.0%				
<b>Total costs</b>				€ 2,000	€ 2,500	€ 3,000
<b>Number of injuries prevented</b>						
- Yearly				0.0015	0.0016	0.0018
- Total vehicle lifetime				0.022	0.024	0.027
- 1 injury prevented per ... vehicles				46	42	37
<b>Quality of life improvement (QALYs)</b>						
- Yearly				0.0014	0.0017	0.0022
- Total vehicle lifetime				0.021	0.026	0.032
- 1 QALY gained per ... vehicle				48	38	31
<b>Benefits</b>						
- Quality of life gains				€ 1,162	€ 1,457	€ 1,806
- Medical costs reduction				€ 111	€ 136	€ 165
- Productivity gains				€ 276	€ 362	€ 465
- Total benefits				€ 1,549	€ 1,955	€ 2,436
<b>Socio-economic return</b>						
- Net present value				-€ 1,451	-€ 545	€ 436
- Benefit-cost ratio				0.5	0.8	1.2

Figure 3-7: Cost-Benefit Analysis for pedestrian to generic Sedan cases.

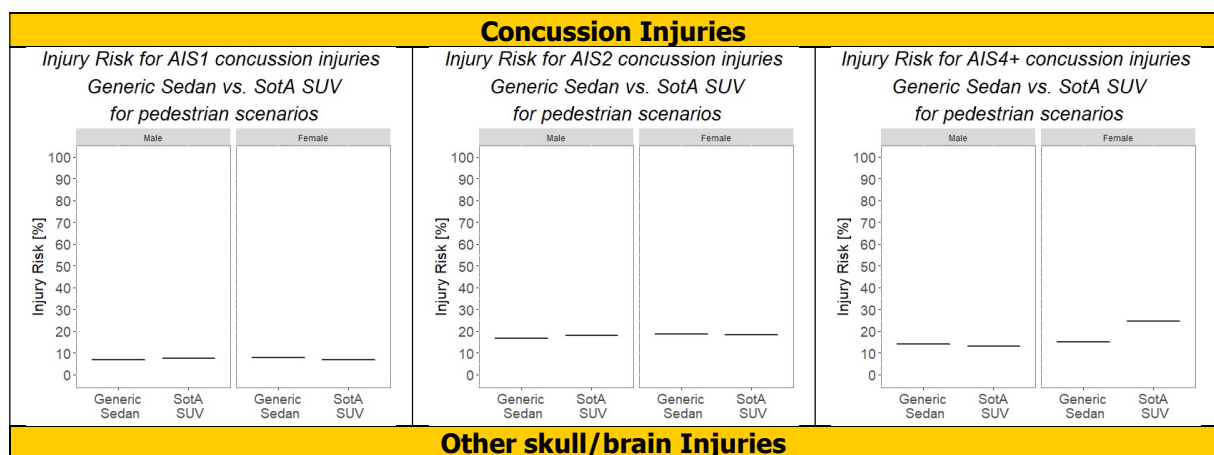
### 3.2.3 State of the Art SUV Model

Simulations with a SotA SUV model were performed to compare the injury risks of the generic Sedan front to a modern SUV model. This was done to study the effect of a more detailed vehicle model and another car shape on the injury risks per body region and the overall benefit.

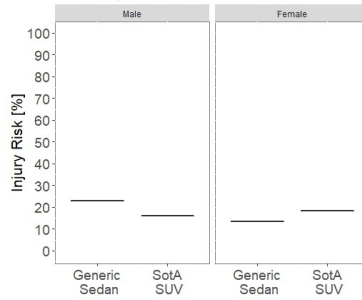
Therefore, in this section the results of the generic and the SotA SUV are presented, for both the AEB scenarios. As baseline, the injury risks derived with the generic Sedan were used for both use cases. The results of these analyses are presented numerically in Figure 14-2 of the Appendix E and also graphically in Table 3-4.

For light concussion injuries (AIS1 and AIS2), the generic Sedan and the SotA SUV showed similar responses, for both males and females. For more severe concussion injuries (AIS4+) the SotA SUV showed a higher risk for female scenarios than the generic Sedan. For males, a similar injury risk was observed for AIS4+ concussion injuries. The generic Sedan showed a higher risk with regard to skull fractures for male scenarios, while compared to the SotA SUV, the risk for female scenarios was lower. For light rib fractures (only 1 rib broken), a similar injury risk was observed with a slightly higher risk for the SotA SUV. Furthermore, the risk appears to be equivalent for both car models with regard to the risk of two broken ribs for males. Females, on the other hand, showed a higher risk of injury for the SUV model. For more severe rib injuries (3+ ribs broken), the generic Sedan showed a slightly higher risk for males while the SotA SUV showed a 20% higher risk of females. For hip fractures, a comparable risk was observed for males between the two cars. The generic Sedan shows a higher risk of hip fractures for the AEB scenarios for females. For femur shaft fractures, the generic Sedan showed a higher risk for the left side for both sexes and a similar risk for the right side. The risk for tibia fracture was found to be generally very low, with slightly higher risks for the SotA SUV. The high ligament rupture risk was slightly lower for the SotA scenarios, than for the generic Sedan.

Table 3-4: Results of the overall injury assessment for AEB pedestrian generic Sedan and SotA SUV scenarios based on the predicted injuries by the meta-model and the occurrence probability.

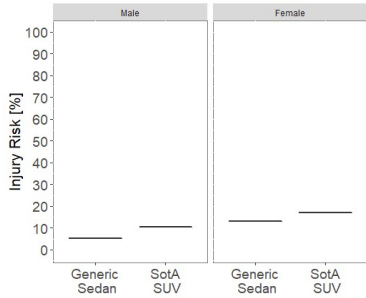


*Injury Risk for other skull/brain injuries  
Generic Sedan vs. SotA SUV  
for pedestrian scenarios*

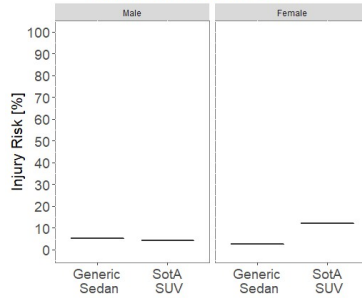


**Rib Injuries**

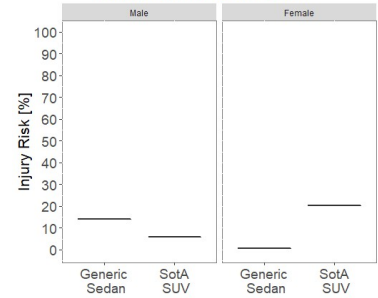
*Injury Risk for 1 broken rib  
Generic Sedan vs. SotA SUV  
for pedestrian scenarios*



*Injury Risk for 2 broken ribs  
Generic Sedan vs. SotA SUV  
for pedestrian scenarios*

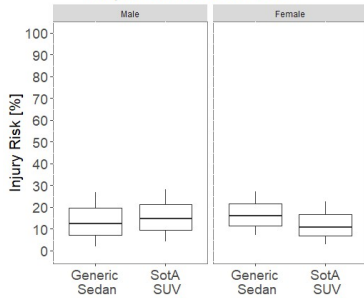


*Injury Risk for 3+ broken ribs  
Generic Sedan vs. SotA SUV  
for pedestrian scenarios*

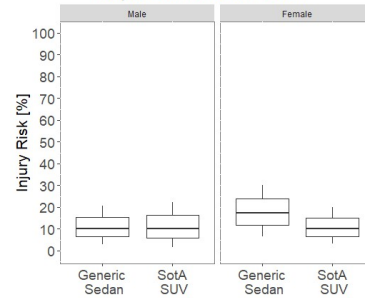


**Hip Injuries**

*Injury Risk for left hip fracture  
Generic Sedan vs. SotA SUV  
for pedestrian scenarios*

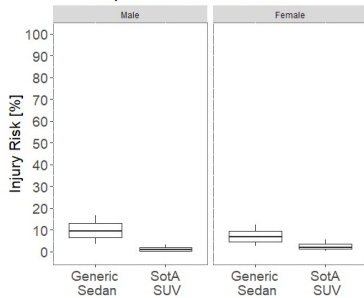


*Injury Risk for right hip fracture  
Generic Sedan vs. SotA SUV  
for pedestrian scenarios*

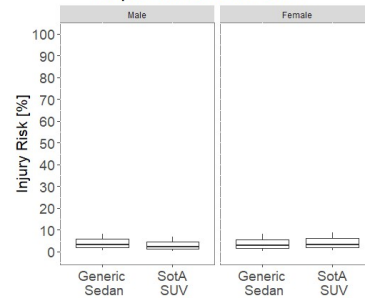


**Femur Injuries**

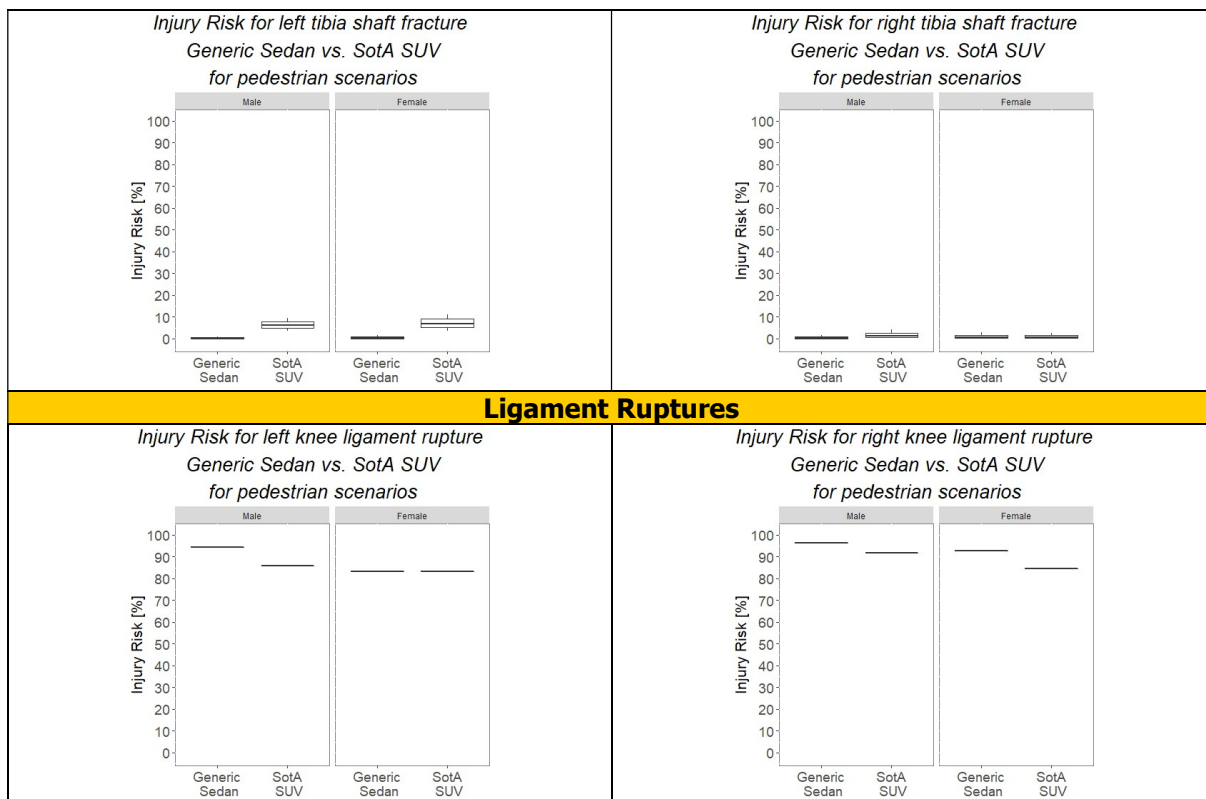
*Injury Risk for left femur shaft fracture  
Generic Sedan vs. SotA SUV  
for pedestrian scenarios*



*Injury Risk for right femur shaft fracture  
Generic Sedan vs. SotA SUV  
for pedestrian scenarios*



**Tibia Injuries**



### 3.3 Discussion

In general, the predicted results seem plausible. However, especially for knee ligament ruptures higher injury risks compared to field data were observed. This effect might have been caused by simplification of the procedure (only one anthropometry, age and posture assumed) and the accuracy of the injury risk curves (often calibrated to data of historical samples, and the knee ligament rupture and rib risk curves not having been specifically calibrated for the VIVA+ model, but based on material test).

The GV use case shows that additionally to the avoided crashes, also the injury risk was lowered in the remaining crashes due to the changed impact configurations. The CBA indicates that extra costs of < €1,500 for an AEB system would ensure a positive net value. It must be considered that not all injury groups have been considered in our analysis, (e.g., upper extremities, neck injuries), hence it can be assumed that the benefit is under-predicted. Moreover, although the same AEB system can be used to address different crash types, our analysis only considered pedestrian crashes.

In the SotA use case, the injury risks caused by the SotA SUV model were comparable to the generic Sedan model. Due to the difference in vehicle shape and more realistic (heterogeneous) vehicle structure, slight differences in the overall injury risks have been identified for some body regions, (e.g., AIS4+ concussion injuries and hip injuries).

If we use the result of the generic Sedan simulations without AEB as baseline for both use cases, the final numbers calculated by the CBA were very similar for the overall benefit for both sets of AEB simulations. For both, one injury per ~42 vehicles can potentially be avoided by the generic AEB system, as seen in Figure 14-3 of Appendix E. It is expected that when using the SotA SUV for baseline simulations, overall numbers would be very similar.

The simulations with the SotA car have also been performed to check feasibility of training the meta-model for the simulation results. The vehicle model is more complex, and therefore it was expected that the scatter in the simulation results for smaller changes would also be greater in these simulations, compared to the generic Sedan model. As shown in Figure 3-8 when using the same number of samples, the errors of the meta-models trained to the SotA SUV were similar to the generic Sedan model for most of the body regions, but remarkably higher for the knee ligament strains

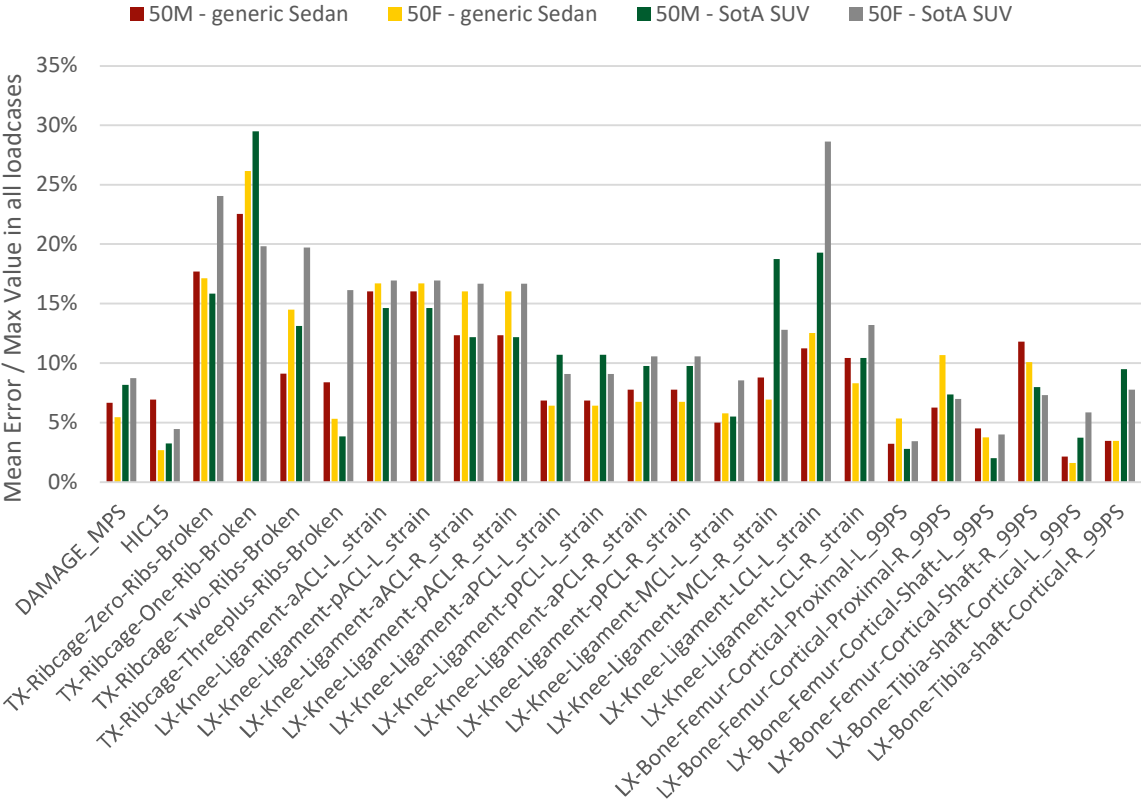


Figure 3-8: Relative mean error for all pedestrian load cases (relative to the max values over all four use cases) comparing 50F, 50M and both vehicle models.

Since there are major differences in some body regions, these meta-models should be improved further in the future.

Different trends were seen in the simulations with the average female and average male models in the two vehicle models, which might mainly be related to the different shapes: Higher risks for AIS4+ concussion and more than three rib fractures were observed for the average female compared to the male for the SotA SUV. For the generic Sedan model, higher risks of skull fracture, more than three rib fractures and knee ligament ruptures were observed for the male compared to the female, and a higher risk for hip fractures was observed for the female compared to the male.

### 3.3.1 Robustness of In-Crash Simulation Results

To investigate the robustness of the in-crash simulation results produced by our simulation models and setups, round-robin simulations have been performed by different partners on their systems. The simulations shown in Table 3-5, with exactly the same two setups, have been performed by the partners.

Table 3-5: Simulation Matrix for Round-robin Simulations.

Simulation Number	Vehicle Velocity [km/h]	VRU Velocity [km/h]	Collision Angle [°]	Collision Location [%]	Anthropometry	GV Model
01	40	0	90	0	50F	Sedan
02	40	0	90	0	50M	Sedan

Table 3-6: System properties used in the simulations performed by the different partners.

	TU Graz	Siemens	University of Ljubljana	VOLVO
FE Solver	LS-Dyna	LS-Dyna	LS-Dyna	LS-Dyna
Solver Version	R12.0	R12.1	R12.1	R12.0
Operating System	Linux	Linux	Windows	Linux
Platform	MPP	MPP	MPP	MPP
Precision	single	single	single	single
Number of Nodes	1	1	1	18
CPUs per Node	32	16	40	28
Total CPU Number	32	16	40	504
MPI Version	Open-MPI 4.0.0 Xeon64	08.02.00.00 [10060] Linux x86-64		Platform-MPI 8.1.1

The results of the round-robin simulations for Load Case 1 are shown in Table 3-7. The rotational velocities of the head resulting in DAMAGE values were consistent over the four different simulations of the same setup on different systems. HIC values varied up to 10%. For the ribs, in case of more than three rib fractures, values varied between 18 and 25%. It must be considered that the risk curves in this area are very steep and consequently small variations in strain can produce such differences in risk, which seems to be generally still acceptable. For the non-struck side proximal femur, a variation from 10-16% was observed, occurring towards the end of the simulation runtime (300 ms), when the pedestrian was not in contact with the car anymore and rotating around the vehicle. Struck-side fractures of the proximal femur, femur shaft fracture and tibia fracture risk were very consistent between the different simulations. The kinematics until the head impact for Load Case 1 can be seen in Table 3-10.

Table 3-7: Results of the round-robin simulations of Load Case 1 with the VIVA+ 50F pedestrian and the generic Sedan (struck side in bold).

		<b>50F</b>				
		<b>Graz</b>	<b>Siemens</b>	<b>UL</b>	<b>VOLVO</b>	
Head	DAMAGE	MPS	0.62	0.61	0.63	0.61
		AIS1	4.82%	5.60%	3.80%	5.91%
		AIS2	44.85%	46.92%	41.53%	47.67%
		AIS4+	50.04%	47.08%	54.50%	45.97%
	HIC	871.79	860.65	827.35	834.90	
Rib	50YO	1	33.31%	35.24%	35.02%	30.77%
		2	35.87%	33.47%	34.43%	34.24%
		3+	20.09%	17.65%	17.87%	24.46%
Femur	Proximal	Left	9.97%	15.63%	15.77%	12.32%
		<b>Right</b>	<b>98.55%</b>	<b>99.01%</b>	<b>98.35%</b>	<b>98.59%</b>
	Shaft	Left	3.17%	3.18%	3.09%	3.72%
		<b>Right</b>	<b>68.75%</b>	<b>69.08%</b>	<b>69.60%</b>	<b>69.59%</b>
Tibia	Shaft	Left	0.88%	0.92%	0.83%	0.89%
		<b>Right</b>	<b>5.16%</b>	<b>5.27%</b>	<b>5.30%</b>	<b>5.07%</b>

For the 50M (Table 3-8), DAMAGE values were much higher causing an AIS4+ risk of more than 96%. This high head injury risk is constantly predicted on all systems, although the precise DAMAGE values vary up to 20%. HIC values varied between 1,440 and 1,606, being all rather high and affected by the failure behaviour of the windshield glass.

For rib fractures, a high scatter was observed for the 50M. While the simulations performed at the VOLVO system indicate a 1.5% risk of two rib fractures, simulations performed on the TU Graz system indicated 61%. This significant variation should be further investigated, although it has been deemed related to the numerical scatter in the glass failure.

An unrealistically high proximal femur fracture risk was observed on the non-struck side. To avoid including such results in the holistic assessments, post-processing procedures have been adjusted to only consider values up to the end of the contact between VRU and vehicle (values are only considered until there is no contact between the thorax and the vehicle anymore). Struck-side proximal femur, femur and tibia shaft fracture risks have been consistent throughout the simulations performed on the different systems. The kinematics until the head impact for Load Case 2 can be seen in Table 3-11.



Table 3-8: Results of the round-robin simulations of Load Case 2 with the VIVA+ 50M pedestrian and the generic Sedan (struck side in bold).

		<b>50M</b>				
		<b>TU Graz</b>	<b>Siemens</b>	<b>UL</b>	<b>VOLVO</b>	
Head	DAMAGE	MPS	0.8	1	0.96	0.87
		AIS1	0.04%	0%	0%	0%
		AIS2	4.47%	0%	0.01%	0.58%
		AIS4+	95.49%	100%	99.99%	99.42%
	HIC	1606.51	1833.72	1549.36	1439.62	
Rib	50YO	1	27.33%	49.07%	67.87%	27.01%
		2	61.34%	43.27%	16.50%	1.50%
		3+	8.21%	6.32%	0.45%	0.02%
Femur	Proximal	Left	57.64%	64.35%	56.57%	23.98%
		<b>Right</b>	<b>5.97%</b>	<b>5.74%</b>	<b>5.95%</b>	<b>5.74%</b>
	Shaft	Left	0.87%	0.89%	0.84%	0.84%
		<b>Right</b>	<b>64.95%</b>	<b>64.18%</b>	<b>64.07%</b>	<b>65.20%</b>
Tibia	Shaft	Left	0.32%	0.34%	0.35%	0.34%
		<b>Right</b>	<b>0.88%</b>	<b>0.90%</b>	<b>0.91%</b>	<b>0.84%</b>

The results for the ribs are shown in detail in Table 3-9, where it becomes clear that the variation in rib fracture risk for the 50M is mainly driven by the 1<sup>st</sup> and 12<sup>th</sup> rib. This should be further investigated in future and monitored in further simulations.

Table 3-9: Variation in maximum principal strains of the single ribs for 50M and 50F simulations performed on the four different systems.

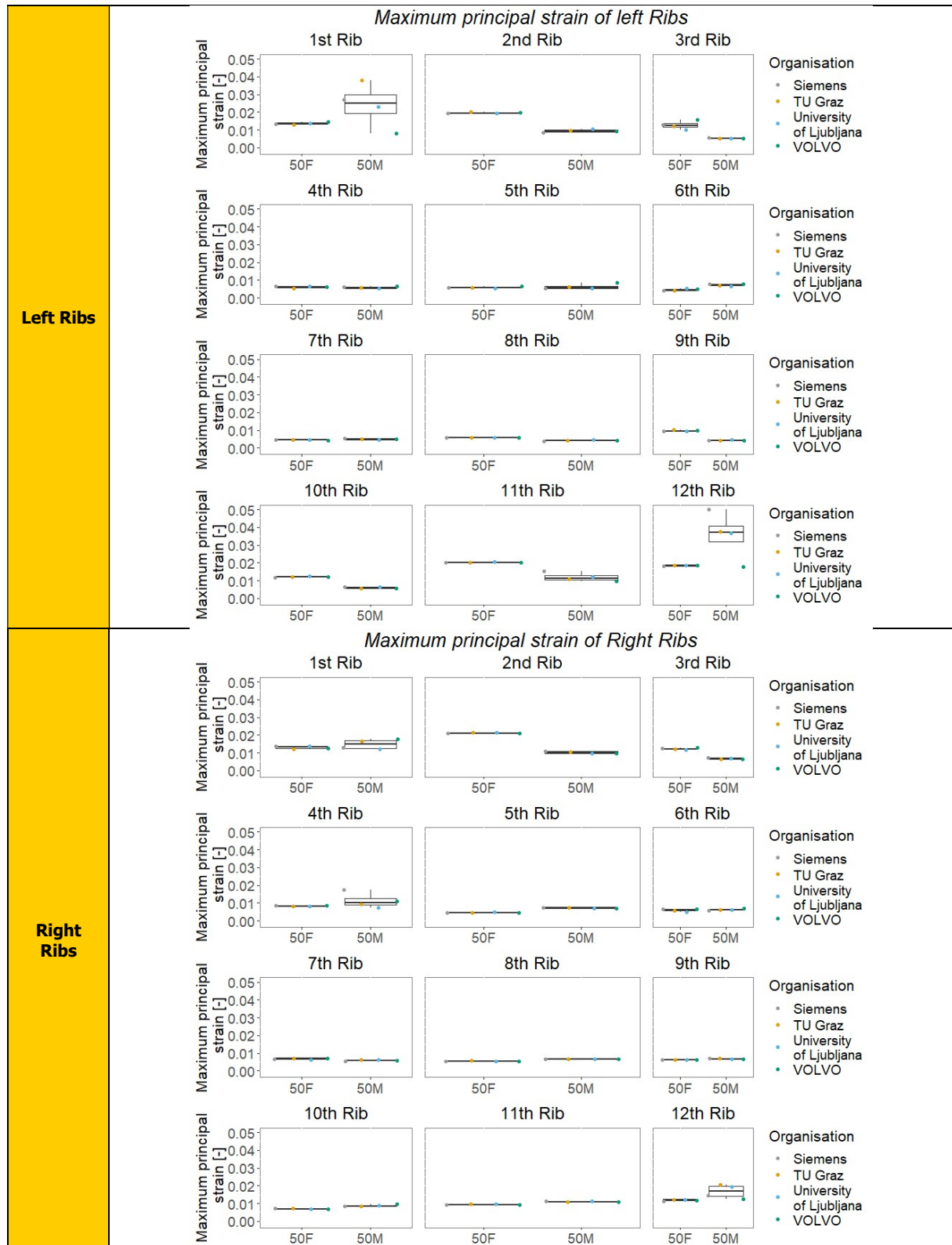


Table 3-10 Kinematics of the VIVA+ 50F model in the generic Sedan crash until head impact.

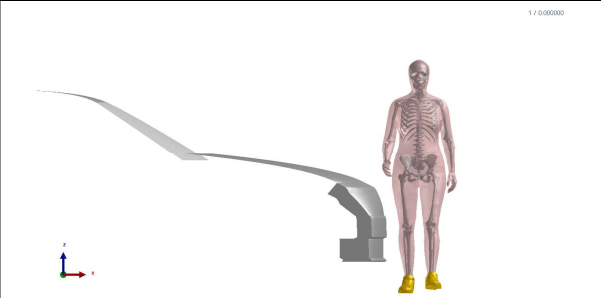
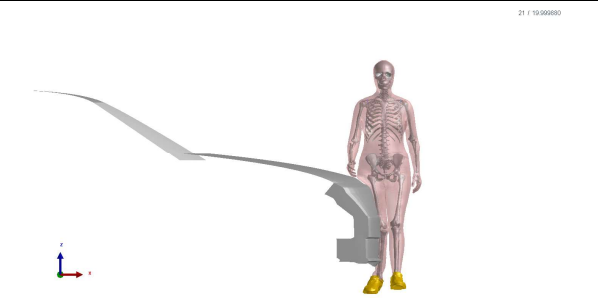
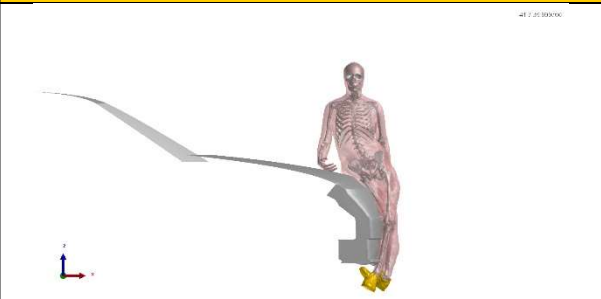
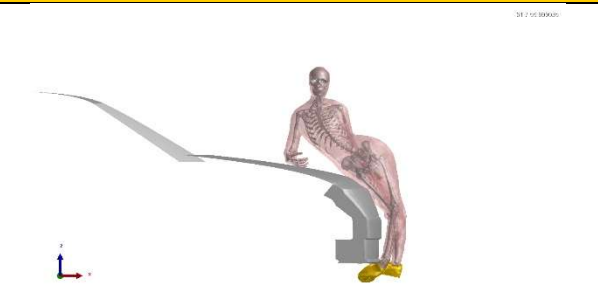

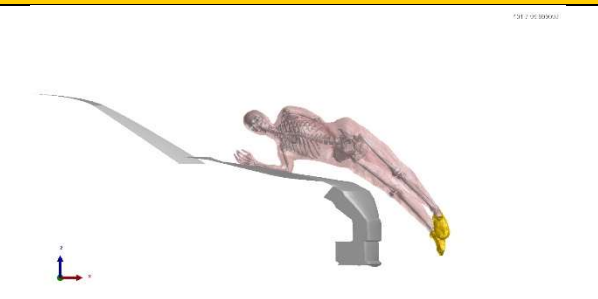
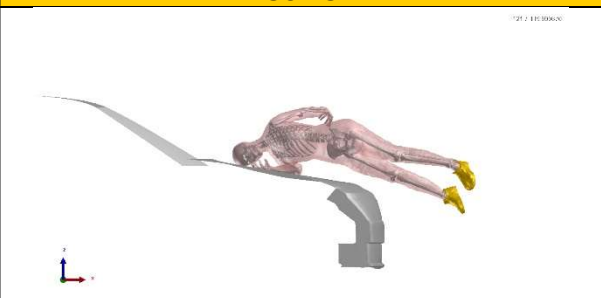
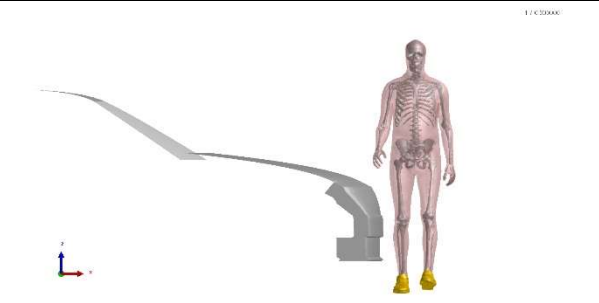
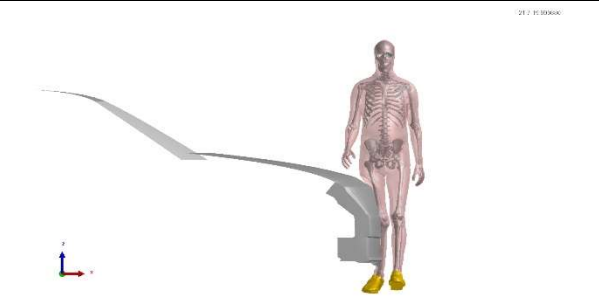
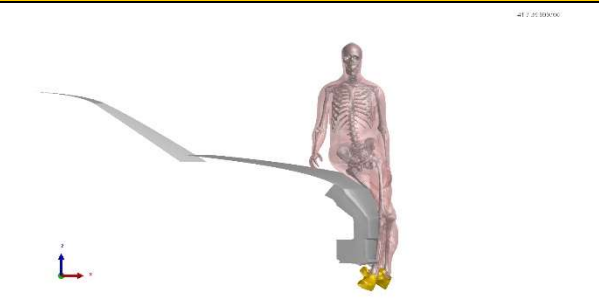
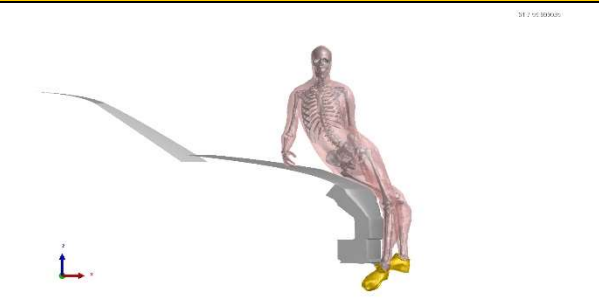
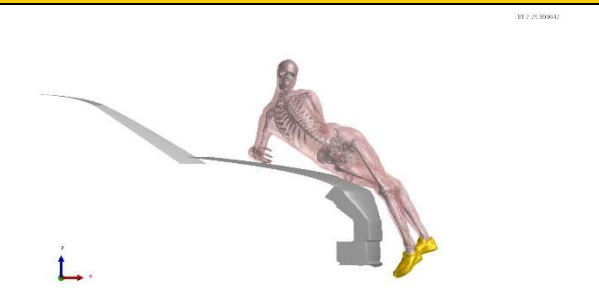
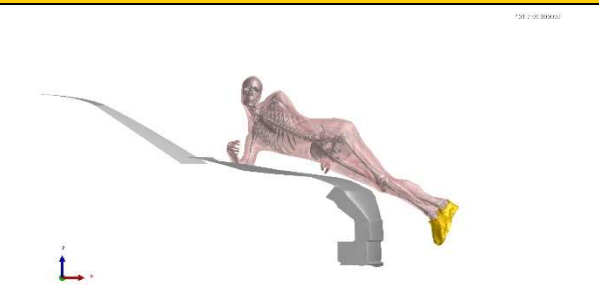

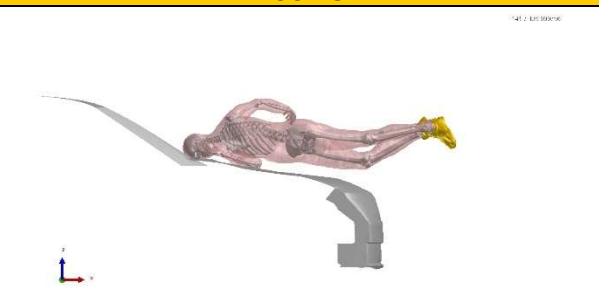
50F	
 <p>1 / 0.00000</p>	 <p>21 / 10.00000</p>
0ms	20ms
 <p>41 / 20.00000</p>	 <p>61 / 30.00000</p>
40ms	60ms
 <p>81 / 20.00000</p>	 <p>101 / 20.00000</p>
80ms	100ms
 <p>121 / 10.00000</p>	
120ms	

Table 3-11: Kinematics of the VIVA+ 50M model in the generic Sedan crash until head impact.

50M	
 <p>0ms</p>	 <p>20ms</p>
 <p>40ms</p>	 <p>60ms</p>
 <p>80ms</p>	 <p>100ms</p>
 <p>120ms</p>	 <p>140ms</p>

# 4 Holistic Assessment of Car-Cyclist cases

The aim of this use-case was to investigate the effect of a generic AEB system on the overall benefit for cyclist protection considering a reduction of the crash and injury risk. For the in-crash, two different vehicle models were used – a generic Sedan and a SotA SUV model - to investigate the vehicle-specific effect on the determined overall benefit.

## 4.1 Method

### 4.1.1 Generic AEB

The same AEB model was used as for the pedestrian simulations, which are described in Section 3.1.1.

### 4.1.2 In-Crash Simulations:

The Simulation Matrix for the in-Crash cyclist simulations can be found in Appendix B for the cyclist baseline and the AEB simulations, where the method described in Section 2.3.1 was applied.

### 4.1.3 Car Models

The same car models as for the pedestrian simulations were used, which are described in Section 3.1.2.1 and 3.1.2.2.

### 4.1.4 Cyclist Model

The VIVA+ pedestrian model (John et al., 2022) was positioned according the values given in Table 4-1 for the 50<sup>th</sup> percentile female and 50<sup>th</sup> percentile male models. A seated decline angle of 68° was selected for the 50F and 70° for the 50M, based on Otte and Facius (2017). The other angles were selected to achieve a realistic driving posture of the target bicycle with the left leg down. To achieve the seated decline, the 50<sup>th</sup> percentile female was rotated 22° forward around the y-axis and the 50<sup>th</sup> percentile male was rotated 20° forward around the y-axis.

A stick figure displaying all the values is given in Figure 4-1. The positioned VIVA+ 50F model can be seen in Figure 4-2 and the positioned VIVA+ 50M in Figure 4-3.

Version 0.3.2.<sup>5</sup> of the VIVA+ (John et al., 2022) models was used in the simulations. In certain simulations performed with the generic Sedan model at high severities, instabilities in the pelvic floor of the HBM were observed. Any such instabilities have been fixed in revision 0.3.2.a<sup>6</sup> of the models and were rerun with these models (50M and 50F).

The same properties were applied for the shoes in these simulations as for the pedestrian described in Section 3.1.2.3.

---

<sup>5</sup> <https://openvt.eu/fem/viva/vivaplus/-/commit/ce7074e7094ff93f3c7af5bf26da78da76f0e7a0>

<sup>6</sup> <https://openvt.eu/fem/viva/vivaplus/-/commit/07cfc0cb1972689a2cd8590396ee55b5350ee4c4>

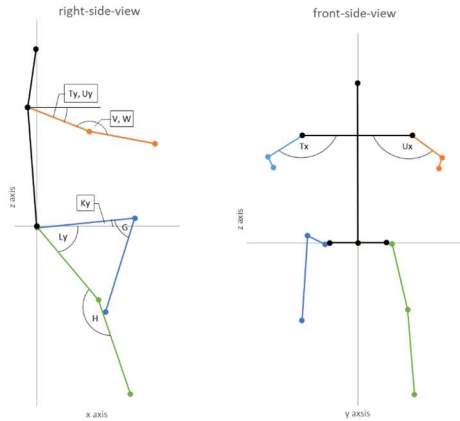


Figure 4-1: Reference Posture of 50F and 50M cyclists with left foot down.

Table 4-1: Reference Postures of 50F and 50M cyclists.

Abbrev.	Measure	50F L-Down	50M L-Down
Px	Heel to heel distance longitudinal	99.627 mm	120.20 mm
Py	Heel to heel distance lateral	301.737 mm	299.60 mm
Pz	Heel to heel distance vertical	319.531 mm	321.5 mm
Ky	Right Upper Leg Angle (around Y w.r.t. horizontal)	4.93°	6.03°
Ly	Left Upper Leg Angle (around Y w.r.t. the horizontal)	52.03°	46.78°
G	Right Knee flexion Angle (Y)	68.77°	75.15°
H	Left Knee flexion Angle (Y)	145.52°	155.23°
Ty	Right Upper Arm Angle (Y w.r.t. horizontal)	22.67°	24.90°
Uy	Left Upper Arm Angle (Y w.r.t. horizontal)	22.80°	24.51°
Tx	Right Upper Arm Angle (X w.r.t. horizontal)	135.27°	114.47°
Ux	Left Upper Arm Angle (X w.r.t. horizontal)	130.25°	116.50°
V	Right Elbow flexion Angle	168.29°	169.77°
W	Left Elbow flexion Angle	168.29°	169.61°
HCx	x-Position of HC relative to AC	-2.411 mm	9.80 mm
	Seated decline	68°	70°



Figure 4-2: Positioned 50F cyclist model in front of GV Sedan Model.



Figure 4-3: Positioned 50M cyclist model in front of GV Sedan Model.

#### 4.1.5 FE Bicycle Model for in-crash simulations

Based on a literature review and discussions amongst the WP4 partners about bicycle types and sizes, it was decided to prepare bicycle models based on the dimensions presented in Figure 4-4 and Figure 4-5. The dimensions were selected to correspond to the VIVA+ 50F (trapeze frame) and VIVA+ 50M (diamond frame) model (height, in seam length). The model also enables a typical seated posture (seated decline) based on literature (Otte & Facius, 2017). The dimensions of the bicycles can be found in Table 4-2 and Table 4-3.

Already available and verified models from TU Graz (Klug et al., 2018) were initially rescaled and modified to allow the proper positioning of the VIVA+ models. For a more accurate simulation of the interaction between the HBM and the bicycle, it was decided to remodel and update the bicycle model with shell elements corresponding to bicycle frame thickness. Both models have been modelled to be deformable and EN 25CrMo4 steel was used for the frame, forks and handlebar.

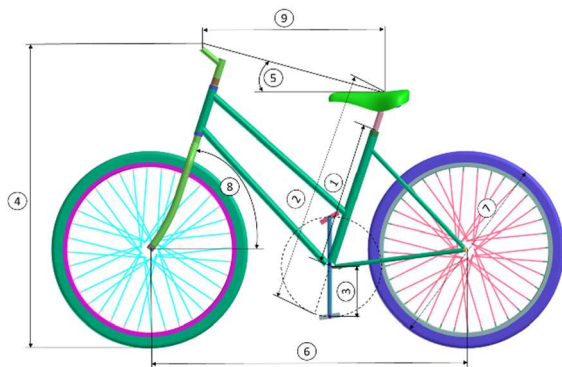


Figure 4-4: Trapeze Frame Bicycle for VIVA+ 50F simulations.

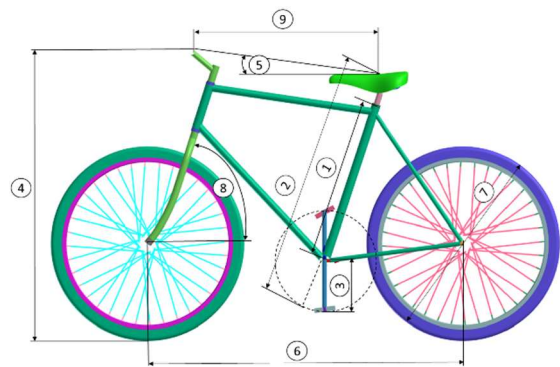


Figure 4-5: Diamond Frame Bicycle for VIVA+ 50M simulations.

Table 4-2: Target geometry for trapeze frame VIVA+ 50F.

#	Measurement	Goal
1	Frame Size	480 mm
2	Saddle Height	790 mm
3	Crank Length	165 mm
4	Handlebar Height	1018 mm
5	Handlebar to Saddle Angle	14°
6	Wheelbase	1062 mm
7	Wheel Diameter	660 mm
8	Head Tube Angle	66.8°
9	Handlebar to Saddle Distance	650 mm
10	Weight	11.7 kg
11	Seated decline	68.0°

Table 4-3: Target geometry for diamond frame VIVA+ 50M.

#	Measurement	Goal
1	Frame Size	550 mm
2	Saddle Height	840 mm
3	Crank Length	165 mm
4	Handlebar Height	966 mm
5	Handlebar to Saddle Angle	7°
6	Wheelbase	1077 mm
7	Wheel Diameter	660 mm
8	Head Tube Angle	66.7°
9	Handlebar to Saddle Distance	623 mm
10	Weight	11.3 kg
11	Seated decline	70.0°

## 4.2 Results

### 4.2.1 Generic AEB simulations

In total 72,035 VT scenarios have been derived for car-cyclist cases, out of which the implemented AEB system avoided 23,566. Although 48,469 cases were unavoidable by the AEB system based on the scenario probability, a total avoidance rate of 53.80% was achieved. The results of the pre-crash



simulations can be seen in Figure 4-6 where the grey bars represent the baseline, and the yellow bars represent the simulations with the AEB system. Furthermore, the implementation of the AEB system revealed a clear trend towards lower collisions speeds.

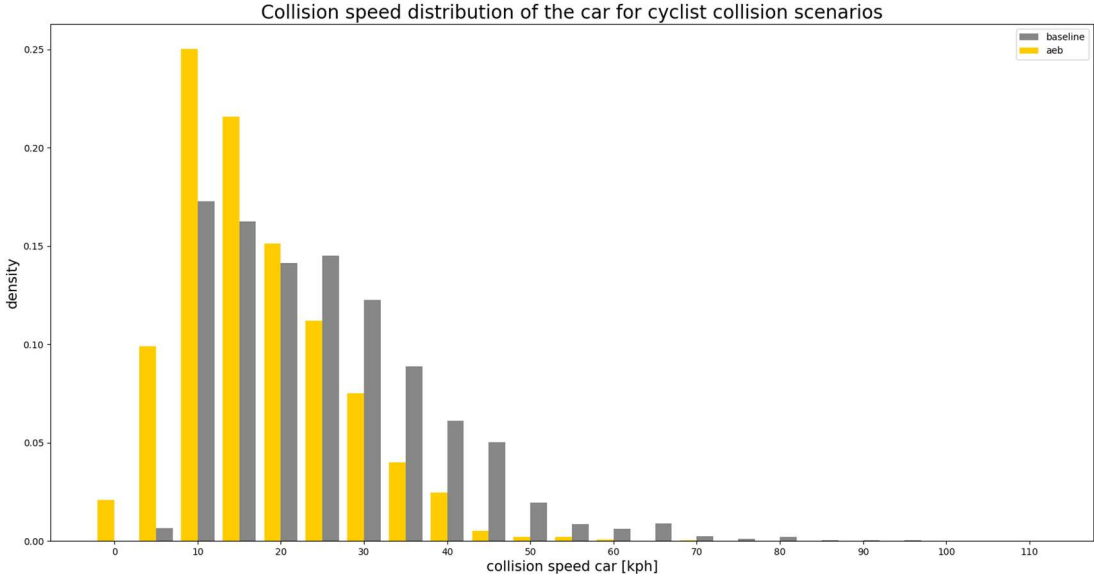


Figure 4-6: Results of the pre-crash simulations for car-cyclist cases.

## 4.2.2 Generic Sedan In-crash Simulations

### 4.2.2.1 Holistic Assessment Simulations

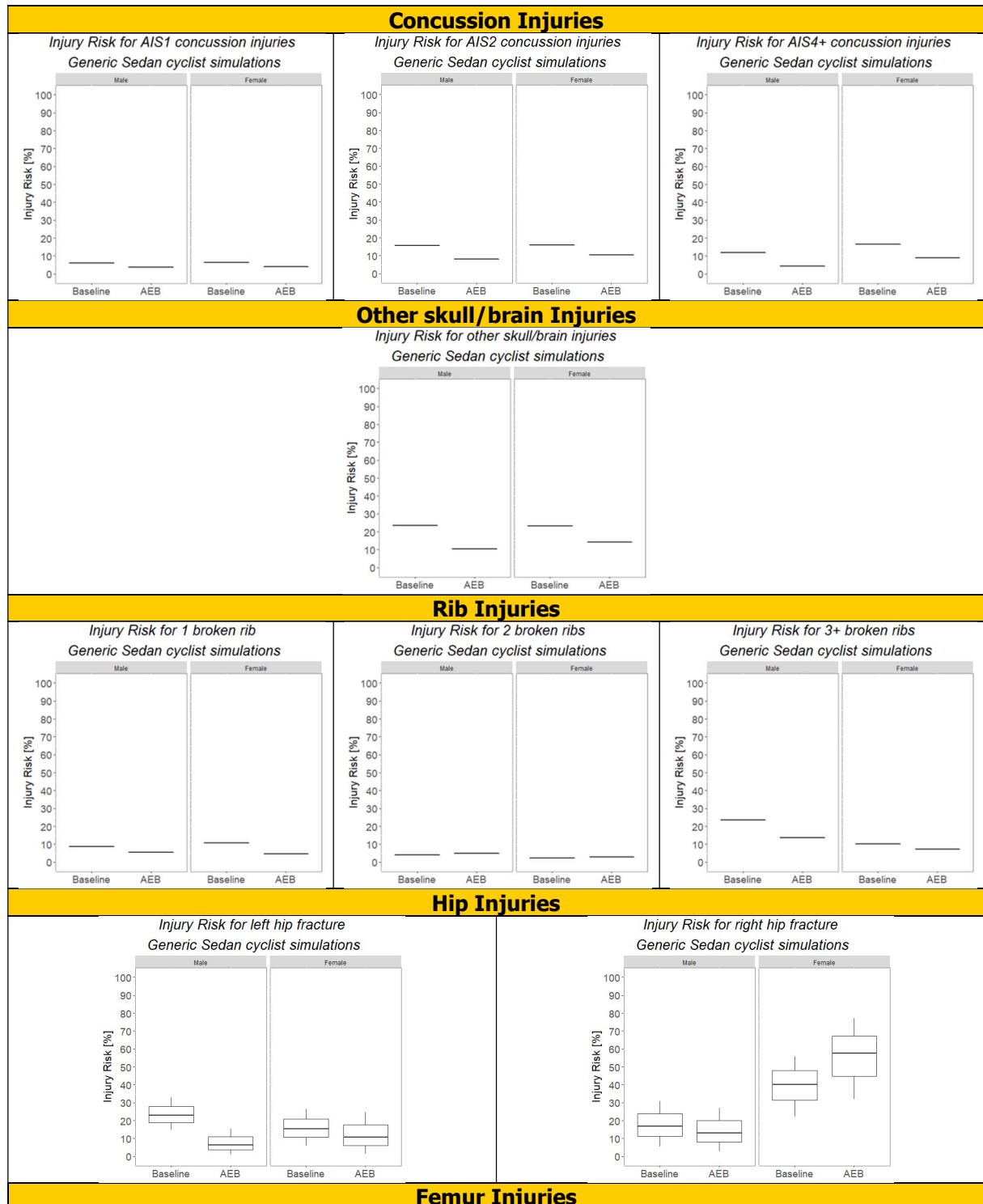
For GV in-crash simulations, baseline as well as AEB cases have been considered. For both cases, 50 in-crash simulations have been conducted for males and females resulting in a total of 200 simulations. These simulations have then been used to train the meta-model, used to predict the injuries of the excluded cases. The performance of the meta-model with regard to different injury criteria can be seen in Table 15-1 and Table 15-2 of Appendix F, which shows that the prediction of the meta-model is performing better for certain injury criteria than others. Hence, the results should be discussed more in the term of trends than in absolute injury values. In Figure 15-1 of Appendix F, the results of the overall injury analysis can be seen based on the injury prediction from the meta-model combined with the occurrence probability of each collision scenario.

The values presented in Figure 15-1 are also presented in Table 4-4. By examining the injury risk for AIS4+ concussion injuries, it can be seen that the injury risk was reduced for males as well as for females, by implementing an AEB system. A similar trend was observed for skull injuries, resulting in a lower injury risk in the AEB scenarios. For AIS3+Rib injuries (3+ Ribs broken) the injury risk can also be lowered by the AEB system, whereby females tend to show a lower AIS3+ rib injury risk than males for the baseline, as well as for the AEB simulations.

For the left hip, reduced fracture risks were observed in the AEB cases for males and females. For the right hip, fracture risk was only lowered for males. For female cyclists, the fracture risk was increasing in the AEB cases. For femur shaft fractures a comparable injury risk can be seen for males and females with lower fracture risks in the AEB cases. For tibia shaft fractures, only a very low injury risk was observed for both sexes, which was further lowered in the AEB cases. The risk of ligament rupture was

very high for the baseline as well as AEB simulations, although they were slightly reduced. The reduction was observed for males as well as females.

Table 4-4: Results of the overall injury assessment for cyclist-generic Sedan cases based on the predicted injuries by the meta-model and the occurrence probability.





#### 4.2.2.2 Cost Benefit Analysis

In Figure 4-7 the final results of the CBA for generic Sedan-cyclist cases can be seen. The manufacturing costs have been estimated due to lack of available data. The crash risk before intervention has been based on data analyses which have been presented in Deliverable 6.1 of the VIRTUAL project (Bützer et al., 2022). By implementing the AEB system for cyclists, an avoidance rate of 53.80% (see Section 4.2.1) could be achieved. This avoidance rate is also affecting the crash risk resulting in a lower crash risk after intervention. The average age was set to 50 years for both males and females as this was found to be the average age in the CARE database (Klug et al., 2020; Linder et al., 2020). The proportion between males and females was also analysed based on the CARE database. With all of this information and the injury risks calculated in Section 3.2.2.1 a total benefit of €1,107 to €1,785 has been predicted by implementing an AEB system. If one system is capable to address both, pedestrian and cyclist crashes, this would add to the benefits described in Section 3.2.2.2.



## COST-BENEFIT TOOL FOR VEHICLE SAFETY

*Measure: AEB cyclist*

Input	lower	best estimate	upper	Results	lower	best estimate	upper
<b>Costs per vehicle</b>				<b>Total costs</b>	€ 2,000	€ 2,500	€ 3,000
- Development costs				<b>Number of injuries prevented</b>			
- Manufacturing costs	€ 2,000	€ 2,500	€ 3,000	- Yearly	0.0011	0.0012	0.0013
- Repair/replacement costs after a crash				- Total vehicle lifetime	0.016	0.018	0.020
<b>Crash risk (number of target crashes per vehicle per year)</b>				- 1 injury prevented per ... vehicles	62	56	50
- before intervention	0.0005151	0.0005189	0.0005227	<b>Quality of life improvement (QALYs)</b>			
- after intervention	0.000238	0.000240	0.000241	- Yearly	0.0010	0.0013	0.0016
<b>Road user characteristics</b>				- Total vehicle lifetime	0.015	0.019	0.024
- Number of target road users per vehicle		1		- 1 QALY gained per ... vehicles	68	53	42
- Average age casualties: - male		50		<b>Benefits</b>			
- female		50		- Quality of life gains	€ 818	€ 1,053	€ 1,321
- Life expectancy: - male		78		- Medical costs reduction	€ 78	€ 98	€ 120
- female		83		- Productivity gains	€ 211	€ 271	€ 344
- Proportion male target road user		66%		- Total benefits	€ 1,107	€ 1,423	€ 1,785
<b>Vehicle life time (years)</b>		15		<b>Socio-economic return</b>			
<b>Discount rate</b>		3.0%		- Net present value	-€ 1,893	-€ 1,077	-€ 215
				- Benefit-cost ratio	0.4	0.6	0.9

Figure 4-7: CBA for cyclist-generic Sedan cases.

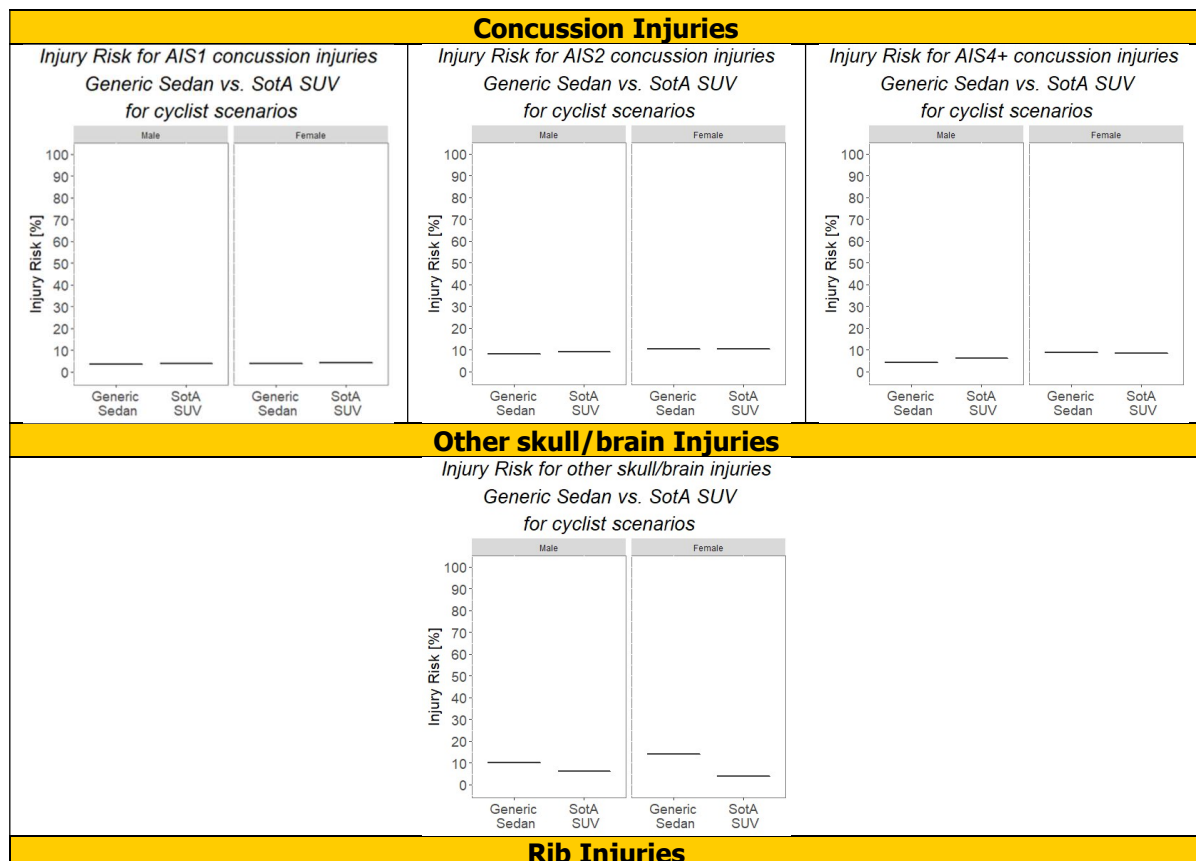
### 4.2.3 State of the Art SUV in-crash simulations

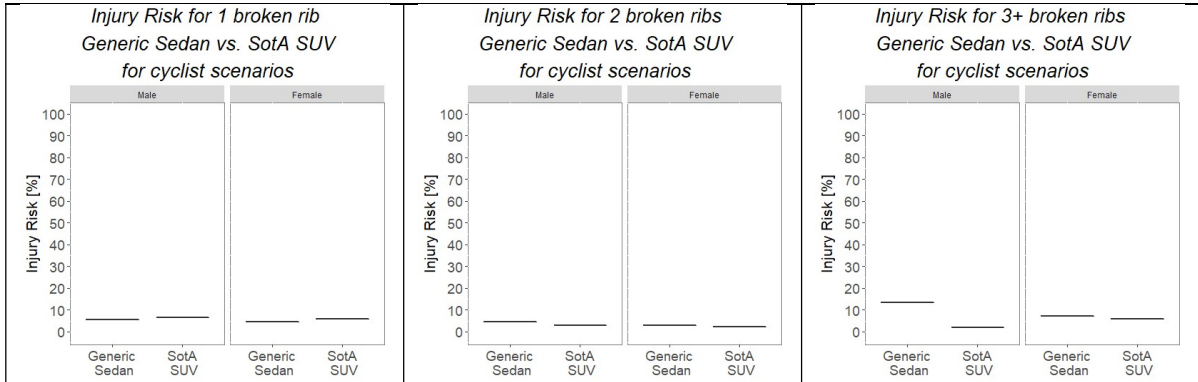
Simulations were performed with a SotA SUV model to compare the injury risks of the generic Sedan front to a modern SUV model. This was done to study the effect on injury risk per body region as well as the overall benefit of a more detailed vehicle model and different car shape.

The results of the generic and the SotA SUVs for both the AEB scenarios are presented in this section. As baseline, the injury risks derived with the generic Sedan were used for both use cases, and the results are presented in Figure 15-2 of Appendix F and Table 4-:5.

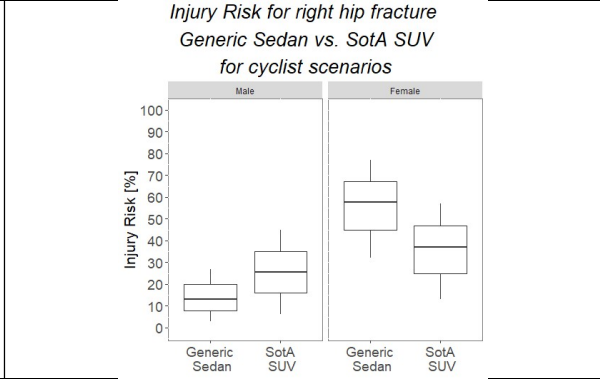
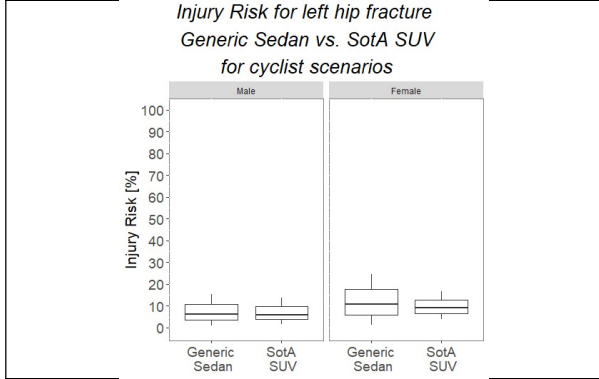
It can be seen, that for all concussion injuries (AIS1, AIS2 and AIS4+) the generic Sedan and the SotA SUV showed similar responses for both males and females. Further examination shows that the injury risk with regard to skull fracture for the generic Sedan were higher for both the 50F and 50M models. For light rib fractures (only 1 or 2 ribs broken), a similar injury risk was observed for both sexes and car models. For more severe rib injuries (3+ ribs broken), the generic Sedan showed a higher risk for males compared to the SotA SUV. For females, both cars show a comparable risk of sustaining rib fractures of more than three ribs. For hip fractures of the left hip, a similar injury risk was observed for both cars and sexes. For the left hip, the SotA SUV model showed a higher risk for male scenarios and a lower risk for female scenarios. Femur shaft fractures appear equally likely for each sex and vehicle, besides the risk of the left femur shaft fractures in female scenarios. Here the generic Sedan shows a higher risk than the SotA SUV. Only a very low injury risk for tibia fractures was observed, with a marginally higher risk for generic Sedan scenarios. Moreover, a high risk of ligament rupture was observed for cyclists which was very similar for both cars and sexes. It was only for the right ligaments that the generic Sedan showed a higher risk for male scenarios.

Table 4-:5 Results of the overall injury assessment for AEB cyclist generic Sedan and SotA SUV scenarios based on the predicted injuries by the meta-model and the occurrence probability.

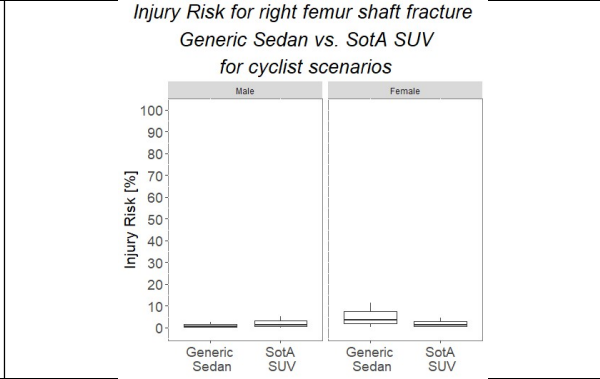
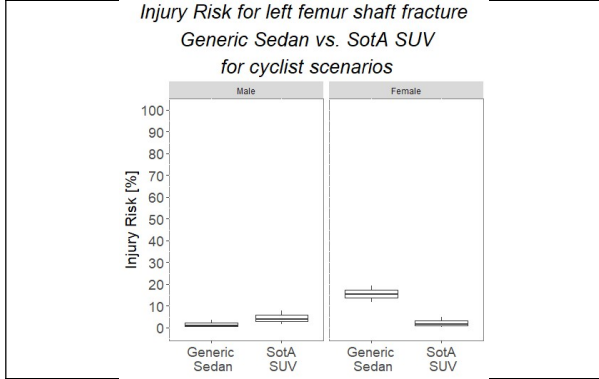




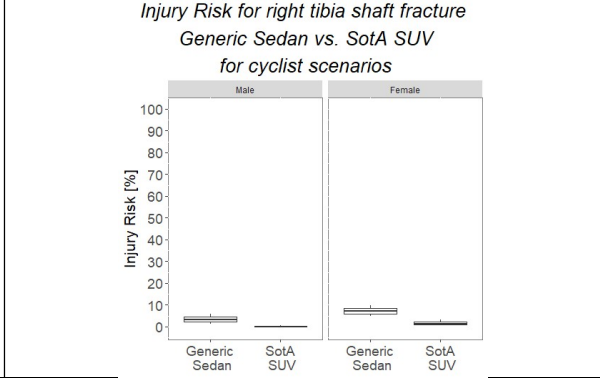
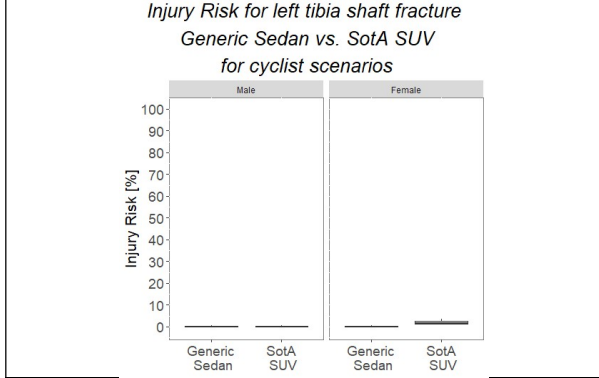
**Hip Injuries**



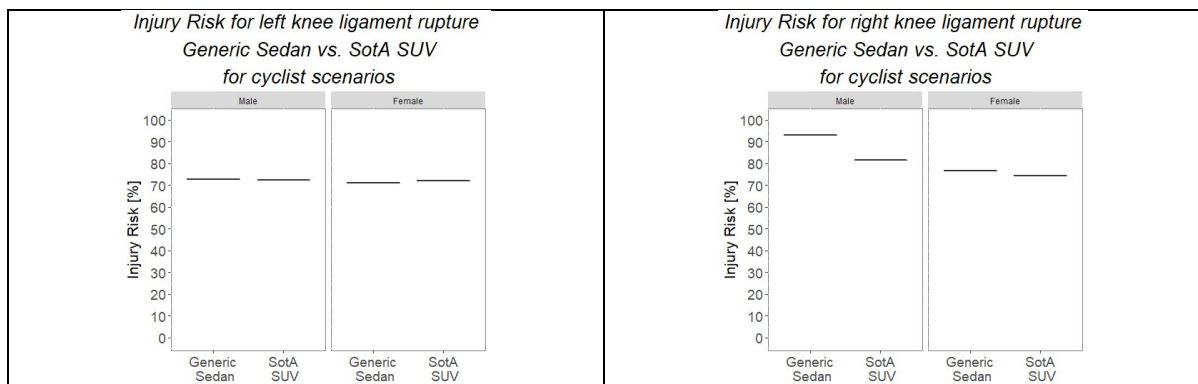
**Femur Injuries**



**Tibia Injuries**



**Ligament Ruptures**



### 4.3 Discussion

In general, the predicted results seem plausible, but higher compared to injury risks in field data, especially for knee ligament ruptures. This might be caused by simplifications in the procedure (only one anthropometry, age and posture assumed) and the accuracy of the injury risk curves (often calibrated to data of historical samples and the knee ligament rupture and rib risk curves, not having been specifically calibrated for the VIVA+ model, instead based on material tests).

The GV use case shows that additionally to the avoided crashes, also the injury risk was lowered in the remaining crashes due to the changed impact configurations. The only risk not reduced due to the AEB system, was the left hip fracture. This may have been caused by the different impact configuration (impact angle, impact point) between baseline and AEB simulations as not only the collision velocity was reduced for the AEB simulations. This circumstance should be examined more closely in the future. The CBA indicates that an extra < €1,107 cost of an AEB system would ensure a positive net value. It must be remembered that not all injury groups have been considered in our analysis, (e.g., upper extremities, neck injuries), hence it can be assumed that the benefits are underpredicted. Furthermore, the same AEB system is suitable for addressing different crash types, while in our analysis we considered cyclist crashes only.

A specific baseline has not been established for the SotA SUV use case. However, injury risks produced by the generic Sedan model can be compared to the SotA SUV model. Due to the different vehicle shapes and a more realistic (heterogeneous) vehicle structure, slight differences in the overall injury risks have been identified for certain body regions, (e.g., hip injuries).

For the generic Sedan, one injury per ~56 vehicles would potentially be avoided (Figure 4-7), while one injury per ~85 vehicles would potentially be avoided for the SotA SUV (Figure 15-3 of Appendix F) when assuming the generic Sedan as baseline for both and applying the same generic AEB as intervention. The reason for this might be the different shape and more detailed modelling of the windshield leading to differences in the injury risk for the intervention simulations, which have not been considered in the baseline.

Therefore, especially for cyclists, it would also be very beneficial to perform in future studies also baseline simulations with the SotA SUV model.

Simulations have also been performed with the SotA SUV to evaluate the feasibility of training the meta-model to the simulation results, as this vehicle model is more complex and hence in comparison to the generic Sedan model, the smaller changes in the simulation result scatter, would be expected to be bigger in these simulations. As shown in Appendix F and Figure 4-8, when using the same number of

samples, the errors of the meta-models trained to the SotA SUV were similar to the generic Sedan model for certain body regions, but higher for the strain of the right tibia shaft, for example.

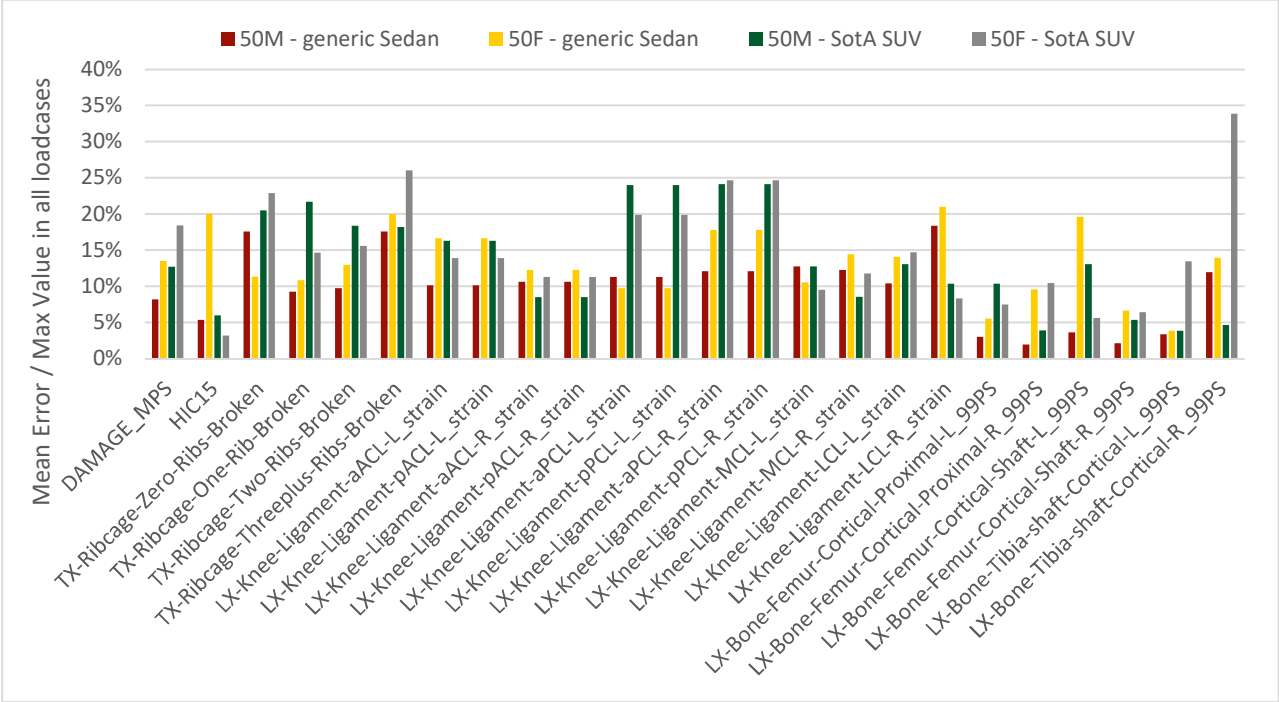


Figure 4-8: Relative mean error for all cyclist load cases (relative to the max values over all four use cases) comparing 50F, 50M and both vehicle models.

Since there are major differences between certain body regions, the meta-models should be improved further in the future.

Different trends were shown in the difference between simulations of the two vehicle models with the average female and average male, which might mainly relate to the different vehicle shapes: Higher risks for more than three rib fractures and hip fractures were observed for the average female compared to the male for the SotA SUV. For the generic Sedan model, a higher risk of more than three rib fractures and knee ligament ruptures were observed for the male compared to the female, and a higher risk of skull fracture, hip fractures and femur shaft fracture, was observed for the female compared to the male.



# 5 Holistic Assessment for tram-pedestrian cases

The aim of this use case was to investigate the potential of a generic AEB system and predict the overall benefit of an improved tram front structure on pedestrian protection.

## 5.1 Method

### 5.1.1 Generic AEB for trams

The conceptual AEB system used for the investigations in Chapter 3 and 4 was reconfigured for the assessment of tram-pedestrian cases. In comparison to cars, tram brake characteristics are different. This concerns the maximum deceleration as well as the braking gradient, which have been observed being approximately  $3 \text{ m/s}^2$ , and  $20 \text{ m/s}^3$ , respectively (Lindemann et al., 2021). Since the lower maximum deceleration also affects the distance required for a full stop, the TTC threshold for triggering the AEB has been selected to 1.5 [s], in line with (Gettman et al., 2008), who proposed scenarios critical if a TTC value below this value has been established. All other parameters of the AEB system have been defined in Section 3.1.1. A summary is shown in Table 5-1.

Table 5-1: Parameters of the conceptual Tram AEB System.

Sensor range [m]	Field of view (sensor angle) [°]	Acquisition time [s]	TTC threshold [s]	Azimuthal resolution [°]	Brake delay [s]	Braking gradient [ $\text{m/s}^3$ ]
60	60	0.15	1.5	0.5	0.2	20.0

### 5.1.2 Generic tram models

The generic tram front model is shown in Figure 5-1. The tram front has been designed in accordance with the geometrical recommendations stated in the technical report on "Railway applications - Vehicle end design for trams and light rail vehicles with respect to pedestrian safety" (Technical Committee CEN/TC, 2019). The model of the tram consists of seven main components which are modelled with an average element edge length of 10 mm, mostly connected by shared nodes. Only the windscreen and side windows have been attached to the frame by applying tied contacts. A 20 tonne lumped mass element centred in the back of the tram and connected by a rigid element to the rearmost points of the chassis represents the mass of a typical tram. This mass element is also connected to the front panels at various positions with beam elements in between. These beam elements are modelled with a very general spring and damper model which represent the behaviour of typically used panel-brackets.

As head injuries are of high interest for the tram impacts, a special focus was set on this area. The windshield has been modelled as laminated glass with three layers: glass (Shell), PVB (Polyvinylbutyral plastics, Solid) and glass (Shell). For the glass, triangular elements (trias) are used to achieve a more accurate fracture pattern and the rather newly developed MAT\_Glass (mat\_280) was used as material model. In comparison to a regular quad-mesh, trias offer the cracks a more random and free way to propagate. The interlayer material PVB has been modelled by 'wedge' elements and the material card MAT\_Simplified\_Rubber (mat\_181). The material behaviour of the windscreen was validated against empirical data (Jezdik, 2019).

For the front skirts, which are made up of glass-fibre reinforced plastics (FRP), a simple material model MAT\_Elastic (mat\_1) with typical strength parameters was used.

These front skirts have been connected to the rigid tram base structure by the beams that can be seen in dark red in Figure 5-1. As a passive countermeasure and "improved" tram front structure, the characteristic of the attachment beams was adjusted and modelled more compliant, allowing a displacement of the panels of about 100 mm (compared to approximately 10 mm in the baseline version). The beams used to model this improvement can be seen in red in Figure 5-2. The stiffness of these beams was adjusted in the improved tram front compared to the baseline. Characteristics are shown in Figure 5-3.

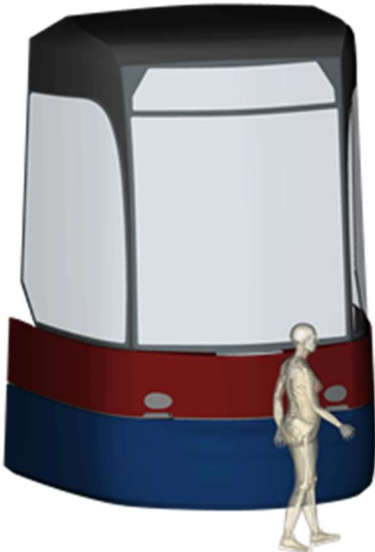


Figure 5-1: Generic tram front model developed within WP4.

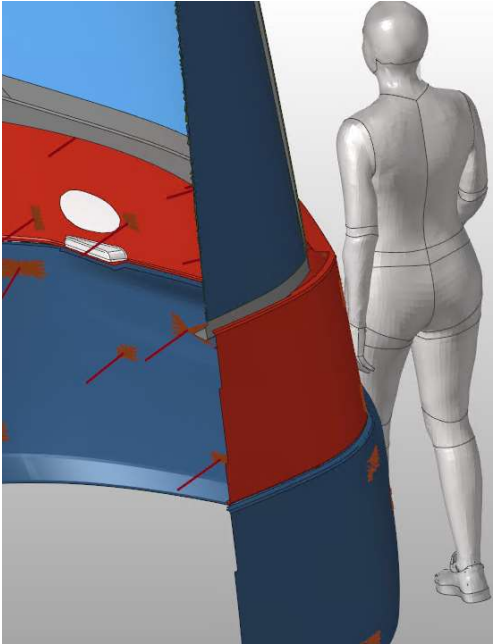


Figure 5-2: Beams (red) at the back of the Tram front to adjust the stiffness and achieve an improved generic tram.

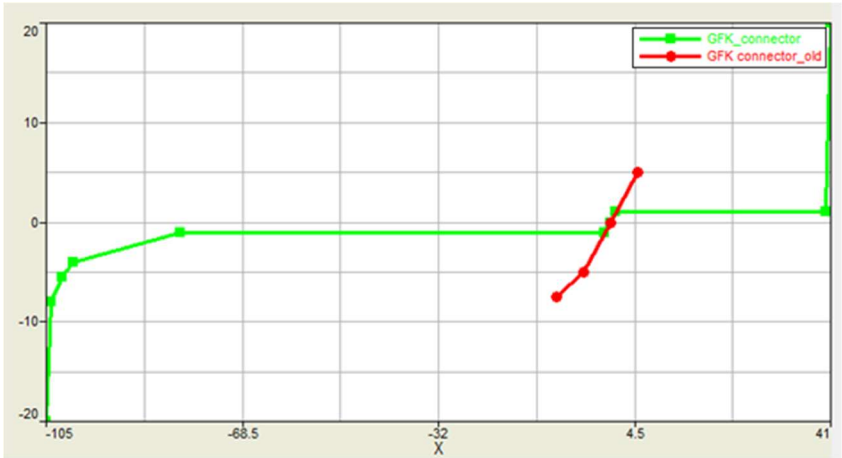


Figure 5-3: Characteristics of the beams fixing the panels to the tram body. The baseline variant is shown red and the "Improved" version in green.

### 5.1.3 Pedestrian Model

The same pedestrian model with fitted shoes as for pedestrian-car simulations was used, which are described in Section 3.1.2.3. All simulations were performed with revision 0.3.2.a<sup>7</sup> of the VIVA+ models.

## 5.2 Results

### 5.2.1 Generic AEB for trams

In total, 2,761 VT scenarios have been derived for tram to pedestrian cases, out of which the generic AEB system avoided 815 simulated cases. When weighting the 1,946 cases unavaoided by the AEB system based on their occurrence probability, the total avoidance rate was 51.9 %. The results of the pre-crash simulations can be seen in Figure 5-4, in which the grey bars represent the occurrence probability for a certain baseline collision speed and the yellow bars represent simulations of the remaining crashes with the generic AEB system.

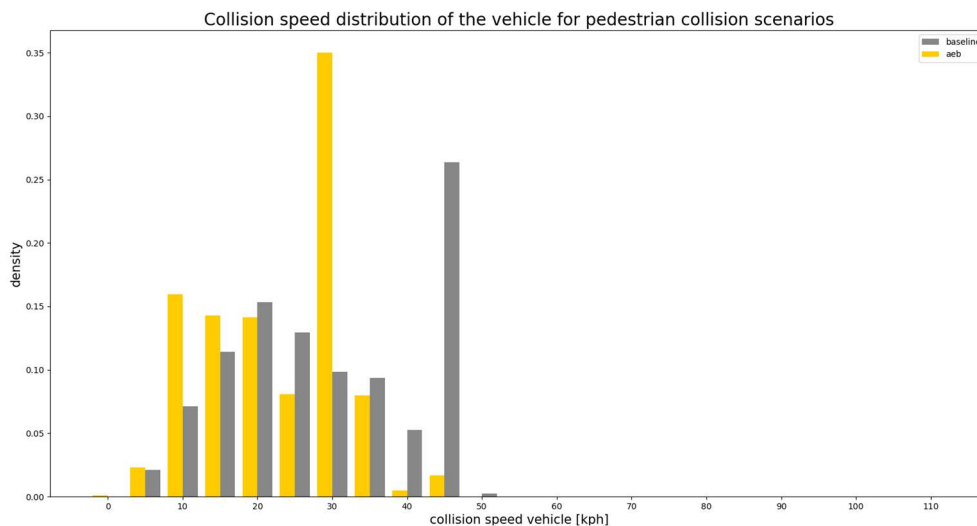


Figure 5-4: Results of the pre-crash simulations for tram-pedestrian cases.

The results for the generic AEB system have been used separately and have not been considered for the overall holistic assessment and CBA, as such systems are currently not available on the market and the focus of this use case was more on the passive side.

### 5.2.2 Generic tram models

#### 5.2.2.1 Holistic Assessment Simulations

The changes of the tram structure led to a reduction in all injury risks or a shift towards lower injury severities for both, 50M and 50F models. For AIS 4+ concussions, the risk was nearly halved as well as significantly reduced for proximal femur and femur shaft fractures. For tibia shaft fractures the risk was reduced from 30% to 4% for the 50M. Also, for the 50F model a reduction in the tibia shaft fracture risk can be seen. For skull fractures, the risk was reduced by ~5% for 50F and 50M models. The results are presented in Figure 16-1 of the Appendix G in a numerical way and in Table 5-2 in a graphical way.

<sup>7</sup> <https://openvt.eu/fem/viva/vivaplus/-/commit/07cfc0cb1972689a2cd8590396ee55b5350ee4c4>

Table 5-2: Results of the overall injury assessment for pedestrian to tram scenarios based on the predicted injuries and the occurrence probability.





### 5.2.2.2 Cost Benefit Analysis

According to D6.1, an estimated crash risk of 1.377-1.512 (with a best estimate of 1.444) per 1 million km was assumed. Unfortunately, a general crash risk per vehicle was not available. Hence, it was decided to use the crash risk per vehicle for Vienna only as this data was also used to derive the VT scenarios described in Lackner et al. (2022).

In Vienna, the mean annual number of trams in operation for the years 2014-2020 was 399.5<sup>8</sup>. In the same period the mean annual number of injury accidents was 67.1 if all injury severities were considered, 49.7 for slight injuries, 16.1 for severe injuries and 1.3 for fatal injuries (Lackner et al., 2022). This results in a crash risk per vehicle of 0.1680 for all accidents. Considering accidents resulting slight injuries only, the crash risk was calculated to 0.1244, while accidents involving severe injuries reached

<sup>8</sup> [https://www.wienerlinien.at/media/files/2020/wl\\_betriebsangaben\\_2019\\_englisch\\_358275.pdf](https://www.wienerlinien.at/media/files/2020/wl_betriebsangaben_2019_englisch_358275.pdf)

0.0403 and the crash risk for accidents resulting in fatal injuries the figure was 0.0033. Assuming a minimum lifetime of 30 years for trams, the total benefit can be calculated and can be seen in Figure 5-5.



## COST-BENEFIT TOOL FOR VEHICLE SAFETY

*Measure: Passive Tram Improvement*

Input				Results			
	<i>lower</i>	<i>best estimate</i>	<i>upper</i>		<i>lower</i>	<i>best estimate</i>	<i>upper</i>
<b>Costs per vehicle</b>				<b>Total costs</b>	€ 2,000	€ 2,500	€ 3,000
- Development costs				<b>Number of injuries prevented</b>			
- Manufacturing costs	€ 2,000	€ 2,500	€ 3,000	- Yearly	0.0037	0.0441	0.1288
- Repair/replacement costs after a crash				- Total vehicle lifetime	0.110	1.323	3.863
<b>Crash risk (number of target crashes per vehicle per year)</b>				- 1 injury prevented per ... vehicles	9	1	0
- before intervention	0.0033	0.0403	0.1244	<b>Quality of life improvement (QALYs)</b>			
- after intervention	0.0033	0.0403	0.1244	- Yearly	0.0091	0.1076	0.3090
<b>Road user characteristics</b>				- Total vehicle lifetime	0.272	3.228	9.270
- Number of target road users per vehicle		1		- 1 QALY gained per ... vehicles	4	0	0
- Average age casualties: - male		50		<b>Benefits</b>			
- female		50		- Quality of life gains	€ 12,441	€ 147,631	€ 423,942
- Life expectancy: - male		78		- Medical costs reduction	€ 949	€ 11,035	€ 30,988
- female		83		- Productivity gains	€ 2,822	€ 36,585	€ 114,217
- Proportion male target road user		50%		- Total benefits	€ 16,211	€ 195,251	€ 569,147
<b>Vehicle life time (years)</b>		30		<b>Socio-economic return</b>			
<b>Discount rate</b>		3.0%		- Net present value	€ 13,211	€ 192,751	€ 567,147
				- Benefit-cost ratio	5.4	78.1	284.6

Figure 5-5: CBA for pedestrian to generic tram cases.

## 5.3 Discussion

A significant reduction in injury risk was observed for the passive improvement of the tram. The passive safety improvements account for a benefit of more than €16,000 per tram. These numbers are surprisingly high and indicate that focus should be enhanced in the product development area.

In general, it would be beneficial to have more details on pedestrian-tram crashes, especially with regard to impact locations and certain detailed crash reconstructions, (e.g., ensuring any deformation of the tram front is documented to reconstruct impact locations).

The current use case shows the importance of VRU protection for public transport vehicles and highlights the need of further innovation in this area.



# 6 Dissemination

## 6.1 OpenVT

All explained parts of the framework have been uploaded to the OpenVT platform, and are available to the project partners at <https://openvt.eu>.

Content on OpenVT:

- Precrash Tool: [https://virtual.openvt.eu/virtual\\_precrash/vru-precash-tool](https://virtual.openvt.eu/virtual_precrash/vru-precash-tool)
- Virtual Testing Scenario catalogue: [https://virtual.openvt.eu/virtual\\_precrash/vru-precash-tool](https://virtual.openvt.eu/virtual_precrash/vru-precash-tool)
- Generic tram front model [https://openvt.eu/fem/generic\\_tram\\_front](https://openvt.eu/fem/generic_tram_front)
- Generic Sedan front <https://openvt.eu/fem/generic-car-front>
- VIVA+ Models: <https://openvt.eu/fem/viva/vivaplus>
- Shoes Models: <https://openvt.eu/fem/shoes>
- Bicycle Models: <https://openvt.eu/fem/bicycle-models>
- Jupyter notebook for analysing the precrash results: <https://OpenVT.eu/VISAFE-VRU>
- Script for DoE: <https://OpenVT.eu/VISAFE-VRU>
- Templates for main files for vehicle impacts (using parameter files generated with the Jupyter notebook): <https://OpenVT.eu/VISAFE-VRU>
- Objects.def + calculation\_porcedure.def file for VIVA+ models covering relevant assessment criteria for postprocessing in Dynasaur: <https://openvt.eu/fem/viva/vivaplus>
- Jupyter notebook which reads binout files from simulations and "converts" simulation results to input table for Cost-Benefit-Analysis-Tool: <https://OpenVT.eu/VISAFE-VRU>
- Script for deriving Meta-models from simulation results: <https://OpenVT.eu/VISAFE-VRU>
- Cost-Benefit-Analysis-Tool: <https://openvt.eu/cost-benefit-analysis/cost-benefit-tool>

## 6.2 Publications

The results of WP4 have been published in the following scientific publications:

- Lackner, C., Heinzl, P., Rizzi, M. C., Leo, C., Schachner, M., Pokorny, P., et al. (2022). Tram to Pedestrian Collisions—Priorities and Potentials. *Front. Future Transp.* 3, 877. Doi: 10.3389/ffutr.2022.913887
- Leo, C., Klug, C., Ohlin, M., and Linder, A. (2019). Analysis of pedestrian injuries in pedestrian-car collisions with focus on age and gender, in 2019 IRCOBI Conference Proceedings, ed. International Research Council on the Biomechanics of Injury (IRCOBI), 256–257.
- Leo, C., Klug, C., Ohlin, M., Bos, N., Davidse, R., and Linder, A. (2019). Analysis of Swedish and Dutch accident data on cyclist injuries in cyclist-car collisions. *Traffic Inj Prev* 20, S160-S162. Doi: 10.1080/15389588.2019.1679551
- Leo, C., Rizzi, M. C., Bos, N. M., Davidse, R. J., Linder, A., Tomasch, E., et al. (2021). Are There Any Significant Differences in Terms of Age and Sex in Pedestrian and Cyclist Accidents? *Front. Bioeng. Biotechnol.* 9. Doi: 10.3389/fbioe.2021.677952
- Schachner, M., Sinz, W., Thomson, R., and Klug, C. (2020). Development and evaluation of potential accident scenarios involving pedestrians and AEB-equipped vehicles to demonstrate the efficiency of an enhanced open-source simulation framework. *Accid Anal Prev* 148, 105831. Doi: 10.1016/j.aap.2020.105831

- Schubert, A., Erlinger, N., Leo, C., Iraeus, J., John, J., and Klug, C. (2021). Development of a 50th Percentile Female Femur Model, in 2021 IRCOBI Conference Proceedings, ed. International Research Council on the Biomechanics of Injury (IRCOBI), 308-332.
- Lackner, C., Heinzl, P., Leo, C., Klug, C. (2022). Investigations on Tram-Pedestrian Impacts by Application of Virtual Testing with Human Body Models. European Transport Research Review

The WP4 methods and results have been presented at:

- AAAM Conference 2019 Madrid
- IRCOBI Conference 2019 Florence
- SafetyUpDate Conference 2019 Graz
- Human Modelling and Simulation in Automotive Engineering Conference 2020 online
- Virtual Testing - Human Modeling in Pedestrian Protection Conference 2021 online
- IRCOBI Conference 2021 online
- Safety UpDate 2022 Graz
- Human Modeling and Simulation in Automotive Engineering Conference 2022 Wiesbaden

## 7 Discussion and Outlook

The developed procedure is an important step towards holistic assessments, moving away from standard-load case assessments only, towards the prediction of real-world safety.

However, the current study still underlies several limitations: Only two adult anthropometries have been considered and one age. In the future, human variability should be further considered as well as VRU crashes with children. Furthermore, only one posture was considered per VRU in our simulations. Analysis of real-world crashes have shown that avoidance-postures might be relevant (Schachner, Schneider et al., 2020) and should be considered in the future.

In the active safety assessment, currently no interaction of the VRU and vehicle (i.e. avoiding reactions) is considered and constant speeds have been chosen. On the other hand, the considered AEB system is very generic and does not consider environmental conditions, (e.g., fog), which limits the detection capabilities. The generic Sedan model is simplified and provides a homogenous stiffness per structural part, (i.e., the foam describing the structural behaviour of the bonnet is homogenous, modelling a constant clearance throughout the whole bonnet). However, the comparison with the SotA SUV shows that the overall behaviour seems to still be comparable to a full FE vehicle model of a serial car.

The collision speed distributions for the tram underlie several assumptions based on the distance between collision and tram stops and an average acceleration only. In areas outside of the acceleration area of the tram, maximum allowed velocities were assumed. It is expected that real collision speeds are lower, as braking might be induced prior to the crash. Therefore, the current assessment of the tram-pedestrian use cases should be considered as conservative worst case assumptions. However, as the same VT load cases with speed distributions are used with and without intervention, conclusions based on the relative comparison can be drawn anyway. In future, it would be beneficial to receive data from tram providers on real-world crashes including collision speeds.

For the in-crash simulations, only 50 simulations were performed with each anthropometry, road user and vehicle model. The injury prediction for the remaining scenarios was done using the meta-models which were trained with 42 of the 50 performed simulations each. Eight load cases were randomly selected for each sample to test the meta-models. This has shown that the prediction accuracy of the meta-models works very well for some body regions (DAMAGE, femur and tibia fractures), but are poor for others (risk of one rib fracture, HIC).

For the pedestrian, the benefit of adding additional simulations to the sample was tested. A manuscript on this study is currently under preparation.

The simulation protocol to replicate the performed simulations in D4.2. with a specific vehicle are described in Deliverable 1.2. Further work is especially needed on the validation procedures to ensure that the virtual vehicle model behaves realistically and represents a real car sufficiently.

## 8 Conclusions

As shown in this report, the developed tools and procedures of VISAFE-VRU can be applied for the assessment of integrated partner protection of cars and trams, addressing pedestrians and cyclists. Safety assessment is performed over a wide range of scenarios while keeping the efforts required for simulations at a feasible level. User-friendly tools were prepared and tested by the WP4 partners to ensure that the developed procedures can easily be replicated by others after the end of the project, enabled by the open-source availability of all tools developed in WP4 on the OpenVT platform.

The potential of AEB systems to reduce crash and injury risks is shown as well as the potential of a more forgiving tram fronts, optimised for improved partner protection. Although the examples used for demonstration are generic, they showcase that the socio-economic benefit of VRU protection is significant.

Future research should focus on further injury risk curves to enable evaluation of further body regions, (e.g., necks and upper extremities), and the consideration of children and other groups of VRUs, (e.g., E-scooter riders).

## 9 References

- Alvarez, V. S., & Kleiven, S. (2016). Importance of Windscreen Modelling Approach for Head Injury Prediction. In International Research Council on the Biomechanics of Injury (Ed.), *IRCOBI Conference Proceedings, 2016 IRCOBI Conference Proceedings* (pp. 813–830). IRCOBI. <http://www.ircobi.org/wordpress/downloads/irc16/pdf-files/100.pdf>
- Barrow, A., Edwards, A., Smith, L., Khatri, R., Kalaiyarasan, A., & Hynd, D. (2018). *Effectiveness estimates for proposed amendments to the EU's General and Pedestrian Safety Regulations (v3.0). Published project report / Transport Research Laboratory, TRL PPR: Vol. 844*. TRL. <https://trl.co.uk/reports/effectiveness-estimates-proposed-amendments-eus-general-and-pedestrian-safety-regulations>
- Budzynski, M., Tubis, A., & Jamroz, K. (2019). Identifying Selected Tram Transport Risks. *IOP Conference Series: Materials Science and Engineering*, 603(4), 42053. <https://doi.org/10.1088/1757-899X/603/4/042053>
- Bützer, D., Wijnen, W., Elvik, R., & Pokorny, P. (2022). *Cost-benefit analysis of innovative automotive safety systems available on the platform accompanied by two scientific papers* (H2020 project VIRTUAL VIRTUAL Deliverable 6.1.).
- Chen, Q., Lin, M., Dai, B., & Chen, J. (2015). Typical Pedestrian Accident Scenarios in China and Crash Severity Mitigation by Autonomous Emergency Braking Systems. In SAE International (Ed.), *SAE Technical Paper Series, SAE 2015 World Congress Proceedings*. SAE International. <https://doi.org/10.4271/2015-01-1464>
- Cho et al (2009). Landing impact analysis of sports shoes using 3-D coupled foot-shoe finite element model. *Journal of Mechanical Science and Technology*(23), 2583–2591.
- Detwiller, M., & Gabler, H. C. (2017). Potential Reduction in Pedestrian Collisions with an Autonomous Vehicle. In NHTSA (Ed.), *ESV Conference Proceedings, The 25th ESV Conference Proceedings* (pp. 1–8). NHTSA. <https://www-esv.nhtsa.dot.gov/Proceedings/25/25ESV-000404.pdf>
- Duvenaud, D. (2014). *The Kernel cookbook: Advice on covariance functions*.
- Euro NCAP (November 2019). *Pedestrian Human Model Certification*. (TB 024). <https://cdn.euroncap.com/media/56949/tb-024-pedestrian-human-model-certification-v20.pdf>
- Euro NCAP (2022, February 7). *Brain Injury Calculation*. (Technical Bulletin, TB0 35). <https://cdn.euroncap.com/media/67886/tb-035-brain-injury-calculation-v10.pdf>
- European Commission. (2021). *Road safety thematic report – Fatigue*. Brussels.
- Feist, F., Sharma, N., Klug, C., Roth, F., Schinke, S., Besch, A., & Dornbusch, F. (2019). GVTR: A Generic Vehicle Test Rig Representative of the Contemporary European Vehicle Fleet. In NHTSA (Ed.), *ESV Conference Proceedings, The 26th ESV Conference Proceedings*. NHTSA. <http://indexsmart.mirasmart.com/26esv/PDFfiles/26ESV-000254.pdf>
- Forman, J. L., Kent, R. W., Mroz, K., Pipkorn, B., Bostrom, O., & Segui-Gomez, M. (2012). Predicting Rib Fracture Risk with Whole-Body Finite Element Models: Development and Preliminary Evaluation of a Probabilistic Analytical Framework. *Annals of Advances in Automotive Medicine*, 56, 109–124.
- Gabler, L. F., Crandall, J. R., & Panzer, M. B. (2019). Development of a Second-Order System for Rapid Estimation of Maximum Brain Strain. *Annals of Biomedical Engineering*, 47(9), 1971–1981. <https://doi.org/10.1007/s10439-018-02179-9>
- Gettman, D., Pu, L., Sayed, T., & Shelby, Steven, G. (2008). *Surrogate Safety Assessment Model and validation: Final report* (FHWA-HRT-08-051). McLean, Va. Federal Highway Administration.
- Gruber, M., Kolk, H., Klug, C., Tomasch, E., Feist, F., Schneider, A., & Roth, F. (2019). The effect of P-AEB system parameters on the effectiveness for real world pedestrian accidents. In NHTSA (Ed.),

- ESV Conference Proceedings, The 26th ESV Conference Proceedings.* NHTSA. <http://indexsmart.mirasmart.com/26esv/PDFfiles/26ESV-000130.pdf>
- Hummel, T., Kühn, M., Bende, J., & Lang, A. (2011). *Advanced Driver Assistance Systems: An investigation of their potential safety benefits based on an analysis of insurance claims in Germany. Forschungsbericht / Gesamtverband der Deutschen Versicherungswirtschaft e.V FS, Fahrzeugsicherheit / Unfallforschung der Versicherer: Vol. 03.* GDV.
- Isaksson-Hellman, I., & Lindman, M. (2019). Real-world evaluation of driver assistance systems for vulnerable road users based on insurance crash data in Sweden. In NHTSA (Ed.), *ESV Conference Proceedings, The 26th ESV Conference Proceedings.* NHTSA. <https://www-esv.nhtsa.dot.gov/Proceedings/26/26ESV-000300.pdf>
- Jeppsson, H., Östling, M., & Lubbe, N. (2018). Real life safety benefits of increasing brake deceleration in car-to-pedestrian accidents: Simulation of Vacuum Emergency Braking. *Accident Analysis & Prevention, 111*, 311–320. <https://doi.org/10.1016/j.aap.2017.12.001>
- Jezdik, R. (2019). Aspect of front end Tram Design with respect to Pedestrian Safety. In *12th International Symposium on Passive Safety of Rail Vehicles*, Berlin, Germany.
- John, J., Klug, C., Kranjec, M., Svenning, E., & Iraeus, J. (2022). Hello, world! Viva+: A human body model lineup to evaluate sex-differences in crash protection. *Frontiers in Bioengineering and Biotechnology, 10*, 918904. <https://doi.org/10.3389/fbioe.2022.918904>
- Joseph, V. R., Gul, E., & Ba, S. (2015). Maximum projection designs for computer experiments. *Biometrika, 102*(2), 371–380. <https://doi.org/10.1093/biomet/asv002>
- Joseph, V. R., Gul, E., & Ba, S. (2020). Designing computer experiments with multiple types of factors: The MaxPro approach. *Journal of Quality Technology, 52*(4), 343–354. <https://doi.org/10.1080/00224065.2019.1611351>
- K. I. Williams, C. (2006). *Gaussian Processes for Machine Learning.* The MIT Press. <http://196.189.45.87/handle/123456789/51320>
- Klug, C., Feist, F., Raffler, M., Sinz, W., Petit, P., Ellway, J., & van Ratingen, M. (2017). Development of a Procedure to Compare Kinematics of Human Body Models for Pedestrian Simulations. In International Research Council on the Biomechanics of Injury (Ed.), *IRCOBI Conference Proceedings, 2017 IRCOBI Conference Proceedings* (pp. 509–530). IRCOBI. <http://www.ircoibi.org/wordpress/downloads/irc17/pdf-files/64.pdf>
- Klug, C., Feist, F., Schneider, B., Sinz, W., Ellway, J., & van Ratingen, M. (2019). Development of a Certification Procedure for Numerical Pedestrian Models. In NHTSA (Ed.), *ESV Conference Proceedings, The 26th ESV Conference Proceedings* (Paper No.19-0310-O). NHTSA. <https://www-esv.nhtsa.dot.gov/Proceedings/26/26ESV-000310.pdf>
- Klug, C., Feist, F., & Wimmer, P. (2018). Simulation of a Selected Real World Car to Bicyclist Accident using a Detailed Human Body Model. In International Research Council on the Biomechanics of Injury (Ed.), *IRCOBI Conference Proceedings, 2018 IRCOBI Conference Proceedings* (pp. 182–183). IRCOBI. <http://www.ircoibi.org/wordpress/downloads/irc18/pdf-files/27.pdf>
- Klug, C., Leo, C., Schachner, M., Rizzi, M., Grumert, E., & Davidse, R. (2020). *Current and future accident and impact scenarios for pedestrians and cyclists* (H2020 project VIRTUAL VIRTUAL Deliverable 4.1.).
- Lackner, C., Heinzl, P., Rizzi, M. C., Leo, C., Schachner, M., Pokorny, P., Klager, P., Buetzer, D., Elvik, R., Linder, A., & Klug, C. (2022). Tram to Pedestrian Collisions—Priorities and Potentials. *Frontiers in Future Transportation, 3*, 877. <https://doi.org/10.3389/ffutr.2022.913887>
- Larsson, K.-J., Blennow, A., Iraeus, J., Pipkorn, B., & Lubbe, N. (2021). Rib Cortical Bone Fracture Risk as a Function of Age and Rib Strain: Updated Injury Prediction Using Finite Element Human Body Models. *Frontiers in Bioengineering and Biotechnology, 9*, Article 677768, 677768. <https://doi.org/10.3389/fbioe.2021.677768>

- Leo, C., Klug, C., Ohlin, M., Bos, N., Davidse, R., & Linder, A. (2019). Analysis of Swedish and Dutch accident data on cyclist injuries in cyclist-car collisions. *Traffic Injury Prevention, 20*(sup2), S160-S162. <https://doi.org/10.1080/15389588.2019.1679551>
- Leo, C., Klug, C., Ohlin, M., & Linder, A. (2019). Analysis of pedestrian injuries in pedestrian-car collisions with focus on age and gender. In International Research Council on the Biomechanics of Injury (Ed.), *IRCOBI Conference Proceedings, 2019 IRCOBI Conference Proceedings* (pp. 256–257). IRCOBI. <http://www.ircobi.org/wordpress/downloads/irc19/pdf-files/40.pdf>
- Leo, C., Rizzi, M. C., Bos, N. M., Davidse, R. J., Linder, A., Tomasch, E., & Klug, C. (2021). Are There Any Significant Differences in Terms of Age and Sex in Pedestrian and Cyclist Accidents? *Frontiers in Bioengineering and Biotechnology, 9*, Article 677952. <https://doi.org/10.3389/fbioe.2021.677952>
- Lindemann, U., Sczuka, K., Becker, C., & Klenk, J. (2021). Perturbation im öffentlichen Nahverkehr als Grundlage für Perturbationstraining zur Vermeidung von Stürzen [Perturbation in public transport as a basic concept for perturbation-based balance training for fall prevention]. *Zeitschrift Fur Gerontologie Und Geriatrie, 54*(6), 571–575. <https://doi.org/10.1007/s00391-020-01755-w>
- Linder, A., Davidse, R. J., Iraeus, J., John, J. D., Keller, A., Klug, C., Krašna, S., Leo, C., Ohlin, M., Silvano, A. P., Svensson, M., Wågström, L., & Schmitt, K.-U. (2020). VIRTUAL - a European approach to foster the uptake of virtual testing in vehicle safety assessment. In TRA (Chair), *Transport Research Arena*, Helsinki, Finland. [https://projectvirtual.eu/wp-content/uploads/2020/03/VIRTUAL-TRA-2020-Linder-et-al\\_12Mar20.pdf](https://projectvirtual.eu/wp-content/uploads/2020/03/VIRTUAL-TRA-2020-Linder-et-al_12Mar20.pdf)
- Lindman, M., Ödblom, A., Bergvall, E., Eidehall, A., Svanberg, B., & Lukaszewicz, T. (2010). Benefit Estimation Model for Pedestrian Auto Brake Functionality. In ESAR (Chair), *4th International Conference on ESAR*, Hanover, Germany. <https://www.saferresearch.com/library/benefit-estimation-model-pedestrian-auto-brake-functionality>
- Luttenberger, P., Tomasch, E., Willinger, R., Mayer, C., Bakker, J., Bourdet, N., Ewald, C., & Sinz, W. (2014). Method for future pedestrian accident scenario prediction. In *Transport Research Arena*.
- Naznin, F., Currie, G., & Logan, D. (2017). Key challenges in tram/streetcar driving from the tram driver's perspective – A qualitative study. *Transportation Research Part F: Traffic Psychology and Behaviour, 49*, 39–48. <https://doi.org/10.1016/j.trf.2017.06.003>
- Naznin, F., Currie, G., Logan, D., & Sarvi, M. (2016). Safety impacts of platform tram stops on pedestrians in mixed traffic operation: A comparison group before-after crash study. *Accident; Analysis and Prevention, 86*, 1–8. <https://doi.org/10.1016/j.aap.2015.10.007>
- Nusia, J., Xu, J. C., Sjöblom, R., Knälmann, J., Linder, A., & Kleiven, S. (2021). *Injury risk functions for the four primary knee ligaments*. <https://doi.org/10.1101/2021.07.30.454445>
- Otte, D., & Facius, T. (2017). Analysis of the Riding Posture of Bicyclists and Influence Parameters on the Helmet Use. *Open Journal of Safety Science and Technology, 07*(01), 58–68. <https://doi.org/10.4236/ojsst.2017.71005>
- Page, Y., Fahrenkrog, F., Fiorentino, A., Gwehenberger, J., Helmer, T., Lindman, M., Op den Camp, O., van Rooij, L., Puch, S., Fränzle, M., Sander, U., & Wimmer, P. (2015). A Comprehensive and Harmonized Method for Assessing the Effectiveness of Advanced Driver Assistance Systems by Virtual Simulation: The P.E.A.R.S. Initiative. In NHTSA (Ed.), *ESV Conference Proceedings, The 24th ESV Conference Proceedings*. NHTSA. <https://www-esv.nhtsa.dot.gov/Proceedings/24/files/24ESV-000370.PDF>
- Pedregosa, F., Varoquaux, G., Gramfort, A., Michel, V., Thirion, B., Grisel, O., Blondel, M., Prettenhofer, P., Weiss, R., Dubourg, V., Vanderplas, J., Passos, A., Cournapeau, D., Brucher, M., Perrot, M., & Duchesnay, E. (2011). Scikit-learn: Machine learning in Python. *Journal of Machine Learning Research, 12*, 2825–2830. [https://www.jmlr.org/papers/volume12/pedregosa11a/pedregosa11a.pdf?source=post\\_page](https://www.jmlr.org/papers/volume12/pedregosa11a/pedregosa11a.pdf?source=post_page)

- Rasmussen, C. E. (2004). Gaussian Processes in Machine Learning. In O. Bousquet, U. von Luxburg, & G. Rätsch (Eds.), *SpringerLink Bücher: Vol. 3176. Advanced Lectures on Machine Learning: ML Summer Schools 2003, Canberra, Australia, February 2-14, 2003, Tübingen, Germany, August 4-16, 2003, Revised Lectures* (Vol. 3176, pp. 63–71). Springer Berlin Heidelberg. [https://doi.org/10.1007/978-3-540-28650-9\\_4](https://doi.org/10.1007/978-3-540-28650-9_4)
- Rosen, E., Källhammer, J.-E., Eriksson, D., Nentwich, M., Fredriksson, R., & Smith, K. (2010). Pedestrian injury mitigation by autonomous braking. *Accident Analysis & Prevention*, *42*(6), 1949–1957. <https://doi.org/10.1016/j.aap.2010.05.018>
- Roth, F., Labenski, V., Gruber, M., & Kolk, H. (2018). Future Traffic Scenario under Consideration of AEB Systems. In CARHS (Chair), *Praxiskonferenz Fußgängerschutz*, Bergisch-Gladbach.
- Schachner, M., Schneider, B., Klug, C., & Sinz, W. (2020). Extracting Quantitative Descriptions of Pedestrian Pre-crash Postures from Real-world Accident Videos. In International Research Council on the Biomechanics of Injury (Ed.), *IRCOBI Conference Proceedings, 2020 IRCOBI Conference Proceedings* (pp. 231–249). IRCOBI. <http://www.ircobi.org/wordpress/downloads/irc20/pdf-files/37.pdf>
- Schachner, M., Sinz, W., Thomson, R., & Klug, C. (2020). Development and evaluation of potential accident scenarios involving pedestrians and AEB-equipped vehicles to demonstrate the efficiency of an enhanced open-source simulation framework. *Accident Analysis & Prevention*, *148*, 105831. <https://doi.org/10.1016/j.aap.2020.105831>
- Schmitt, K.-U., Niederer, P. F., Cronin, D. S., Morrison III, B., Muser, M. H., & Walz, F. (2019). *Trauma Biomechanics: An Introduction to Injury Biomechanics* (5th ed. 2019). Springer eBook Collection. Springer. <https://doi.org/10.1007/978-3-030-11659-0>
- Schubert, A., Erlinger, N., Leo, C., Iraeus, J., John, J., & Klug, C. (2021). Development of a 50th Percentile Female Femur Model. In International Research Council on the Biomechanics of Injury (Ed.), *IRCOBI Conference Proceedings, 2021 IRCOBI Conference Proceedings* (308-332). IRCOBI. <http://www.ircobi.org/wordpress/downloads/irc21/pdf-files/2138.pdf>
- Strandroth, J., Nilsson, P., Sternlund, S., Rizzi, M., & Krafft, M. (2016). Characteristics of future crashes in Sweden – identifying road safety challenges in 2020 and 2030. In International Research Council on the Biomechanics of Injury (Ed.), *IRCOBI Conference Proceedings, 2016 IRCOBI Conference Proceedings* (pp. 47–60). IRCOBI. <http://www.ircobi.org/wordpress/downloads/irc16/pdf-files/15.pdf>
- Technical Committee CEN/TC. (2019). *Railway Applications - Vehicle End Design for Trams and Light Rail Vehicles with Respect to Pedestrian Safety* (European Committee for Standardization No. 30). Brussels.
- TRL, CEESAR, & ACEA. (September 2018). *Accident Analysis - General Safety Regulation: accident analysis assesses effectiveness of proposed safety measures*. [https://www.acea.be/uploads/publications/Accident\\_Analysis\\_TRL\\_CEESAR\\_2018.pdf](https://www.acea.be/uploads/publications/Accident_Analysis_TRL_CEESAR_2018.pdf)
- UIC: International union of Railways. (2009). *UIC: International Union of Railways: ERRAC Road Map*. France.
- Vertal, P., & Steffan, H. (2016). Evaluation of the Effectiveness of Volvo's Pedestrian Detection System Based on Selected Real-Life Fatal Pedestrian Accidents. In SAE International (Ed.), *SAE Technical Paper Series, SAE 2016 World Congress Proceedings*. SAE International. <https://doi.org/10.4271/2016-01-1450>
- Wimmer, P., Düring, M., Chajmowicz, H., Granum, F., King, J., Kolk, H., Op den Camp, O., Scognamiglio, P., & Wagner, M. (2019). Toward harmonizing prospective effectiveness assessment for road safety: Comparing tools in standard test case simulations. *Traffic Injury Prevention*, *20*(sup1), S139-S145. <https://doi.org/10.1080/15389588.2019.1616086>



Wu, T., Sato, F., Antona-Makoshi, J., Gabler, L. F., Giudice, J. S., Alshareef, A., Yaguchi, M., Masuda, M., Margulies, S. S., & Panzer, M. B. (2022). Integrating Human and Nonhuman Primate Data to Estimate Human Tolerances for Traumatic Brain Injury. *Journal of Biomechanical Engineering*, *144*(7). <https://doi.org/10.1115/1.4053209>

# 10 Appendix A: Pedestrian Simulations Matrix

Table 10-1: In-Crash Simulation Matrix for Pedestrian baseline simulations.

Collision Angle [°]	Collision Position [%]	Collision Speed Vehicle [km/h]	Collision Speed Pedestrian [km/h]
90	0	40	6
270	20	35	6
270	-40	25	4
270	-20	25	12
270	40	35	12
270	0	20	5
270	-20	45	8
270	40	15	2
90	20	30	12
270	0	40	12
270	20	15	12
90	20	50	6
90	40	45	7
90	-40	35	12
270	-40	50	7
90	0	20	10
90	-40	25	3
90	-20	15	12
270	-20	10	4
270	-40	10	12
270	20	10	2
90	-40	60	10
90	-20	35	2
270	20	50	11
90	20	10	4

90	40	10	10
240	-40	10	4
90	-20	65	10
90	20	65	2
240	-20	20	2
270	0	55	2
270	20	60	3
60	40	15	5
90	0	70	12
90	40	20	2
90	40	75	12
270	40	55	9
60	0	10	9
240	0	10	2
240	20	10	10
240	40	10	5
240	40	25	10
60	-40	15	10
300	-5	35	11
300	-40	20	3
300	-40	35	8
300	0	25	5
300	20	25	9
60	20	35	9
0	5	40	6

Table 10-2: In-Crash Simulation Matrix for Pedestrian AEB simulations.

Collision Angle [°]	Collision Position [%]	Collision Speed Vehicle [km/h]	Collision Speed Pedestrian [km/h]
270	-40	15	12
270	45	10	8
90	40	15	10
90	-50	30	4

270	25	20	6
270	-15	15	5
270	20	25	5
90	-10	25	7
270	5	15	8
90	-25	35	10
90	-45	15	8
270	35	15	3
270	-10	5	4
270	-30	20	2
90	-15	20	6
60	15	5	3
90	-20	30	12
90	-30	10	12
90	-5	5	12
90	15	10	5
60	10	10	6
90	-35	5	8
90	-35	35	5
90	10	25	2
60	0	20	10
270	30	30	2
60	35	20	4
60	-5	15	7
270	0	10	2
270	-20	30	7
270	-15	35	9
90	-5	50	10
90	20	40	8
90	35	45	2
240	-15	25	3
60	-25	30	5
90	20	5	2
90	15	45	10
90	30	50	4

90	-10	45	12
90	-40	25	12
90	-45	40	12
90	-50	50	8
90	10	35	12
60	-30	5	9
60	-50	10	10
240	-10	10	7
240	-30	10	2
240	-35	20	10
240	25	5	5

# 11 Appendix B: Cyclist Simulations Matrix

Table 11-1: In-crash Simulation Matrix for Cyclist baseline simulations.

Collision Angle [°]	Collision Position [%]	Collision Speed Vehicle [km/h]	Collision Speed Cyclist [km/h]
270	40	10	15
270	-20	15	15
270	-40	10	10
270	20	15	20
90	0	15	15
90	-40	25	20
270	-40	20	20
90	-20	30	10
270	0	20	5
270	-20	35	20
270	0	40	20
270	40	45	20
330	-50	5	10
270	20	35	5
90	40	45	10
270	20	50	15
210	40	10	10
240	-20	10	25
150	-40	20	10
60	-20	20	15
300	40	30	15
330	20	20	15
210	40	35	20
270	-20	55	10
240	40	20	10
300	45	20	25
90	-40	55	15
150	5	25	10
240	0	35	25
300	0	35	10

240	20	25	20
150	40	10	20
300	5	15	15
330	45	15	15
150	-20	35	15
240	20	10	5
240	-40	35	10
60	0	25	10
330	40	35	25
270	-40	65	5
270	40	60	5
330	-20	45	15
300	20	40	15
330	15	30	25
150	20	5	15
300	35	10	15
300	40	50	10
330	35	25	20
210	20	30	25
150	0	10	5

Table 11-2: In-crash Simulation Matrix for Cyclist AEB simulations.

Collision Angle [°]	Collision Position [%]	Collision Speed Vehicle [km/h]	Collision Speed Cyclist [km/h]
270	-20	10	15
270	40	15	20
60	50	10	20
330	-50	25	30
330	-50	5	10
90	-20	5	20
270	-40	40	20
90	-15	10	15
210	35	5	20
240	-40	25	10
330	-25	30	25
90	-10	40	10
150	5	25	20
60	40	30	15
330	5	20	10
270	25	20	10
150	-40	15	5
330	-35	15	15
60	-20	15	10
210	20	35	15
150	0	35	10
90	-40	20	10
150	20	20	10
90	-50	25	15
210	-10	5	10
330	35	30	30
270	-15	15	5
150	-20	40	20
150	40	35	15
180	-45	5	15
270	30	40	5
270	5	35	15
240	-25	15	10
240	-35	30	25



150	-20	5	10
30	40	25	10
240	0	5	5
240	40	25	20
330	-40	35	30
330	-5	40	30
330	45	35	15
240	50	5	10
270	10	20	20
60	20	40	10
300	-50	15	25
240	0	25	25
90	10	10	5
60	0	35	25
30	0	50	10
90	25	15	20

# 12 Appendix C: Tram Simulations Matrix

Table 12-1: Probabilities for tram collision speeds.

Collision Speeds Tram Range [km/h]	Probability
0 – 10	0.0253
10 – 15	0.0805
15 – 20	0.1149
20 – 25	0.1471
25 – 30	0.1241
30 – 35	0.0943
35 – 40	0.0897
40 – 50	0.3034
50 – 60	0.0207

Table 12-2: Probabilities for pedestrian collision speeds.

Collision Speeds Tram Range [km/h]	Probability
< 2	0.0913
2 – 3	0.0936
3 – 4	0.1106
4 – 5	0.1169
5 – 6	0.1142
6 – 7	0.1047
7 – 8	0.0909
8 – 9	0.0752
9 – 10	0.0595
> 10	0.143

Table 12-3: Probability for tram conflict situations.

SCPPR	SCPPL	RTSD	RTOD	LTSD	SD
0.676	0.279	0.0165	0.002364	0.014	0.01182

Table 12-4: In-crash Simulation Matrix for Tram simulations.

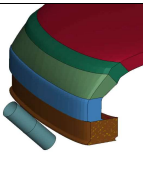
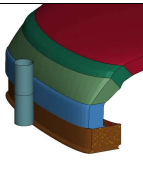
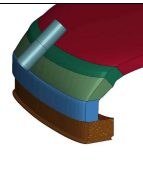
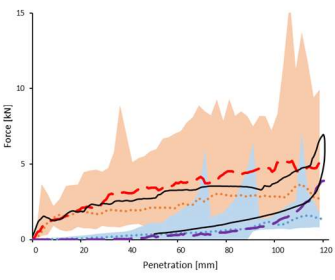
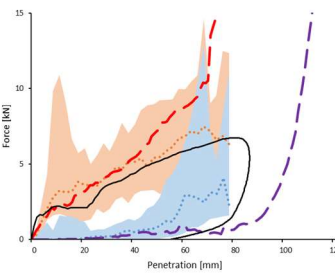
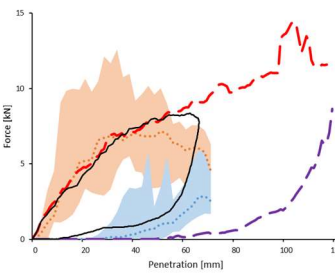
<b>Collision Speed Tram [km/h]</b>	<b>Collision Position [%]</b>	<b>Tram Front</b>
10	0% & 25%	Baseline & Improved
15	0% & 25%	Baseline & Improved
20	0% & 25%	Baseline & Improved
25	0% & 25%	Baseline & Improved
30	0% & 25%	Baseline & Improved
35	0% & 25%	Baseline & Improved
40	0% & 25%	Baseline & Improved
50	0% & 25%	Baseline & Improved
60	0% & 25%	Baseline & Improved

# 13 Appendix D: GV and Windscreen Validation

## 13.1 GVE Validation

The stiffness characteristics of the spoiler, bumper and bonnet leading edge of the GV models were compared to corridors from current fleet data from Feist et al. (2019). The results of the impactor tests can be seen in Table 13-1.

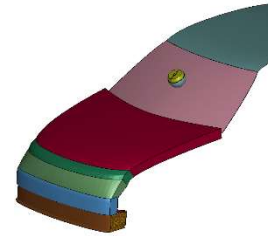
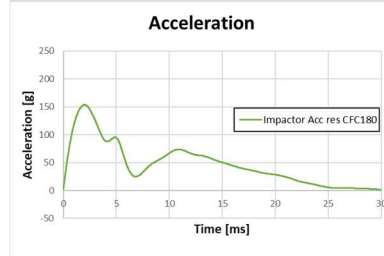
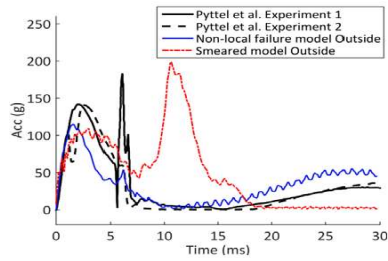
Table 13-1: Response of the impactor test (black) compared to the results reported in Feist et al. (2019).

Oblique spoiler test (SPV)	Bumper impact, horizontal (BMP)	Bonnet leading edge impact, oblique (BLE)
		
<p style="text-align: center;">SPV All</p> 	<p style="text-align: center;">BMP All</p> 	<p style="text-align: center;">BLE All</p> 
<p> <span style="color: orange;">■</span> CoHerent Study - Corridor Loading  <span style="color: orange;">●●●</span> CoHerent Study - Loading - Median  <span style="color: red;">—</span> GVTRv1 Study - Loading - Median         </p>		<p> <span style="color: blue;">■</span> CoHerent Study - Corridor Unloading  <span style="color: blue;">●●●</span> CoHerent Study - Unloading - Median  <span style="color: purple;">—</span> GVTRv1 Study - Unloading - Median         </p>

## 13.2 Windscreen Validation

As in the original GV models in accordance with the Euro NCAP Technical Bulletin TB024, the windscreen was modelled rigid, for injury assessment this windscreen has to be adjusted. Therefore, the windscreen was modelled with a solid PVC layer covered by two shell glass layers. By applying a head impactor test on the outside of the windscreen, the response of the windscreen was compared with the values reported in Alvarez and Kleiven (2016). Consequently, the impact velocity of the 4.58kg heavy head impactor was adjusted to 10.24m/s to achieve the same kinetic energy of 240J as reported by Alvarez and Kleiven (2016). The results can be seen in Table 13-2.

Table 13-2: Results reported by Alvarez and Kleiven (2016) (left), Impactor results with CFC180 filtered impactor acceleration (middle) and location of the head impactor impact on the windscreen (right).



# 14 Appendix E: Results of the meta-model for pedestrian-car cases

Table 14-1: Results of the meta-model for generic Sedan pedestrian Baseline in-crash cases.

Baseline								
	50M				50F			
	Min Value	Max Value	Max Error	Mean Absolut error	Min Value	Max Value	Max Error	Mean Absolut error
DAMAGE_MPS	0.0045	1.4489	0.3841	0.1411	0.0717	2.0519	0.2750	0.1156
HIC15	0.2256	11101	1702	816	0.1833	24801	2801	813
TX-Ribcage-Zero-Ribs-Broken	0.0000	1.0000	0.4733	0.1581	0.0000	1.0000	0.5461	0.2520
TX-Ribcage-One-Rib-Broken	0.0000	0.6170	0.2406	0.1276	0.0000	0.7911	0.3410	0.1640
TX-Ribcage-Two-Ribs-Broken	0.0000	0.3901	0.4437	0.1067	0.0000	0.5333	0.3079	0.0850
TX-Ribcage-Threepus-Ribs-Broken	0.0000	1.0000	0.2615	0.1025	0.0000	1.0000	0.3675	0.1148
LX-Knee-Ligament-aACL-L_strain	0.0634	0.4127	0.1246	0.0555	0.0633	0.3147	0.1205	0.0552
LX-Knee-Ligament-pACL-L_strain	0.0634	0.4127	0.1246	0.0555	0.0633	0.3147	0.1205	0.0552
LX-Knee-Ligament-aACL-R_strain	0.0321	0.4261	0.1565	0.0596	0.0708	0.5075	0.0779	0.0495
LX-Knee-Ligament-pACL-R_strain	0.0321	0.4261	0.1565	0.0596	0.0708	0.5075	0.0779	0.0495
LX-Knee-Ligament-aPCL-L_strain	0.0000	0.4880	0.0896	0.0340	0.0867	0.3777	0.1458	0.0368
LX-Knee-Ligament-pPCL-L_strain	0.0000	0.4880	0.0896	0.0340	0.0867	0.3777	0.1458	0.0368
LX-Knee-Ligament-aPCL-R_strain	0.0473	0.4875	0.1384	0.0492	0.0424	0.3958	0.1053	0.0562
LX-Knee-Ligament-pPCL-R_strain	0.0473	0.4875	0.1384	0.0492	0.0424	0.3958	0.1053	0.0562
LX-Knee-Ligament-MCL-L_strain	0.0343	0.5220	0.0985	0.0578	0.0622	0.3712	0.1664	0.0437
LX-Knee-Ligament-MCL-R_strain	0.0595	0.4087	0.1186	0.0513	0.0798	0.2946	0.0680	0.0366
LX-Knee-Ligament-LCL-L_strain	0.1292	0.8873	0.1428	0.0811	0.0762	0.6391	0.1410	0.0744

LX-Knee-Ligament-LCL-R_strain	0.1363	0.9596	0.1991	0.1071	0.1242	0.7561	0.1902	0.0779
LX-Bone-Femur-Cortical-Proximal-L_99PS	0.0015	0.1547	0.0052	0.0026	0.0013	0.0952	0.0131	0.0037
LX-Bone-Femur-Cortical-Proximal-R_99PS	0.0012	0.0768	0.0067	0.0026	0.0013	0.1033	0.0210	0.0062
LX-Bone-Femur-Cortical-Shaft-L_99PS	0.0011	0.1045	0.0207	0.0043	0.0016	0.0774	0.0230	0.0041
LX-Bone-Femur-Cortical-Shaft-R_99PS	0.0010	0.0640	0.0052	0.0016	0.0019	0.0633	0.0119	0.0028
LX-Bone-Tibia-shaft-Cortical-L_99PS	0.0010	0.0426	0.0008	0.0004	0.0014	0.0143	0.0011	0.0004
LX-Bone-Tibia-shaft-Cortical-R_99PS	0.0010	0.0242	0.0009	0.0004	0.0012	0.0114	0.0013	0.0006

Table 14-2: Results of the meta-model for generic Sedan pedestrian in-crash AEB cases.

AEB								
	50M				50F			
	Min Value	Max Value	Max Error	Mean Absolut error	Min Value	Max Value	Max Error	Mean Absolut error
DAMAGE_MPS	0.0357	0.9718	0.2548	0.0924	0.0306	1.2929	0.2495	0.0757
HIC15	0	5768	1785	484	0	6999	349	188
TX-Ribcage-Zero-Ribs-Broken	0.0000	1.0000	0.4875	0.1770	0.0477	1.0000	0.4819	0.1712
TX-Ribcage-One-Rib-Broken	0.0000	0.4290	0.6445	0.1271	0.0000	0.5178	0.2840	0.1474
TX-Ribcage-Two-Ribs-Broken	0.0000	0.4460	0.0649	0.0409	0.0000	0.3686	0.1662	0.0651
TX-Ribcage-Threeplus-Ribs-Broken	0.0000	0.9999	0.1556	0.0837	0.0000	0.1147	0.3430	0.0531
LX-Knee-Ligament-aACL-L_strain	0.0335	0.3293	0.1036	0.0528	0.0145	0.2892	0.1296	0.0550
LX-Knee-Ligament-pACL-L_strain	0.0335	0.3293	0.1036	0.0528	0.0145	0.2892	0.1296	0.0550
LX-Knee-Ligament-aACL-R_strain	0.0250	0.3706	0.0817	0.0493	0.0186	0.3596	0.1283	0.0641
LX-Knee-Ligament-pACL-R_strain	0.0250	0.3706	0.0817	0.0493	0.0186	0.3596	0.1283	0.0641
LX-Knee-Ligament-aPCL-L_strain	0.0000	0.4165	0.1148	0.0285	0.0229	0.3612	0.0956	0.0267
LX-Knee-Ligament-pPCL-L_strain	0.0000	0.4165	0.1148	0.0285	0.0229	0.3612	0.0956	0.0267
LX-Knee-Ligament-aPCL-R_strain	0.0257	0.4596	0.0941	0.0357	0.0094	0.3317	0.0714	0.0310
LX-Knee-Ligament-pPCL-R_strain	0.0257	0.4596	0.0941	0.0357	0.0094	0.3317	0.0714	0.0310
LX-Knee-Ligament-MCL-L_strain	0.0270	0.3937	0.0917	0.0223	0.0432	0.3016	0.0891	0.0257
LX-Knee-Ligament-MCL-R_strain	0.0000	0.3120	0.1033	0.0339	0.0000	0.2192	0.0484	0.0268
LX-Knee-Ligament-LCL-L_strain	0.0280	0.5130	0.1426	0.0608	0.0243	0.4833	0.2184	0.0678
LX-Knee-Ligament-LCL-R_strain	0.1118	0.8857	0.2508	0.0932	0.0513	0.6766	0.2158	0.0743
LX-Bone-Femur-Cortical-Proximal-L_99PS	0.0013	0.0110	0.0035	0.0015	0.0012	0.0367	0.0049	0.0025
LX-Bone-Femur-Cortical-Proximal-R_99PS	0.0006	0.0175	0.0040	0.0017	0.0007	0.0272	0.0077	0.0029



LX-Bone-Femur-Cortical-Shaft-L_99PS	0.0009	0.0369	0.0029	0.0018	0.0012	0.0400	0.0037	0.0015
LX-Bone-Femur-Cortical-Shaft-R_99PS	0.0006	0.0265	0.0112	0.0034	0.0006	0.0241	0.0079	0.0029
LX-Bone-Tibia-shaft-Cortical-L_99PS	0.0006	0.0046	0.0008	0.0004	0.0006	0.0054	0.0006	0.0003
LX-Bone-Tibia-shaft-Cortical-R_99PS	0.0009	0.0056	0.0008	0.0004	0.0009	0.0086	0.0008	0.0004

**INPUT INJURY PROBABILITIES**



Injury group		Injury probability											
		Male						Female					
		before intervention			after intervention			before intervention			after intervention		
		lower	best estimate	upper	lower	best estimate	upper	lower	best estimate	upper	lower	best estimate	upper
1a	Concussion AIS1	8.09%	8.09%	8.09%	6.88%	6.88%	6.88%	7.21%	7.21%	7.21%	8.02%	8.02%	8.02%
1b	Concussion AIS2	24.43%	24.43%	24.43%	16.59%	16.59%	16.59%	22.93%	22.93%	22.93%	18.52%	18.52%	18.52%
1c	Concussion AIS4+	38.87%	38.87%	38.87%	14.20%	14.20%	14.20%	45.79%	45.79%	45.79%	15.12%	15.12%	15.12%
2	Other skull-brain injury	43.17%	43.17%	43.17%	22.88%	22.88%	22.88%	40.62%	40.62%	40.62%	13.58%	13.58%	13.58%
11a	Fracture of 1 rib AIS1	14.67%	14.67%	14.67%	5.10%	5.10%	5.10%	13.60%	13.60%	13.60%	12.97%	12.97%	12.97%
11b	Fracture of 2 ribs AIS2	8.64%	8.64%	8.64%	5.30%	5.30%	5.30%	8.10%	8.10%	8.10%	2.68%	2.68%	2.68%
11c	Fracture of 3+ ribs AIS3+	27.39%	27.39%	27.39%	14.16%	14.16%	14.16%	17.54%	17.54%	17.54%	0.54%	0.54%	0.54%
22a	Fracture of hip - left	7.14%	17.74%	30.82%	2.00%	12.58%	27.00%	16.21%	25.98%	37.63%	7.28%	15.93%	27.27%
22b	Fracture of hip - right	9.69%	18.01%	28.73%	2.78%	10.07%	20.64%	36.94%	47.95%	57.37%	6.42%	17.32%	30.27%
23a	Fracture of femur shaft - left	12.08%	18.35%	25.25%	3.68%	9.49%	16.62%	11.34%	17.14%	23.89%	2.66%	6.82%	12.44%
23b	Fracture of femur shaft - right	15.88%	26.39%	36.97%	0.55%	3.21%	8.32%	12.48%	22.75%	33.55%	0.47%	3.08%	8.23%
24a	Fracture of knee/lower leg - left	1.54%	2.61%	5.28%	0.02%	0.10%	1.04%	0.16%	1.22%	4.66%	0.02%	0.21%	1.58%
24b	Fracture of knee/lower leg - right	1.61%	3.51%	7.46%	0.02%	0.24%	1.74%	0.53%	3.58%	9.64%	0.04%	0.61%	2.78%
27a	Dislocation/sprain/strain of knee - left	98.22%	98.22%	98.22%	94.57%	94.57%	94.57%	92.94%	92.94%	92.94%	83.26%	83.26%	83.26%
27b	Dislocation/sprain/strain of knee - right	99.60%	99.60%	99.60%	96.52%	96.52%	96.52%	98.96%	98.96%	98.96%	92.92%	92.92%	92.92%

Figure 14-1: Results of the overall injury assessment for pedestrian to generic Sedan scenarios based on the predicted injuries by the meta-model and the occurrence probability.

Table 14-3: Results of the meta-model for the SotA SUV pedestrian in-crash AEB scenarios.

AEB								
	50M				50F			
	Min Value	Max Value	Max Error	Mean Absolut error	Min Value	Max Value	Max Error	Mean Absolut error
DAMAGE_MPS	0.0197	1.0764	0.2711	0.1134	0.0061	1.3891	0.2250	0.1211
HIC15	0	3811	539	227	0	4529	1036	312
TX-Ribcage-Zero-Ribs-Broken	0.0007	1.0000	0.3762	0.1583	0.0000	1.0000	0.4028	0.2404
TX-Ribcage-One-Rib-Broken	0.0000	0.5056	0.3924	0.1663	0.0000	0.5639	0.2760	0.1117
TX-Ribcage-Two-Ribs-Broken	0.0000	0.4288	0.1857	0.0589	0.0000	0.4492	0.1711	0.0885
TX-Ribcage-Threepius-Ribs-Broken	0.0000	0.8974	0.0970	0.0384	0.0000	0.9999	0.5623	0.1612
LX-Knee-Ligament-aACL-L_strain	0.0271	0.2913	0.0849	0.0482	0.0212	0.2653	0.1296	0.0558
LX-Knee-Ligament-pACL-L_strain	0.0271	0.2913	0.0849	0.0482	0.0212	0.2653	0.1296	0.0558
LX-Knee-Ligament-aACL-R_strain	0.0127	0.3973	0.1180	0.0487	0.0046	0.3999	0.1948	0.0667
LX-Knee-Ligament-pACL-R_strain	0.0127	0.3973	0.1180	0.0487	0.0046	0.3999	0.1948	0.0667
LX-Knee-Ligament-aPCL-L_strain	0.0000	0.3114	0.0983	0.0446	0.0164	0.3432	0.1469	0.0378
LX-Knee-Ligament-pPCL-L_strain	0.0000	0.3114	0.0983	0.0446	0.0164	0.3432	0.1469	0.0378
LX-Knee-Ligament-aPCL-R_strain	0.0095	0.3348	0.0767	0.0448	0.0019	0.3451	0.1491	0.0485
LX-Knee-Ligament-pPCL-R_strain	0.0095	0.3348	0.0767	0.0448	0.0019	0.3451	0.1491	0.0485
LX-Knee-Ligament-MCL-L_strain	0.0346	0.4337	0.0464	0.0245	0.0431	0.4462	0.0516	0.0381
LX-Knee-Ligament-MCL-R_strain	0.0080	0.3529	0.1180	0.0724	0.0279	0.3861	0.0884	0.0494
LX-Knee-Ligament-LCL-L_strain	0.0538	0.5414	0.1808	0.1044	0.0000	0.4701	0.2464	0.1550
LX-Knee-Ligament-LCL-R_strain	0.0104	0.8939	0.2009	0.0933	0.0000	0.7185	0.2741	0.1180
LX-Bone-Femur-Cortical-Proximal-L_99PS	0.0017	0.0468	0.0025	0.0013	0.0006	0.0381	0.0040	0.0016

LX-Bone-Femur-Cortical-Proximal-R_99PS	0.0003	0.0163	0.0046	0.0020	0.0004	0.0257	0.0047	0.0019
LX-Bone-Femur-Cortical-Shaft-L_99PS	0.0008	0.0174	0.0018	0.0008	0.0011	0.0305	0.0033	0.0016
LX-Bone-Femur-Cortical-Shaft-R_99PS	0.0004	0.0233	0.0061	0.0023	0.0005	0.0288	0.0036	0.0021
LX-Bone-Tibia-shaft-Cortical-L_99PS	0.0005	0.0188	0.0019	0.0007	0.0008	0.0166	0.0026	0.0011
LX-Bone-Tibia-shaft-Cortical-R_99PS	0.0006	0.0116	0.0025	0.0011	0.0007	0.0081	0.0018	0.0009

**INPUT INJURY PROBABILITIES**



Injury group		Injury probability											
		Male						Female					
		Generic Sedan			SotA SUV			Generic Sedan			SotA SUV		
	lower	best estimate	upper	lower	best estimate	upper	lower	best estimate	upper	lower	best estimate	upper	
1a	Concussion AIS1	6.88%	6.88%	6.88%	7.51%	7.51%	7.51%	8.02%	8.02%	8.02%	6.82%	6.82%	6.82%
1b	Concussion AIS2	16.59%	16.59%	16.59%	17.96%	17.96%	17.96%	18.52%	18.52%	18.52%	18.25%	18.25%	18.25%
1c	Concussion AIS4+	14.20%	14.20%	14.20%	13.24%	13.24%	13.24%	15.12%	15.12%	15.12%	24.63%	24.63%	24.63%
2	Other skull-brain injury	22.88%	22.88%	22.88%	15.94%	15.94%	15.94%	13.58%	13.58%	13.58%	18.47%	18.47%	18.47%
11a	Fracture of 1 rib AIS1	5.10%	5.10%	5.10%	10.47%	10.47%	10.47%	12.97%	12.97%	12.97%	16.97%	16.97%	16.97%
11b	Fracture of 2 ribs AIS2	5.30%	5.30%	5.30%	4.34%	4.34%	4.34%	2.68%	2.68%	2.68%	12.26%	12.26%	12.26%
11c	Fracture of 3+ ribs AIS3+	14.16%	14.16%	14.16%	6.02%	6.02%	6.02%	0.54%	0.54%	0.54%	20.30%	20.30%	20.30%
22a	Fracture of hip - left	2.00%	12.58%	27.00%	4.30%	14.61%	28.12%	7.28%	15.93%	27.27%	2.84%	10.80%	22.56%
22b	Fracture of hip - right	2.78%	10.07%	20.64%	1.61%	10.07%	22.44%	6.42%	17.32%	30.27%	3.16%	10.13%	20.15%
23a	Fracture of femur shaft - left	3.68%	9.49%	16.62%	0.07%	0.84%	3.21%	2.66%	6.82%	12.44%	0.37%	1.98%	5.49%
23b	Fracture of femur shaft - right	0.55%	3.21%	8.32%	0.30%	2.37%	6.78%	0.47%	3.08%	8.23%	0.60%	3.41%	8.74%
24a	Fracture of knee/lower leg - left	0.02%	0.10%	1.04%	3.55%	6.14%	9.56%	0.02%	0.21%	1.58%	3.71%	7.02%	11.29%
24b	Fracture of knee/lower leg - right	0.02%	0.24%	1.74%	0.21%	1.40%	4.14%	0.04%	0.61%	2.78%	0.03%	0.57%	2.74%
27a	Dislocation/sprain/strain of knee - left	94.57%	94.57%	94.57%	85.74%	85.74%	85.74%	83.26%	83.26%	83.26%	83.38%	83.38%	83.38%
27b	Dislocation/sprain/strain of knee - right	96.52%	96.52%	96.52%	91.65%	91.65%	91.65%	92.92%	92.92%	92.92%	84.53%	84.53%	84.53%

Figure 14-2: Results of the overall injury assessment for the AEB pedestrian generic Sedan and SotA SUV scenarios based on the predicted injuries by the meta-model and the occurrence probability.



## COST-BENEFIT TOOL FOR VEHICLE SAFETY

*Measure: Generic Sedan baseline simulations vs. SotA SUV AEB simulations for pedestrians*

Input	<i>lower</i>	<i>best estimate</i>	<i>upper</i>	Results	<i>lower</i>	<i>best estimate</i>	<i>upper</i>
<b>Costs per vehicle</b>				<b>Total costs</b>	€ 2,000	€ 2,500	€ 3,000
- Development costs				<b>Number of injuries prevented</b>			
- Manufacturing costs	€ 2,000	€ 2,500	€ 3,000	- Yearly	0.0014	0.0016	0.0018
- Repair/replacement costs after a crash				- Total vehicle lifetime	0.022	0.024	0.027
<b>Crash risk (number of target crashes per vehicle per year)</b>				- 1 injury prevented per ... vehicles	46	42	37
- before intervention	0.0003959	0.0003993	0.0004027	<b>Quality of life improvement (QALYs)</b>			
- after intervention	0.0000740	0.0000747	0.0000753	- Yearly	0.0014	0.0017	0.0022
<b>Road user characteristics</b>				- Total vehicle lifetime	0.021	0.026	0.033
- Number of target road users per vehicle		1		- 1 QALY gained per ... vehicles	48	38	31
- Average age casualties: - male		50		<b>Benefits</b>			
- female		50		- Quality of life gains	€ 1,164	€ 1,462	€ 1,813
- Life expectancy: - male		78		- Medical costs reduction	€ 111	€ 137	€ 166
- female		83		- Productivity gains	€ 275	€ 362	€ 466
- Proportion male target road user		52%		- Total benefits	€ 1,551	€ 1,961	€ 2,445
<b>Vehicle life time (years)</b>		15		<b>Socio-economic return</b>			
<b>Discount rate</b>		3.0%		- Net present value	-€ 1,449	-€ 539	€ 445
				- Benefit-cost ratio	0.5	0.8	1.2

Figure 14-3: CBA analysis of generic Sedan baseline simulations compared with SotA SUV AEB simulations for pedestrians.

# 15 Appendix F: Results of the meta-model for cyclist-car cases

Table 15-1: Results of the meta-model for generic Sedan cyclist in-crash baseline scenarios.

AEB								
	50M				50F			
	Min Value	Max Value	Max Error	Mean Absolut error	Min Value	Max Value	Max Error	Mean Absolut error
DAMAGE_MPS	0.0222	1.1995	0.5750	0.2118	0.0000	1.4450	0.7400	0.3490
HIC15	0	4715	1322	737	0	7093	13831	3576
TX-Ribcage-Zero-Ribs-Broken	0.0000	1.0000	0.3716	0.2329	0.0000	1.0000	0.7486	0.4017
TX-Ribcage-One-Rib-Broken	0.0000	0.8656	0.4172	0.1406	0.0000	0.8471	0.3326	0.1719
TX-Ribcage-Two-Ribs-Broken	0.0000	0.4270	0.2077	0.0622	0.0000	0.3346	0.3408	0.1594
TX-Ribcage-Threepius-Ribs-Broken	0.0000	1.0000	0.6886	0.3175	0.0000	0.9999	0.8271	0.2410
LX-Knee-Ligament-aACL-L_strain	0.0136	0.3711	0.0779	0.0420	0.0530	0.3365	0.1305	0.0635
LX-Knee-Ligament-pACL-L_strain	0.0136	0.3711	0.0779	0.0420	0.0530	0.3365	0.1305	0.0635
LX-Knee-Ligament-aACL-R_strain	0.0093	0.4089	0.1066	0.0460	0.0000	0.4451	0.1143	0.0484
LX-Knee-Ligament-pACL-R_strain	0.0093	0.4089	0.1066	0.0460	0.0000	0.4451	0.1143	0.0484
LX-Knee-Ligament-aPCL-L_strain	0.0376	0.3947	0.1039	0.0302	0.0772	0.2898	0.1018	0.0523
LX-Knee-Ligament-pPCL-L_strain	0.0376	0.3947	0.1039	0.0302	0.0772	0.2898	0.1018	0.0523
LX-Knee-Ligament-aPCL-R_strain	0.0567	0.3497	0.1829	0.0455	0.0190	0.3304	0.1614	0.0776
LX-Knee-Ligament-pPCL-R_strain	0.0567	0.3497	0.1829	0.0455	0.0190	0.3304	0.1614	0.0776
LX-Knee-Ligament-MCL-L_strain	0.0496	0.4642	0.0665	0.0356	0.0395	0.3024	0.1177	0.0461
LX-Knee-Ligament-MCL-R_strain	0.0532	0.4131	0.1075	0.0449	0.0138	0.2930	0.0961	0.0424
LX-Knee-Ligament-LCL-L_strain	0.0081	0.6433	0.1710	0.0806	0.0000	0.6580	0.2787	0.1097

LX-Knee-Ligament-LCL-R_strain	0.0774	0.7876	0.2885	0.1251	0.0161	0.8285	0.2196	0.0967
LX-Bone-Femur-Cortical-Proximal-L_99PS	0.0019	0.1117	0.0470	0.0109	0.0013	0.0551	0.0068	0.0020
LX-Bone-Femur-Cortical-Proximal-R_99PS	0.0005	0.0561	0.0087	0.0024	0.0003	0.1055	0.0511	0.0160
LX-Bone-Femur-Cortical-Shaft-L_99PS	0.0005	0.0968	0.0097	0.0027	0.0009	0.0955	0.0936	0.0363
LX-Bone-Femur-Cortical-Shaft-R_99PS	0.0004	0.0654	0.0125	0.0051	0.0004	0.1572	0.1310	0.0260
LX-Bone-Tibia-shaft-Cortical-L_99PS	0.0002	0.0099	0.0031	0.0012	0.0004	0.0090	0.0027	0.0012
LX-Bone-Tibia-shaft-Cortical-R_99PS	0.0002	0.0384	0.0184	0.0054	0.0001	0.0449	0.0225	0.0088



Table 15-2: Results of the meta-model for the generic Sedan cyclist in-crash AEB scenarios.

AEB								
	50M				50F			
	Min Value	Max Value	Max Error	Mean Absolut error	Min Value	Max Value	Max Error	Mean Absolut error
DAMAGE_MPS	0.0225	1.3332	0.2756	0.1091	0.0026	1.1139	0.5047	0.1802
HIC15	0	3987	1116	276	0	5142	3499	1028
TX-Ribcage-Zero-Ribs-Broken	0.0000	1.0000	0.3963	0.1757	0.0000	1.0000	0.3517	0.1132
TX-Ribcage-One-Rib-Broken	0.0000	0.7805	0.2155	0.0736	0.0000	0.6310	0.3834	0.0862
TX-Ribcage-Two-Ribs-Broken	0.0000	0.4440	0.0674	0.0484	0.0000	0.4756	0.2072	0.0645
TX-Ribcage-Threepius-Ribs-Broken	0.0000	1.0000	0.4757	0.1758	0.0000	0.9775	0.5414	0.1998
LX-Knee-Ligament-aACL-L_strain	0.0000	0.4518	0.1221	0.0458	0.0217	0.3328	0.1836	0.0753
LX-Knee-Ligament-pACL-L_strain	0.0000	0.4518	0.1221	0.0458	0.0217	0.3328	0.1836	0.0753
LX-Knee-Ligament-aACL-R_strain	0.0044	0.4770	0.1841	0.0507	0.0000	0.3277	0.1419	0.0585
LX-Knee-Ligament-pACL-R_strain	0.0044	0.4770	0.1841	0.0507	0.0000	0.3277	0.1419	0.0585
LX-Knee-Ligament-aPCL-L_strain	0.0280	0.4119	0.1223	0.0466	0.0285	0.3081	0.0927	0.0402
LX-Knee-Ligament-pPCL-L_strain	0.0280	0.4119	0.1223	0.0466	0.0285	0.3081	0.0927	0.0402
LX-Knee-Ligament-aPCL-R_strain	0.0414	0.3524	0.0948	0.0460	0.0190	0.3315	0.1240	0.0677
LX-Knee-Ligament-pPCL-R_strain	0.0414	0.3524	0.0948	0.0460	0.0190	0.3315	0.1240	0.0677
LX-Knee-Ligament-MCL-L_strain	0.0215	0.4341	0.1447	0.0553	0.0192	0.3368	0.1294	0.0457
LX-Knee-Ligament-MCL-R_strain	0.0432	0.6262	0.4587	0.0768	0.0138	0.3599	0.3804	0.0904

LX-Knee-Ligament- LCL-L_strain	0.0000	0.5242	0.2451	0.0730	0.0081	0.7029	0.3708	0.0991
LX-Knee-Ligament- LCL-R_strain	0.0788	0.7263	0.4318	0.1386	0.0161	0.7550	0.3834	0.1585
LX-Bone-Femur- Cortical-Proximal- L_99PS	0.0015	0.0388	0.0034	0.0017	0.0014	0.0560	0.0095	0.0031
LX-Bone-Femur- Cortical-Proximal- R_99PS	0.0005	0.0487	0.0119	0.0042	0.0003	0.1584	0.0726	0.0206
LX-Bone-Femur- Cortical-Shaft-L_99PS	0.0005	0.0658	0.0189	0.0045	0.0006	0.1240	0.1023	0.0243
LX-Bone-Femur- Cortical-Shaft-R_99PS	0.0004	0.0363	0.0151	0.0034	0.0004	0.1591	0.0245	0.0106
LX-Bone-Tibia-shaft- Cortical-L_99PS	0.0002	0.0108	0.0015	0.0007	0.0003	0.0102	0.0015	0.0008
LX-Bone-Tibia-shaft- Cortical-R_99PS	0.0002	0.0218	0.0198	0.0036	0.0001	0.0301	0.0143	0.0042

**INPUT INJURY PROBABILITIES**



Injury group		Injury probability											
		Male						Female					
		before intervention			after intervention			before intervention			after intervention		
		lower	best estimate	upper	lower	best estimate	upper	lower	best estimate	upper	lower	best estimate	upper
1a	Concussion AIS1	5.91%	5.91%	5.91%	3.61%	3.61%	3.61%	6.19%	6.19%	6.19%	4.00%	4.00%	4.00%
1b	Concussion AIS2	15.64%	15.64%	15.64%	8.13%	8.13%	8.13%	15.91%	15.91%	15.91%	10.38%	10.38%	10.38%
1c	Concussion AIS4+	11.73%	11.73%	11.73%	4.32%	4.32%	4.32%	16.57%	16.57%	16.57%	8.99%	8.99%	8.99%
2	Other skull-brain injury	23.57%	23.57%	23.57%	10.28%	10.28%	10.28%	23.24%	23.24%	23.24%	14.24%	14.24%	14.24%
11a	Fracture of 1 rib AIS1	8.57%	8.57%	8.57%	5.58%	5.58%	5.58%	10.74%	10.74%	10.74%	4.59%	4.59%	4.59%
11b	Fracture of 2 ribs AIS2	4.10%	4.10%	4.10%	4.73%	4.73%	4.73%	2.10%	2.10%	2.10%	2.94%	2.94%	2.94%
11c	Fracture of 3+ ribs AIS3+	23.44%	23.44%	23.44%	13.49%	13.49%	13.49%	10.25%	10.25%	10.25%	7.25%	7.25%	7.25%
22a	Fracture of hip - left	14.69%	22.96%	32.73%	1.10%	6.19%	15.49%	6.13%	15.23%	26.55%	1.39%	10.70%	24.61%
22b	Fracture of hip - right	5.54%	16.93%	30.68%	2.85%	13.06%	27.01%	22.37%	40.10%	55.94%	32.03%	57.71%	76.97%
23a	Fracture of femur shaft - left	9.81%	13.92%	18.56%	0.23%	1.07%	3.69%	12.08%	17.39%	23.21%	11.83%	15.54%	19.37%
23b	Fracture of femur shaft - right	0.85%	3.11%	7.12%	0.07%	0.60%	2.54%	1.36%	5.94%	14.11%	0.31%	3.73%	11.44%
24a	Fracture of knee/lower leg - left	0.04%	0.53%	2.33%	0.02%	0.07%	0.63%	0.03%	0.38%	2.18%	0.02%	0.09%	0.76%
24b	Fracture of knee/lower leg - right	10.88%	14.53%	18.60%	1.42%	3.12%	5.80%	21.20%	25.31%	29.53%	4.80%	7.06%	9.84%
27a	Dislocation/sprain/strain of knee - left	78.30%	78.30%	78.30%	72.90%	72.90%	72.90%	90.02%	90.02%	90.02%	71.22%	71.22%	71.22%
27b	Dislocation/sprain/strain of knee - right	93.04%	93.04%	93.04%	93.23%	93.23%	93.23%	94.00%	94.00%	94.00%	76.57%	76.57%	76.57%

Figure 15-1: Results of the overall injury assessment for cyclist-GV scenarios based on the predicted injuries by the meta-model and the occurrence probability.

Table 15-3: Results of the meta-model for SotA SUV cyclist in-crash AEB scenarios.

AEB								
	50M				50F			
	Min Value	Max Value	Max Error	Mean Absolut error	Min Value	Max Value	Max Error	Mean Absolut error
DAMAGE_MPS	0.0001	1.2176	0.3692	0.1696	0.0002	1.3040	0.5514	0.2457
HIC15	0	1919	924	307	0	2037	378	163
TX-Ribcage-Zero-Ribs-Broken	0.0000	1.0000	0.6309	0.2050	0.0000	1.0000	0.4763	0.2290
TX-Ribcage-One-Rib-Broken	0.0000	0.4883	0.3869	0.1725	0.0000	0.7955	0.2565	0.1167
TX-Ribcage-Two-Ribs-Broken	0.0000	0.4968	0.3393	0.0912	0.0000	0.4325	0.2310	0.0775
TX-Ribcage-Threeplus-Ribs-Broken	0.0000	0.9953	0.9564	0.1821	0.0000	0.9950	0.7283	0.2605
LX-Knee-Ligament-aACL-L_strain	0.0000	0.2857	0.1604	0.0737	0.0000	0.3076	0.1405	0.0629
LX-Knee-Ligament-pACL-L_strain	0.0000	0.2857	0.1604	0.0737	0.0000	0.3076	0.1405	0.0629
LX-Knee-Ligament-aACL-R_strain	0.0097	0.3149	0.1293	0.0406	0.0000	0.2954	0.1557	0.0539
LX-Knee-Ligament-pACL-R_strain	0.0097	0.3149	0.1293	0.0406	0.0000	0.2954	0.1557	0.0539
LX-Knee-Ligament-aPCL-L_strain	0.0081	0.3740	0.2138	0.0988	0.0238	0.3227	0.1585	0.0818
LX-Knee-Ligament-pPCL-L_strain	0.0081	0.3740	0.2138	0.0988	0.0238	0.3227	0.1585	0.0818
LX-Knee-Ligament-aPCL-R_strain	0.0068	0.3801	0.1625	0.0917	0.0039	0.3328	0.1427	0.0937
LX-Knee-Ligament-pPCL-R_strain	0.0068	0.3801	0.1625	0.0917	0.0039	0.3328	0.1427	0.0937
LX-Knee-Ligament-MCL-L_strain	0.0099	0.3294	0.1669	0.0553	0.0068	0.3386	0.1016	0.0414
LX-Knee-Ligament-MCL-R_strain	0.0000	0.4476	0.1239	0.0535	0.0000	0.3722	0.1518	0.0738
LX-Knee-Ligament-LCL-L_strain	0.0000	0.6676	0.2618	0.0917	0.0000	0.6583	0.2922	0.1033
LX-Knee-Ligament-LCL-R_strain	0.0128	0.7230	0.1694	0.0783	0.0030	0.3767	0.1532	0.0629
LX-Bone-Femur-Cortical-Proximal-L_99PS	0.0002	0.0456	0.0194	0.0058	0.0002	0.0252	0.0152	0.0042

LX-Bone-Femur-Cortical-Proximal-R_99PS	0.0002	0.1295	0.0389	0.0084	0.0002	0.2149	0.0815	0.0225
LX-Bone-Femur-Cortical-Shaft-L_99PS	0.0004	0.0607	0.0308	0.0162	0.0003	0.0608	0.0161	0.0070
LX-Bone-Femur-Cortical-Shaft-R_99PS	0.0002	0.1017	0.0259	0.0085	0.0003	0.0716	0.0523	0.0102
LX-Bone-Tibia-shaft-Cortical-L_99PS	0.0001	0.0079	0.0020	0.0008	0.0003	0.0208	0.0090	0.0028
LX-Bone-Tibia-shaft-Cortical-R_99PS	0.0001	0.0066	0.0043	0.0014	0.0001	0.0228	0.0295	0.0102

**INPUT INJURY PROBABILITIES**



Injury group	Injury probability											
	Male						Female					
	Generic Sedan			SotA SUV			Generic Sedan			SotA SUV		
	lower	best estimate	upper	lower	best estimate	upper	lower	best estimate	upper	lower	best estimate	upper
1a Concussion AIS1	3.61%	3.61%	3.61%	3.98%	3.98%	3.98%	4.00%	4.00%	4.00%	4.16%	4.16%	4.16%
1b Concussion AIS2	8.13%	8.13%	8.13%	9.17%	9.17%	9.17%	10.38%	10.38%	10.38%	10.46%	10.46%	10.46%
1c Concussion AIS4+	4.32%	4.32%	4.32%	6.08%	6.08%	6.08%	8.99%	8.99%	8.99%	8.38%	8.38%	8.38%
2 Other skull-brain injury	10.28%	10.28%	10.28%	6.23%	6.23%	6.23%	14.24%	14.24%	14.24%	3.81%	3.81%	3.81%
11a Fracture of 1 rib AIS1	5.58%	5.58%	5.58%	6.62%	6.62%	6.62%	4.59%	4.59%	4.59%	6.00%	6.00%	6.00%
11b Fracture of 2 ribs AIS2	4.73%	4.73%	4.73%	2.91%	2.91%	2.91%	2.94%	2.94%	2.94%	2.43%	2.43%	2.43%
11c Fracture of 3+ ribs AIS3+	13.49%	13.49%	13.49%	2.00%	2.00%	2.00%	7.25%	7.25%	7.25%	5.79%	5.79%	5.79%
22a Fracture of hip - left	1.10%	6.19%	15.49%	1.73%	5.93%	13.77%	1.39%	10.70%	24.61%	4.00%	9.10%	16.71%
22b Fracture of hip - right	2.85%	13.06%	27.01%	6.35%	25.67%	44.75%	32.03%	57.71%	76.97%	12.96%	36.91%	57.16%
23a Fracture of femur shaft - left	0.23%	1.07%	3.69%	1.58%	4.03%	7.89%	11.83%	15.54%	19.37%	0.45%	1.79%	4.85%
23b Fracture of femur shaft - right	0.07%	0.60%	2.54%	0.07%	1.20%	5.21%	0.31%	3.73%	11.44%	0.16%	1.24%	4.70%
24a Fracture of knee/lower leg - left	0.02%	0.07%	0.63%	0.02%	0.07%	0.55%	0.02%	0.09%	0.76%	0.88%	1.75%	3.48%
24b Fracture of knee/lower leg - right	1.42%	3.12%	5.80%	0.02%	0.07%	0.52%	4.80%	7.06%	9.84%	0.49%	1.32%	3.25%
27a Dislocation/sprain/strain of knee - left	72.90%	72.90%	72.90%	72.42%	72.42%	72.42%	71.22%	71.22%	71.22%	72.23%	72.23%	72.23%
27b Dislocation/sprain/strain of knee - right	93.23%	93.23%	93.23%	81.52%	81.52%	81.52%	76.57%	76.57%	76.57%	74.36%	74.36%	74.36%

Figure 15-2: Results of the overall injury assessment for AEB cyclist generic Sedan and SotA SUV scenarios based on the predicted injuries by the meta-model and the occurrence probability.



## COST-BENEFIT TOOL FOR VEHICLE SAFETY

*Measure: Generic Sedan baseline simulations vs. SotA SUV AEB simulations for cyclists*

Input	<i>lower</i>	<i>best estimate</i>	<i>upper</i>	Results	<i>lower</i>	<i>best estimate</i>	<i>upper</i>
<b>Costs per vehicle</b>				<b>Total costs</b>	€ 2,000	€ 2,500	€ 3,000
- Development costs				<b>Number of injuries prevented</b>			
- Manufacturing costs	€ 2,000	€ 2,500	€ 3,000	- Yearly	0.0007	0.0008	0.0009
- Repair/replacement costs after a crash				- Total vehicle lifetime	0.011	0.012	0.013
<b>Crash risk (number of target crashes per vehicle per year)</b>				- 1 injury prevented per ... vehicles	94	85	74
- before intervention	0.0005151	0.0005189	0.0005227	<b>Quality of life improvement (QALYs)</b>			
- after intervention	0.000238	0.000240	0.000241	- Yearly	0.0005	0.0007	0.0010
<b>Road user characteristics</b>				- Total vehicle lifetime	0.008	0.011	0.015
- Number of target road users per vehicle		1		- 1 QALY gained per ... vehicles	130	93	67
- Average age casualties: - male		50		<b>Benefits</b>			
- female		50		- Quality of life gains	€ 429	€ 596	€ 831
- Life expectancy: - male		78		- Medical costs reduction	€ 46	€ 60	€ 80
- female		83		- Productivity gains	€ 90	€ 120	€ 167
- Proportion male target road user		66%		- Total benefits	€ 564	€ 776	€ 1,077
<b>Vehicle life time (years)</b>		15		<b>Socio-economic return</b>			
<b>Discount rate</b>		3.0%		- Net present value	-€ 2,436	-€ 1,724	-€ 923
				- Benefit-cost ratio	0.2	0.3	0.5

Figure 15-3: CBA analysis of generic Sedan baseline simulations compared with SotA SUV AEB simulations for cyclists.

# 16 Appendix G: Results of Tram in-crash simulations

Injury group		Injury probability											
		Male						Female					
		before intervention			after intervention			before intervention			after intervention		
		lower	best estimate	upper	lower	best estimate	upper	lower	best estimate	upper	lower	best estimate	upper
1a	Concussion AIS1	12.58%	12.58%	12.58%	14.41%	14.41%	14.41%	8.55%	8.55%	8.55%	12.60%	12.60%	12.60%
1b	Concussion AIS2	38.88%	38.88%	38.88%	37.23%	37.23%	37.23%	34.34%	34.34%	34.34%	34.95%	34.95%	34.95%
1c	Concussion AIS4+	30.20%	30.20%	30.20%	17.66%	17.66%	17.66%	41.64%	41.64%	41.64%	26.19%	26.19%	26.19%
2	Other skull-brain injury	35.29%	35.29%	35.29%	31.62%	31.62%	31.62%	36.16%	36.16%	36.16%	30.99%	30.99%	30.99%
11a	Fracture of 1 rib AIS1	4.07%	4.07%	4.07%	7.30%	7.30%	7.30%	5.32%	5.32%	5.32%	6.47%	6.47%	6.47%
11b	Fracture of 2 ribs AIS2	3.77%	3.77%	3.77%	6.03%	6.03%	6.03%	4.13%	4.13%	4.13%	7.48%	7.48%	7.48%
11c	Fracture of 3+ ribs AIS3+	83.77%	83.77%	83.77%	76.30%	76.30%	76.30%	85.33%	85.33%	85.33%	80.39%	80.39%	80.39%
22a	Fracture of hip - left	45.42%	58.49%	69.65%	9.41%	29.87%	48.98%	71.33%	78.42%	84.47%	40.31%	59.08%	73.58%
22b	Fracture of hip - right	8.00%	19.01%	31.00%	1.33%	8.30%	19.08%	34.35%	43.48%	52.13%	2.53%	11.03%	22.94%
23a	Fracture of femur shaft - left	38.41%	52.26%	63.87%	16.98%	31.18%	45.23%	38.01%	45.30%	52.96%	30.91%	37.12%	43.45%
23b	Fracture of femur shaft - right	0.50%	2.76%	7.61%	0.04%	0.62%	3.07%	1.30%	6.17%	13.69%	0.08%	1.28%	5.06%
24a	Fracture of knee/lower leg - left	1.23%	4.36%	10.49%	0.20%	2.62%	7.97%	21.57%	23.92%	28.04%	1.24%	4.40%	9.82%
24b	Fracture of knee/lower leg - right	23.68%	30.00%	34.52%	1.22%	3.79%	8.27%	18.33%	23.72%	29.50%	10.71%	14.22%	17.87%

Figure 16-1: Results of the overall injury assessment for pedestrian-tram scenarios based on the predicted injuries and the occurrence probability.



